Volume 42
Number 2
February 2025
Pages 197–422

Natural Product Reports

rsc.li/npr

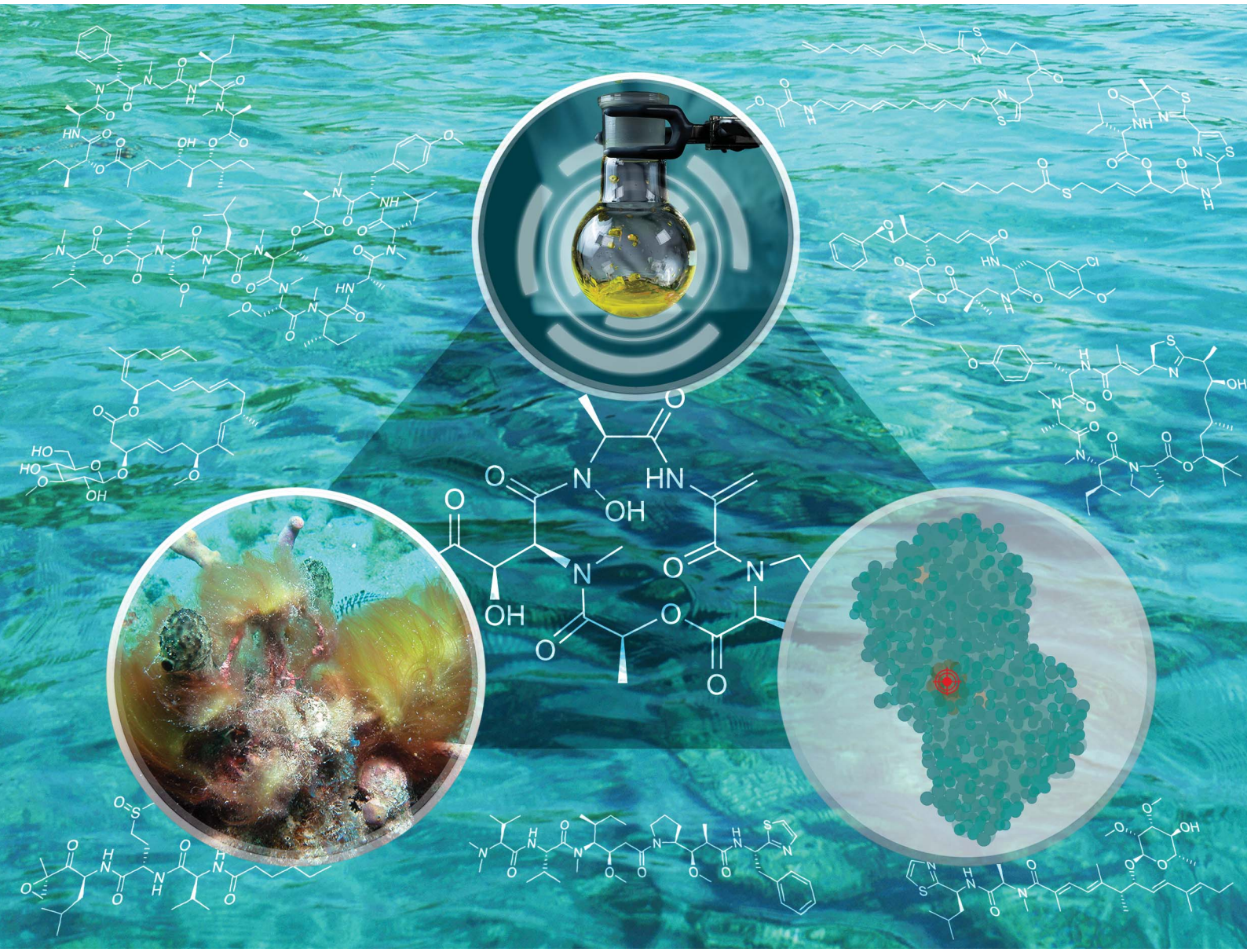

ISSN 0265-0568

ROYAL SOCIETY OF CHEMISTRY

REVIEW ARTICLE
Hendrik Luesch *et al.*
Progress in the discovery and development of anticancer agents from marine cyanobacteria

Natural Product Reports

ROYAL SOCIETY OF CHEMISTRY

REVIEW

View Article Online
View Journal | View Issue

Cite this: *Nat. Prod. Rep.*, 2025, **42**, 208

Progress in the discovery and development of anticancer agents from marine cyanobacteria

Hendrik Luesch, *[ab] Emma K. Ellis, [a] Qi-Yin Chen [a] and Ranjala Ratnayake [a]

Covering 2010–April 2024

There have been tremendous new discoveries and developments since 2010 in anticancer research based on marine cyanobacteria. Marine cyanobacteria are prolific sources of anticancer natural products, including the tubulin agents dolastatins 10 and 15 which were originally isolated from a mollusk that feeds on cyanobacteria. Decades of research have culminated in the approval of six antibody-drug conjugates (ADCs) and many ongoing clinical trials. Antibody conjugation has been enabling for several natural products, particularly cyanobacterial cytotoxins. Targeting tubulin dynamics has been a major strategy, leading to the discovery of the gatorbulin scaffold, acting on a new pharmacological site. Cyanobacterial compounds with different mechanisms of action (MOA), targeting novel or validated targets in a range of organelles, also show promise as anticancer agents. Important advances include the development of compounds with novel MOA, including apratoxin and coibamide A analogues, modulating cotranslational translocation at the level of Sec61 in the endoplasmic reticulum, largazole and santacruzamate A targeting class I histone deacetylases, and proteasome inhibitors based on carmaphycins, resembling the approved drug carfilzomib. The pipeline extends with SERCA inhibitors, mitochondrial cytotoxins and membrane-targeting agents, which have not yet advanced clinically since the biology is less understood and selectivity concerns remain to be addressed. In addition, efforts have also focused on the identification of chemosensitizing and antimetastatic agents. The review covers the state of current knowledge of marine cyanobacteria as anticancer agents with a focus on the mechanism, target identification and potential for drug development. We highlight the importance of solving the supply problem through chemical synthesis as well as illuminating the biological activity and in-depth mechanistic studies to increase the value of cyanobacterial natural products to catalyze their development.

Received 1st May 2024

DOI: 10.1039/d4np00019f

rsc.li/npr

[a]*Department of Medicinal Chemistry and Center for Natural Products, Drug Discovery and Development (CNPD3), University of Florida, 1345 Center Drive, Gainesville, Florida 32610, USA. E-mail: luesch@cop.ufl.edu*

[b]*Program in Cancer and Stem Cell Biology, Duke-NUS Medical School, Singapore, 169857, Singapore*

1. Introduction

Natural products have played a key role in delivering drug candidates or provided the inspiration for the development of agents with new targets or new mechanisms of action, especially for infectious diseases and cancer.[1–3] Historically, roughly 50% of all drugs are inspired by natural products and for cancer even 60%.[3] Critical to the continuous success of natural products is the identification of biological sources with high biosynthetic potential and genetic diversity that translates into new chemical space and therefore therapeutic space, which has been increasingly realized by investigating marine sources that represent the greatest biodiversity on the planet. Through advances in genomics and target identification methodology, natural products are

Hendrik Luesch

Hendrik Luesch received his Diplom in Chemistry at the University of Siegen (Germany) in 1997 and his PhD with Professor Richard Moore at the University of Hawaii at Manoa in 2002. After postdoctoral studies at The Scripps Research Institute with Professor Peter Schultz, he joined the faculty at the University of Florida in 2005, where he is leading a comprehensive marine natural products program with chemistry- and genomics-based discovery platforms. Since 2024 he holds a joint appointment at Duke-NUS Medical School in Singapore. Research highlights include the discovery and characterization of dolastatin 10, apratoxins, largazole, and gatorbulins from marine cyanobacteria.

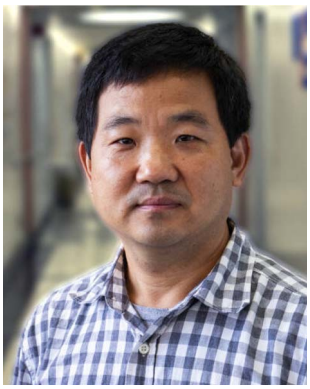

Qi-Yin Chen

Qi-Yin Chen received BSc and MS in Chemistry from Henan Normal University (1997) and Central South University (2000), respectively, and PhD in Organic Chemistry in 2005 from the Institute of Chemistry (CAS). He completed postdoctoral training with Professors Yujiro Hayashi (Tokyo University of Science), Alan Katritzky (UF), and Hendrik Luesch (UF). He currently is a Research Associate Professor and serves as the leader for Synthetic Chemistry Core at Center for Natural Products, Drug Discovery and Development (CNPD3) at UF. His research focuses on the synthesis of bioactive marine natural products, and small-molecule drug leads. He has co-authored over 40 peer-reviewed articles.

Emma K. Ellis

Emma Ellis received her BSc in Biochemistry from Oklahoma Baptist University in 2022. After graduation, she joined the Department of Medicinal Chemistry at the University of Florida as a predoctoral candidate. She was selected as a trainee in the UF Chemistry–Biology Interface Predoctoral Training Program (T32) and is mentored by Professor Hendrik Luesch. Her research is focused on the isolation and characterization of novel metabolites from marine cyanobacteria, including synthesis and biological evaluation of lead compounds with pharmacological relevance for the treatment of cancer.

Ranjala Ratnayake

Ranjala Ratnayake obtained her BSc (1996) and MPhil (2002) from the Open University in Sri Lanka. She obtained her PhD at the University of Queensland, Australia with Professor Robert J Capon in 2007. She completed postdoctoral trainings at the National Cancer Institute (NCI) in the Molecular Targets Development Program (MTDP), in Frederick, Maryland and at UF. She is currently a Research Associate Professor in the Department of Medicinal Chemistry at UF. She has co-authored over 50 peer-reviewed research articles in small molecule characterization, assay development, screening, and mechanistic studies of natural products including dolastatin 15, apratoxins, gatorbulins, lagunamides and largazole.

experiencing a renaissance, especially marine natural products that suffered most from the drawbacks of supply issue, structural complexity associated with difficulty in chemical synthesis and target identification.[4–6] However, we have learned that novel biology exerted by these compounds justifies chemistry efforts, exemplified by the FDA approval of the sponge natural product (halichondrin B) inspired eribulin, requiring a 61-step synthesis.[7] Requisites for successful drug development are the identification of novel chemical scaffolds with biological functions, a scalable total synthesis to solve the supply issue and explore structure–activity relationships (SAR) for further optimization, and the characterization of the mechanism of action (MOA) and the direct biological targets. The latter tends to be highly rewarding, since natural products point us to new ways to combat diseases, which translates into first-in-class agents.

Among marine organisms, cyanobacteria have become a validated source of drug leads and perhaps most successful organisms, with five current FDA approvals based on dolastatin 10 for the treatment of various cancers, accounting for 33% of FDA-approved marine drugs.[8] Marine cyanobacteria's genetic diversity is associated with diverse and novel pharmacological space of the encoded compounds that are mainly modified peptides or peptide-polyketide hybrids. Cyanobacteria have also been demonstrated to produce most-potent-in-class natural products.[9–11] Target discovery and mechanisms of action have been the catalyst to drive focused preclinical studies, to identify potential liabilities and rational application, and even combination therapy. Our review focuses on the recent progress in the discovery and development of anticancer agents from marine cyanobacteria, which usually required that structure determination was coupled with imperative chemical synthesis and in-depth mechanistic studies to recognize and maximize therapeutic opportunities. This review, covering the period from 2010 to April 2024, represents an extension of our group's 2015 review on general and representative biological targets and mechanisms of action of marine cyanobacterial compounds, now with an in-depth focus on anticancer activities and critical developmental issues and status.[12] In contrast to other recent reviews focusing on structures and the vast array of biological activities,[9,13–16] our review highlights promising anticancer activities of marine cyanobacterial compounds through the lens of potential drug development opportunities, with emphasis on target identification and mechanism of action, in addition to solving the supply issue. We present the most promising and well-characterized cyanobacterial compounds with distinct activity profiles, established synthetic strategies for obtaining material for rigorous preclinical assessment, classified compounds based on their MOA and target or target organelle, and application of enabling technologies for their development as ADCs.

2 Tubulin agents and their enablement as antibody-drug conjugates (ADCs)

2.1. Target engagement and mechanism of action

Tubulin-targeted chemotherapy has been highly successful, and the various marketed drugs are based on natural products scaffold, including cyanobacterial compounds.[17,18] Tubulin heterodimers, composed of α-and β-subunits, form polarized polymers and these microtubules are involved in cellular structure, cell division and proliferation, motility, and intramolecular trafficking.[17,19–21] Binding of pharmacological agents affects the tubulin dynamics and ultimately leads to anticancer activity.[22] Tubulin agents are categorized based on their binding site at α/β-tubulin or the dimer interface and whether they stabilize or destabilize microtubules. Eight distinct sites are known (six of which lead to destabilization and two causing stabilization), including one of the first marine derived tubulin destabilizers, curacin A, which binds to the colchicine site based off biochemical data[23,24] and the discovery of the seventh binding site targeted by the cyanobacterial microtubule-destabilizing depsipeptide, gatorbulin-1 (Fig. 1).[25] The eighth binding site was recently discovered using computer-aided molecular design to create the first rationally designed tubulin binder to the interface between the maytansine site and the end of the pironetin pocket.[26] The most well-known cyanobacterial tubulin agents in clinical use and advanced development include dolastatins 10 and 15 as well as the cryptophycins (Fig. 1), all of which are known to target the vinca site to interfere with tubulin assembly and destabilize microtubules.[27–30] The recently discovered gatorbulins induce depolymerization targeting tubulin near the colchicine binding site at the interface between the α,β subunits.[25,31] Target engagement in all cases leads to interference with tubulin dynamics, and one of the downstream effects is the disruption of mitotic spindle, leading to G2/M cell cycle arrest.[32] These agents also produce a similar cytotoxicity profile in the NCI-60

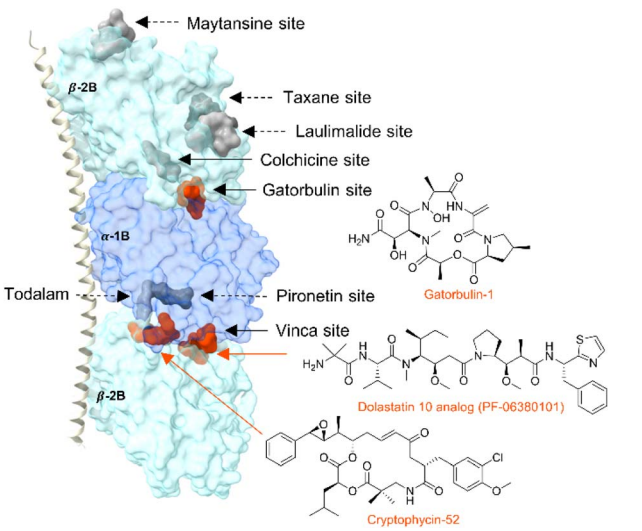

Fig. 1 Tubulin structure (PDBID: 5LA6) showing the known tubulin binding sites: maytasine (PDBID: 4TV8), taxane (zampanolide, 4I4T), laulimalide (4O4H), colchicine (plinabulin, 6S8K), gatorbulin (7ALR), pironetin (5LA6), todalam (todalam 4, 5SB3) and vinca (dolastatin 10 analogue, 4X1I and cryptophycin-52, 7LXB). Sites are indicated by a surface representation of the co-crystallized molecules (in parenthesis, when differing from the site name). Sites known to be targeted by marine cyanobacterial compounds are in orange.

cancer cell line screen, which indicates that they share a similar mechanism of action.[25,33] However, despite these and other striking commonalities, the pharmacology appears to have left a distinct fingerprint and unique intricacies include drug-like properties. Targeting the gatorbulin site induces proteasome-mediated tubulin degradation,[31] which is a unique characteristic compared with tubulin agents against other pharmacological sites.[25]

2.2. Dolastatin 10

Dolastatin 10 (**1a**, Fig. 2) was originally isolated from the Indian Ocean sea hare *Dolabella auricularia*,[34] but in 2001 the true producer was identified as a marine cyanobacterium, taxonomically classified in 2015 as a new genus *Caldora penicillata*.[34–36] The compound (**1a**) has been isolated from cyanobacteria collected from Micronesia, Hawaii and Florida.[34,35,37] Dolastatin 10 (**1a**) showed exquisite potency at the cellular level against cancer cells in the picomolar range (10–100 pM), notably with an IC_{50} of 0.03 nM for L1210 leukemia, 0.059 nM for small cell lung cancer NCI-H169, and 0.5 nM for human prostate cancer DU-145 cell lines.[28,38–40] Dolastatin 10 reached Phase II clinical trials but was discontinued due to granulocytopenia and neutropenia at dose-limiting toxicities.[41] The synthesis was achieved in various ways but always following a sequential elongation approach that was amenable to structure diversification, leading to TZT-1027 (**1b**) and monomethyl auristatin E (MMAE, **2a**), which advanced to clinical trials (Fig. 2).[42–44] Dolastatin 10 analogues did not progress further in clinical trials due to non-selectivity, but MMAE (**2a**) and monomethyl auristatin F (MMAF, **2b**) were developed into the cytotoxic payload for antibody-drug conjugates (ADCs, **3a–3e**, **3f**) with tremendous success (Fig. 2).[45–47]

MMAE linked to the CD30 antibody *via* a protease-cleavable linker led to brentuximab vedotin (**3a**), approved in 2011 for the treatment of Hodgkin's lymphoma and anaplastic large cell lymphoma.[48] (Fig. 2) The same cathepsin B-cleavable maleimidocaproyl-valyl-citrulline-*p*-aminobenzyl-carbamate linker ((mc-Val-Cit-PABC)-citrulline) was pivoted for polatuzumab vedotin (**3b**), where MMAE was linked to a CD79B-directed ADC that was approved in 2019 to treat non-Hodgkin lymphoma, chronic lymphocytic leukemia and refractory B-cell lymphoma.[49] By utilizing an anti-nectin-4 monoclonal antibody, the ADC enfortumab vedotin (**3c**) (using the same payload and linker) was approved in 2019 to effectively target metastatic urothelial cancer.[50]

The success of these drugs prompted the launching of similar ADCs with the same payload and proven linker, differing only by the antibody, to target different cancers.[51] In some instances, linkers were changed with the advances of linker technologies. MMAE-based tisotumab vedotin-tftv was the most recent FDA approved ADC (2021) with implications for recurrent or metastatic cervical cancer possessing disease progression during or post chemotherapeutic treatment.[52] Belantamab mafodotin-blmf (**3f**) was the only MMAF-based FDA approved ADC (2020) as the first anti-B-cell maturation antigen therapy for patients with released or refractory multiple myeloma.[53,54]

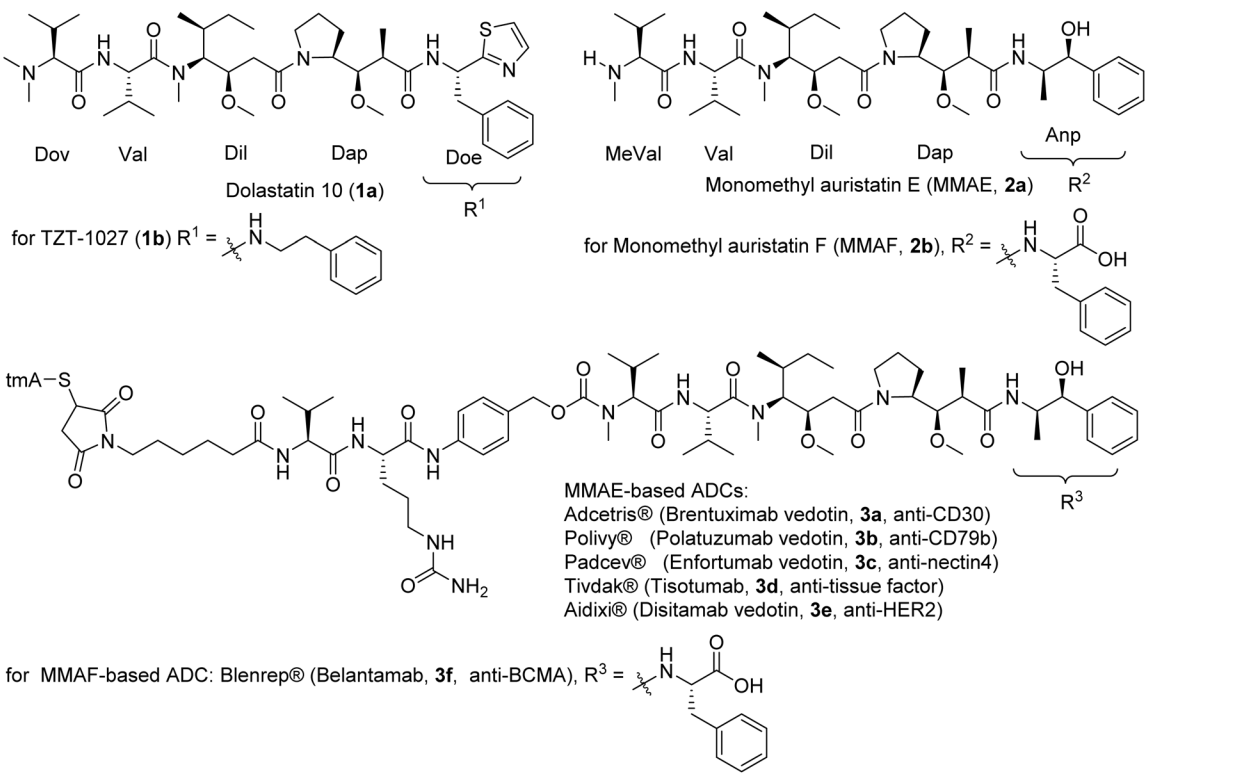

Fig. 2 Structures of dolastatin 10 (**1a**), and the synthetic analogues of monomethyl auristatins developed as ADCs approved by FDA for clinical use. The MMAF-based ADC has been withdrawn.

Table 1 Dolastatin 10 (**1a**) based ADCs approved or in clinical/preclinical trials

Trade name (ADC)	Company	Target (mAb mode)	Payload	Linker	FDA approved/clinical phase	Disease indication	Ref.
Adcetris® (brentuximab vedotin[BV], SGN-35)	Seattle Genetics/Takeda (Washington, U.S./Tokyo, Japan)	CD30 (cAC10 chimeric IgG1)	MMAE	Protease-cleavable linker, maleimidocaproyl-valine–citrulline-*p*-aminobenzyloxycarbonyl linker	2011	Relapsed/refractory Hodgkin lymphoma and anaplastic large cell lymphoma	45
Padcev® (enfortumab vedotin [EV], ASG-22ME, AGS-22M6E)	Seattle Genetics/Astella (Washington, U.S./Tokyo, Japan)	Nectin 4 (IgG1)	MMAE	Cleavable maleimidocaproyl-valine–citrulline-*p*-aminobenzyloxycarbonyl linker	2019	Locally advanced or metastatic urothelial cancer	50
Polivy® (polatuzumab vedotin-piiq[PV], DCDS4501, RG7596)	Roche (Basel, Switzerland)	CD79b (IgG1)	MMAE	Protease-cleavable maleimidocaproyl-valine–citrulline-*p*-aminobenzyloxycarbonyl linker	2019	Diffuse large B-cell lymphoma	57
Tisotumab vedotin (HuMax-TF-ADC)	Genmab (Vably, Denmark)	CD142 (Hu IgG1)	MMAE	Valine–citrulline peptide linker	2021	Multiple solid tumours	52 and 58
Disitamab vedotin (Aidixi)	RemeGene (California, U.S.)	HER2	MMAE	Valine–citrulline peptide linker	2021	Multiple solid tumors	59
Telisotuzumab vedotin (ABBV-399)	AbbVie/Pierre Fabre (Illinois, U.S./Castres, France)	HGFR/cMet (Engineered IgG1)	MMAE	Valine–citrulline peptide linker	2021	Non-small cell lung cancer	60
ARX788	Zhejiang Medicine/Ambrax (Zhejiang, China/California, U.S.)	HER2	MMAF (Amberstatin 269)	Hydroxylamine-PEG4	Phase III	Metastatic breast cancer/gastric cancer	61
BT8009	Bicycle (Cambridge, U.K./Massachusetts, U.S.)	Nectin-4 (PVRL4)	MMAE	Valine–citrulline dipeptide linker	Phase II	Bladder and breast neoplasms, non-small cell lung and ovarian cancer, solid tumors	62
BT5528	Bicycle (Cambridge, U.K./Massachusetts, U.S.)	EphA2	MMAE	Valine–citrulline peptide linker	Phase II	Breast, gastric, and urothelial cancer, head/neck cancer, non-small cell lung, and ovarian cancer, solid tumors	63
Upifitamab rilsodotin (XMT-1536)	Mersana therapeutics (Massachusetts, U.S.)	NaPi2b & microtubules	Auristatin F-HPA	Poly-1-hydroxymethylethylene hydroxymethylformal	Phase II	Solid tumors	64 and 65
STI-6129	Sorrento (California, USA)	CD38	Duostatin 5	Non-polyethylene glycol linker	Phase II	Relapsed/refractory systemic amyloidosis	66
RC-88	RemeGen (China/U.S.)	Mesothelin	MMAE	Valine–citrulline peptide linker	Phase II	Solid tumors	67
A-166	Klus Pharma (New Jersey, U.S.)	HER2	Duostatin 5	Stable protease-cleavable valine citrulline linker	Phase II	HER2-expressing cancer	68
MRG003	Lepu Biopharma (China)	EGFR	MMAE	Valine–citrulline linker	Phase II	Non-small cell lung cancer	69

Table 1 (*Contd.*)

Trade name (ADC)	Company	Target (mAb mode)	Payload	Linker	FDA approved/clinical phase	Disease indication	Ref.
W0101	Pierre Fabre (Paris, France)	IGF-R1	Ab-auristatin	Noncleavable maleimidocaproyl (mc) linker	Phase II	Advanced or metastatic solid tumors	70
SolidAGS-16C3F	Astellas (Tokyo, Japan)	ENPP3 (Hu IgG1)	MMAF	Maleimidocaproyl linker	Phase II	Metastatic renal cell carcinoma	71
Ozuriftamab vedotin (BA-3021)	BioAtla (California, U.S.)	ROR2	MMAE	Cleavable maleimidocaproyl-valyl-citrullinyl-*p*-aminobenzyloxycarbonyl linker	Phase II	NSCLC, triple – Breast cancer, and soft tissue sarcoma	72
Telisotuzumab vedotin (ABBV-399)	Abbvie (Illinois, U.S.)	c-Met	MMAE	Cleavable valine–citrulline peptide linker	Phase II	Solid tumors	73
Ladiratuzumab vedotin (SGN-LIV1A)	Seattle Genetics (Washington, U.S.)	LIV1 (Hz IgG1)	MMAE	Valine–citrulline peptide linker	Phase II	Breast cancer	74
CAB-AXL (BA-3011, Mecbotamab vedotin)	BioAlta (California, U.S.)	AXL	MMAE	Cleavable linker	Phase II	Solid tumor, non-small cell lung cancer, melanoma, sarcoma	75
ARX-517	AmbRX (California, U.S.)	PSMA	MMAF (Amberstatin 269)	Hydroxylamine-PEG4	Phase I	Prostate cancer	76
Cofetuzumab pelidotin (ABBV-647)	Abbvie (Illinois, U.S.)	PTK7	Auristatin-0101	Cleavable valine–citrulline based linker	Phase I	Non-small cell lung cancer	77
SGN-B6A	Pfizer (New York, U.S.)	Integrin beta-6	MMAE	Valine–citrulline peptide linker	Phase I	Solid tumors	78
Zanidatamab zovodotin (ZW-49)	Zymeworks/BeiGene (BC, Canada/Beijing, China)	HER2	Proprietary auristatin	Protease cleavable linker	Phase I	HER2 expressing cancer	79
ALT-P7	3Sbio/Alteogen (China/Korea)	HER2 & microtubules	MMAE	Cysteine-containing peptide motif	Phase I	Breast and gastric cancers	80

The ADC contains a non-cleavable linker and an afucosylated Fc-engineered antibody.[55] Later, approval was withdrawn due to inferior efficacy in progression-free survival of the patient.[56] Table 1 shows ADCs with dolastatin 10 analogues as the cytotoxic payload.[8]

Requisite for the success of the dolastatin 10-based ADC development was both the understanding of the biological and clinical relevance, as well as solving the supply issue by total synthesis.

The total synthesis of dolastatin 10 (**1a**) always followed the sequential elongation approach using the five subunits. The difference between each method is the construct of the three key units, *i.e.*, dolaisoleuine (Dil), dolaproine (Dap) and (*S*)-dolaphenine (Doe).[81] The earlier synthesis of unit Dil and Dap was effected by using an Aldol reaction.[82] A β-ketone ester approach was developed for the synthesis of the Dil fragment (Fig. 3a): the imidazole intermediate of isoleucine was reacted with magnesium enolate of ethyl hydrogen malonate to provide β-ketone ester.[83,84] Sequential asymmetric reduction and methylation then gave the Dil fragment (Fig. 3a). Similarly, Genet followed the β-ketone ester approach to construct the Dap fragment.[84] Wei developed a straightforward chiral *N*-sulfinyl imine method to generate both Dil and Doe fragments (Fig. 3b and c).[85] However, when the Doe fragment was synthesized through a benzyl thiazolyl ketone, more than six steps were required (Fig. 3d).[84] With the five subunits in hand, the synthesis of the final target started from Doe, and other units were installed in a stepwise manner by standard peptide coupling protocols (Fig. 3e). However, the general strategy of the total synthesis of MMAE (**2a**) is a little different: two subunits Dap-Anp and MeVal-Val-Dil were pre-synthesized and then coupled together to yield the final product MMAE (**2a**, Fig. 3f).[86,87] The different strategies resulted from the different polarity of Dov and *N*-MeVal: the *N*,*N*-diMeVal is a polar moiety and its attachment at late-stage could avoid additional side reactions and a harsh purification process, while Fmoc protected MeVal does not face similar issues. Therefore a convergent approach was adopted in the synthesis of MMAE.[88]

Nishio synthesized a series of dolastatin 10 derivatives with the replacement of Doe for versatile conjugations, and Mendelsohn modified the pyrrolidine ring (Dap unit) and synthesized a series of linear and macrocyclic dolastatin 10 analogues.[89,90]

2.3. Dolastatin 15

Dolastatin 15 (**26a**) was also first discovered from the shell-less mollusk *D. auricularia* by the Pettit group and only in 2020

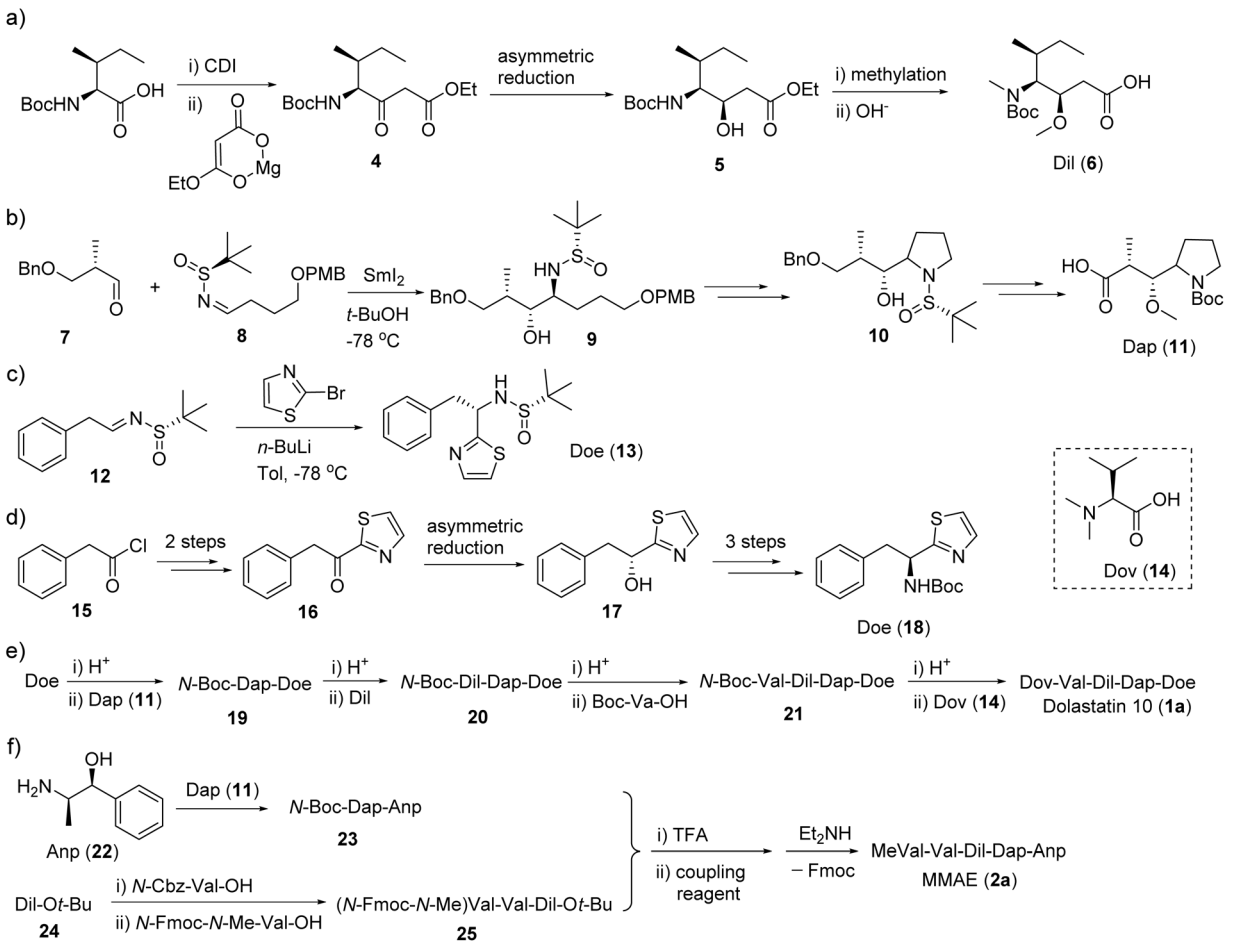

Fig. 3 Synthesis steps (a–e) for dolastatin 10 (**1a**) and (f) MMAE (**2a**).

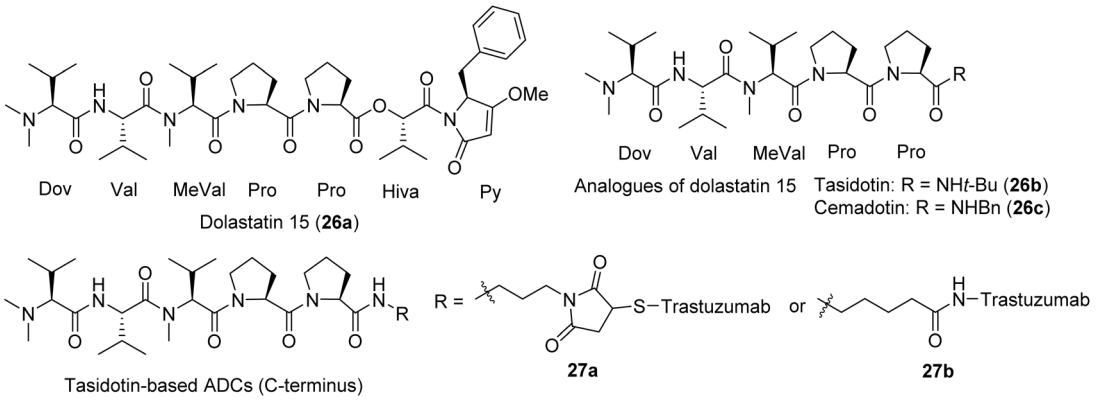

Fig. 4 Dolastatin 15 (**26a**) and clinically evaluated analogues, including relevant ADCs that advanced to clinical trials.

Table 2 Dolastatin 15 (**26a**) ADCs advanced to clinical trials

ADC (other names)	Company	Target	Clinical phase	Indication	Ref.
Tasidotin (**26b**, ILX651)	Genzyme (Massachusetts, U.S.)	Tubulin	Phase I	Advanced solid malignancies	94
Cemadotin (**26c**)	Hu and Hang	Tubulin	Phase I	Solid tumors	95
LU 103793	BASF (Massachusetts, U.S.)	Tubulin	Phase II, discontinued	Non-small cell lung cancer, breast cancer, malignant melanoma	96–98

published to be of proven cyanobacterial origin with its direct isolation from the marine cyanobacterium *Symploca* sp. by the Luesch group[91] (Fig. 4). Dolastatin 15 possesses lower potency than dolastatin 10 in the nanomolar range (IC_{50} 3–5 nM), and has been heavily investigated due to its action on tubulin.[29,92] Dolastatin 15 is believed to target the vinca site, similar to dolastatin 10, although biochemical and cellular data also indicated differences.[29,91,93] The dolastatin 15 analogues tasidotin (**26b**) and cemadotin (**26c**) (Fig. 4) have shown promising activity against solid tumors in preclinical models, and conjugation to trastuzumab on N- and C-terminus led to its evaluation as an ADC against human epidermal growth factor receptor (HER) 2+ ovarian cancer (Table 2).[99] Only the ADCs derived from C-terminus maintained anti-tubulin activity (Fig. 4); the ones derived from N-terminus lost activity.[100] Cemadotin (**26c**), a dolastatin 15 pentapeptide synthetic analogue, has been shown to cause tumor growth delays *in vitro* when conjugated through a thiazolidine linker to the fibronectin antibody (Fig. 4).[81,82,101]

There are two main strategies published for the synthesis of dolastatin 15 (Fig. 5). Pettit's group used the [1 + 1] strategy through liquid solution method (Fig. 5a), first synthesizing the fragments Dov-Val-MeVal-Pro (**28**) and Pro-Hiva-Py (**29**), then fusing the two fragments aided by a coupling reagent to obtain the final product that was identical to the natural product.[102,103] Akaji's group applied a similar strategy but used solid phase peptide synthesis (SPPS) to synthesize the same two fragments, in which a new coupling reagent, 2-chloro- 1,3-dimethylimidazolinium hexafluorophosphate (CIP), was utilized in multiple steps.[104] However, the Jouin group applied a slightly different strategy (Fig. 5b), first synthesizing two fragments 2Val-MeVal-2Pro (**30**) and Hiva-Py (**32**), then fusing these two fragments

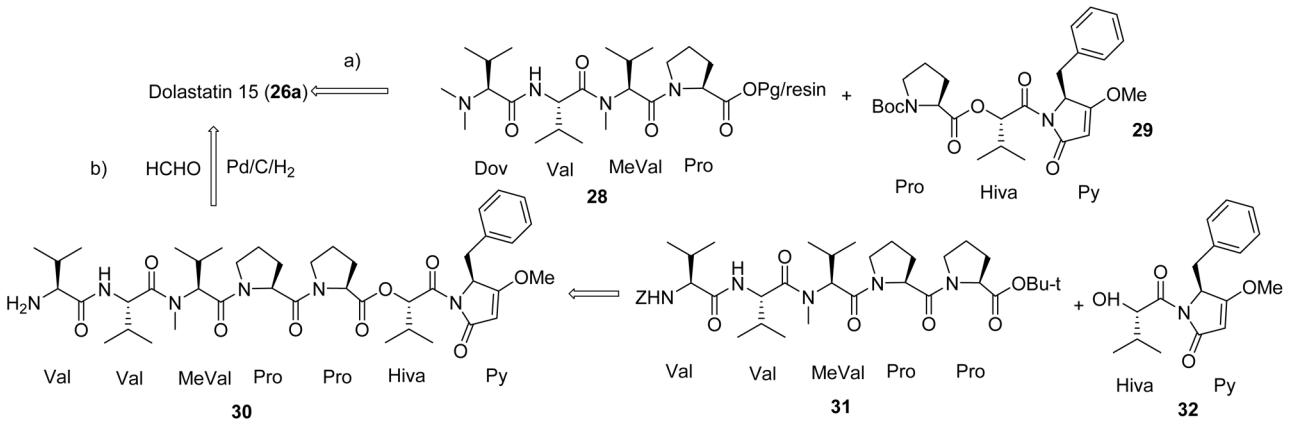

Fig. 5 Synthetic strategies (a and b) for dolastatin 15 (**26a**) that is also applicable to tasidotin (**26b**) and cemadotin (**26c**).

into the linear peptide (Val to Py).[105] The methylation of the end Val of the linear peptide with reductive hydrogenation using the system Pd/C/H_2/HCHO provided the proposed product. However, their product did not match the synthesized natural product from Pettit's group but was comparable to the isolated natural product dolastatin 15 (**26a**). The Jouin group proposed the discrepancies were due to the lack of purity from the originally isolated compound and the lack of diastereomeric purity of an intermediate from Pettit's synthesis of dolastatin 15.[105] The more purified synthetic product had slightly better activity than the isolated dolastatin 15 against the U.S. National Cancer Institute's P388 lymphocytic leukemia cell line (ED_{50} of 0.48 ng mL^{-1} *vs.* 2.4 ng mL^{-1}).[105] Tasidotin (**26b**) and cemadotin (**26c**) are simplified analogues of dolastatin 15 (**26a**) and their total synthesis was straightforward, starting from its proline precursor.[94,106]

2.4. Cryptophycins

The super potent microtubule disruptors cryptophycins were originally isolated from terrestrial cyanobacteria as antifungal agents in 1990, and later characterized as anticancer agents by the Moore group in 1997.[27,107] Subsequently, hundreds of analogues were either isolated or synthesized, many from the Moore group.[108–110] Cryptophycins are presumably also produced by marine cyanobacteria, evidenced by cryptophycin-24 (arenastatin A) that was isolated from the cyanobacteria-harboring marine sponge *Dysidea arenaria*.[111–113] The most abundant naturally occurring cryptophycin-1, demonstrated spectacular potency with IC_{50} values ranging from low-nanomolar to picomolar against many cancer cell lines (IC_{50} 4.58 pM, KB cells; 7.63 pM, LoVo; 0.4 nM, C6 glioma; and 0.8 nM, HepG2) and was an ineffective substrate of P-glycoprotein (Pgp) in multidrug resistant cell lines.[108,109,114,115] Cryptophycin-52 (HeLa IC_{50} 0.011 nM) was selected as a clinical candidate but failed in Phase II clinical trials due to neurological toxicity (DLT 1.5 mg m^{-2}) and limited efficacy.[116–118] However, due to the exquisite potency, cryptophycins were predestined to be recognized as an attractive cytotoxic payload for ADCs, which led to their resurrection[110,119] (Fig. 6). Met-Val-

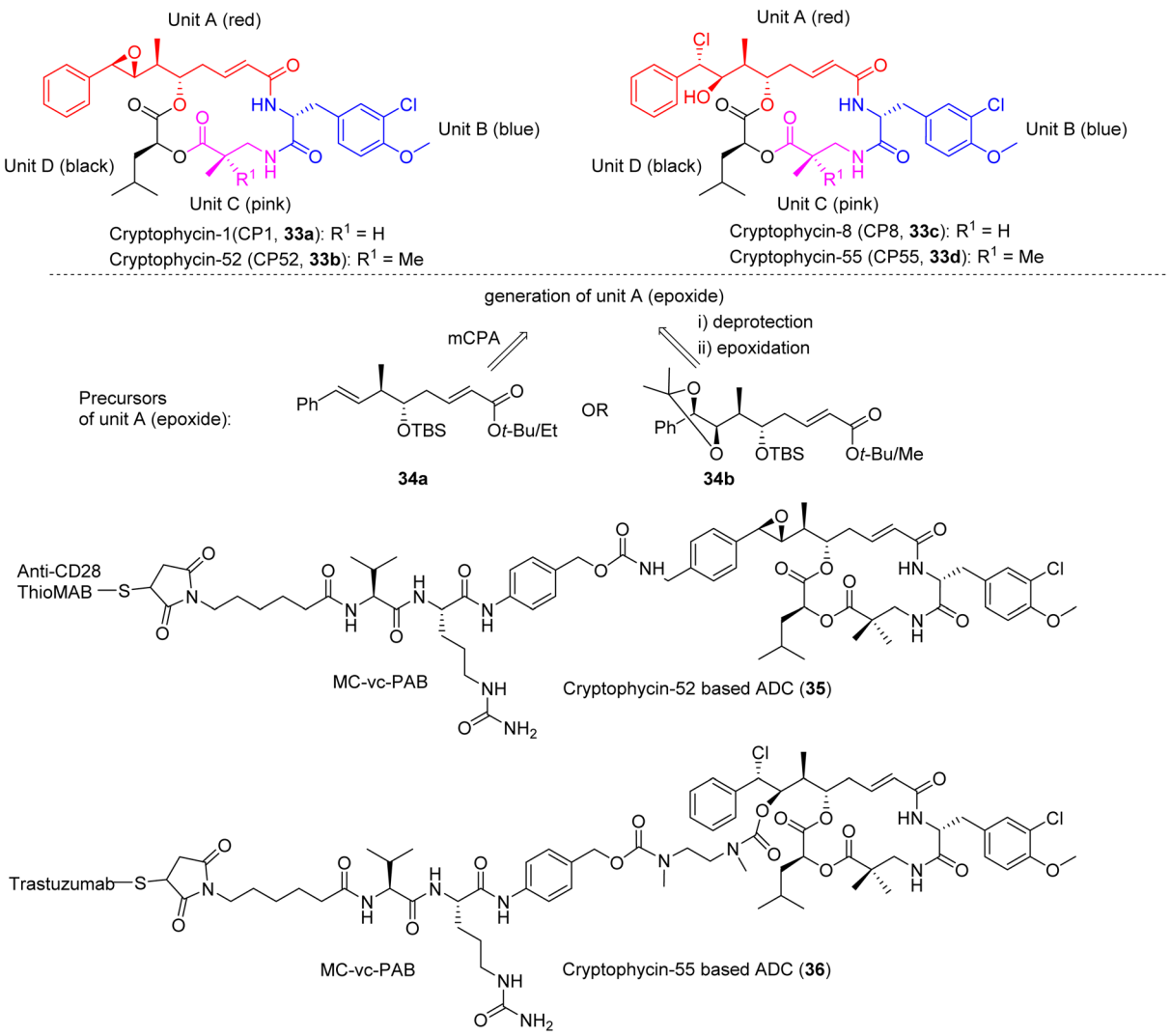

Fig. 6 Selected structures and units of cryptophycins (**33a–d**), including unit A precursors (**34a,b**) and ADCs (**35**, **36**).

Cit-PABC was used as the linker to thiomab and trastuzumab as antibodies for cryptophycins-52 and -55 based ADCs, respectively.[108,119,120] Cryptophycin-55-based ADC exhibited nanomolar cytotoxicity in HER2+ tumor cells (IC_{50} 0.58–1.19 nM) and antitumor activity in xenograft models at 10 mg kg^{-1} (SKOV3 and NCIeN87).[119]

Natural cryptophycins are composed of four units A–D (Fig. 6). Epoxide-containing (*e.g.*, CP1, **33a** or CP52, **33b**) and chlorohydrin-containing (*e.g.*, CP8, **33c** or CP55, **33d**) analogues represent two types of the most cytotoxic analogues. Unit A is the key fragment with respect to synthetic accessibility and bioactivity, *i.e.*, it represents the most complex part for synthesis and the most important part in the determination of activity. The synthesis of unit A is challenging because it possesses four chiral centers, a labile epoxide and an unsaturated amide. Since the chlorohydrin could be readily obtained from the epoxide by transformation using acid-mediated ring opening (HCl), we here discuss the synthesis of epoxide-containing cryptophycins.[121] The epoxide could be introduced at a late-stage by oxidation of the styrene moiety or at an early stage *via* protection by an acetonide that would be cleaved at a late-stage.[121]

A scalable and economically feasible synthesis was the key for rigorous biological evaluation in preclinical and clinical trials. Over 300 cryptophycins have been generated and tested, and, more recently, the biosynthesis was effectively constituted and chemoenzymatic synthesis were performed.[122,123] However, the development of cryptophycin is attributed to its total synthesis.

There are many published methods for the synthesis of unit A. Generally, there are two strategies for the generation of the epoxide moiety, using both the styrene moiety approach and the acetonide moiety approach, as shown in Fig. 7.[124–127] In the former approach, styrene was designed as the precursor for the epoxide moiety, which was generated by oxidation of styrene at a late-stage, while in the latter approach acetonide was designed as the precursor of epoxide moiety, generated by the deprotection-epoxidation sequence of the acetonide moiety.[125,126] However, lower stereoselectivity was observed using the styrene approach (**34a**), *i.e.*, the product was a mixture of diastereomers and the ratio of (*R*,*R*) and (*S*,*S*) varied from 1 : 1 to 2.5 : 1. This method is straightforward, as the diastereomers could be separated by HPLC but is only suitable for small-scale

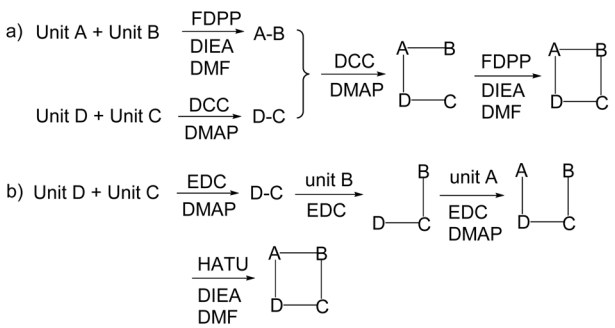

Fig. 7 Two strategies (a and b), for macrocyclization in the synthesis of cryptophycins.

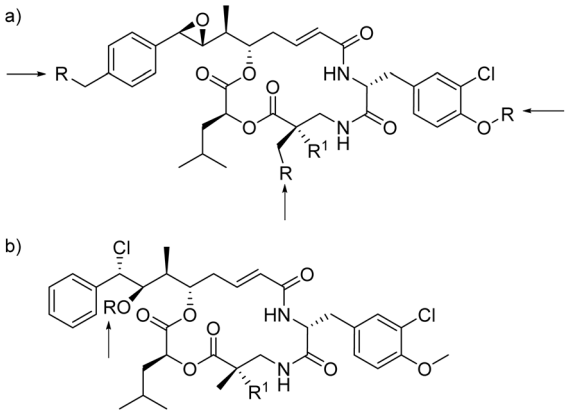

Fig. 8 Linker-antibody attachment sites for cryptophycin-based ADCs for (a) **35** and (b) **36** (R: derived moieties, R^1: H or Me).

preparation.[125] In the acetonide approach, the stereocenters were generated first and masked as acetonide and unmasked at a late-stage to produce an epoxide through another step. Though there are three more steps, this method could generate the (*R*,*R*) configuration, rendering it suitable for a scalable preparation of cryptophycins.[126] In 2011, Sherman developed a novel chemoenzymatic approach to synthesize cryptophycin using the enzyme CrpD-M2 to incorporate a 2-hydroxy acid moiety (unit D) into cryptophycin analogues.[128] The carboxy or amino terminus of 4-*O*-Me-phenylalanine (unit B) was frequently selected as the site of macrocyclization.

Due to the failure of cryptophycin-52 (**33b**) in Phase II clinical studies, ADCs have emerged as an important direction in the field of cryptophycin research (**35**, **36**, Fig. 6).[110,120,129] For the epoxide analogues (Fig. 8a), three sites were frequently chosen as a modification site, being the *para*-position of the aromatic ring of unit A, the OH site of unit B, and the methyl group of unit C. For the chlorohydrin analogue (Fig. 8b), the OH was derivatized to obtain ADCs.[110]

Recently, Sewald comprehensively reviewed the cryptophycins, including the fluorinated analogues and conjugates, biological activities, and SAR.[108]

2.5. Gatorbulins

The gatorbulin family is the most recent addition to the microtubule-destabilizing agents derived from marine cyanobacteria. Gatorbulin-1 (GB1, **37a**, Fig. 9) was described in 2021 from a Floridian *Lyngbya confervoides* by the Luesch group.[25] The structure determination was achieved through standard 2D NMR coupled with ^{15}N NMR, pinpointing the presence of a primary, secondary and tertiary amide as well as a hydroxamate group that was critical for the antiproliferative effects.[25] This distinct cyclodepsipeptide of comparatively low molecular weight is a modified pentapeptide that displayed unique pharmacology, targeting a seventh tubulin pharmacological site, as revealed through multidimensional characterization in complementary mechanistic and phenotypic assays.[25] Using fluorescent bona fide probes, it was found that GB1 could not displace fluorescent probes of eribulin (vinca site) or

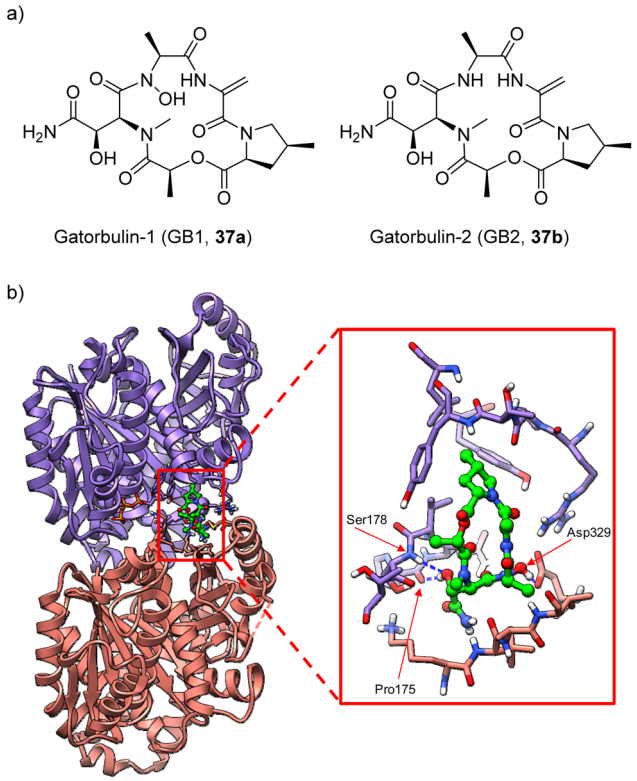

Fig. 9 (a) Structures of gatorbulin-1 (**37a**) and gatorbulin-2 (**37b**) and (b) crystal structure of the tubulin–gatorbulin-1 complex (PDBID: 7ALR). Purple: tubulin α-1B chain. Salmon: tubulin β-3 chain. Gatorbulin-1 carbons atoms are highlighted in green.

maytansine (maytansine/tip site) but competed successfully with a fluorescent probe for the colchicine site.[31] This data initially suggested that GB1 might be the first peptide targeting the colchicine site; however, both the pharmacological data and mechanistic probing indicated that GB1 may not target the classic colchicine pocket.[25] This hypothesis was successfully probed using macromolecular crystallography, culminating in the high-resolution structure determination of the α/β-tubulin-GB1 complex to reveal a new tubulin regulatory site near the colchicine site to modulate tubulin dynamics (Fig. 9).[25,31] The tubulin-colchicine and tubulin-GB1 showed main differences in the β-tubulin loop T7 and α-tubulin loop T5, which imperatively change their conformations upon colchicine binding.[31] GB1 binding precludes the concurrent ligand binding at the colchicine site, rationalizing the competition assay results and underscoring the distinct pharmacology of GB1.[25,31]

GB1 exhibited GI_{50} of 800 nM and IC_{50} of 300 nM in the primary screen against HCT116 colorectal cancer cells, without significantly affecting the cell viability of normal colon cells (IC_{50} > 10 μM).[25] Of the cancer cells tested, GB1 was the most cytotoxic to colon cancer cells COLO205 (GI_{50} 92 nM) and had strong activity in other cell lines, including melanoma (SK-MEL-5), ovarian (OVCAR-3), and prostate (DU-145).[25] However, the activity of GB1 in Pgp and βIII-expressing HeLa cell lines was strongly attenuated, initially suggesting room for optimization.[25] However, subsequent studies with MDCK cells stably transduced with the human efflux transporter MDR1/Pgp, showing similar permeability with and against transporter gradient, indicated that GB1 (**44a**) is a poor Pgp substrate.[31]

The co-isolated gatorbulin-2 (GB2, **37b**), the *N*-deoxy derivative of GB1, lacked antiproliferative activity and provided preliminary SAR information. The structure of the α/β-tubulin-GB1 complex underscored that the *N*-hydroxy group shows wide-ranging interactions with loop 5's α- and β-tubulins.[25] The synthesis of GB1 (**37a**) was achieved in 5.6% overall yield over 20 steps, solving the supply issue and established the basis for the synthesis of gatorbulins with simplified structures, GB2–7.[31]

The presence of almost exclusively unusual moieties (*N*-OH-Ala, DhAla, 4-MePro, OH-Asn) posed challenges for the total synthesis (Fig. 10a). Starting from *trans*-2,3-epoxysuccinic acid, the fully masked acid **38** was efficiently synthesized. Amidation of **38** by allyloxyamine **39** is a key step in this total synthesis, which was accomplished using the acid chloride method with AgCN as base. Fmoc–Fm pair was designed as the protection groups of amino and carboxy termini, respectively and Sec (Ph) was proposed as the precursor unit of DhAla. The PyBOP-mediated macrocyclization proceeded with good yield (60%). The Luesch group also synthesized six analogues (GB2–7, **37b–37g**, Fig. 10b) applying a similar synthetic strategy.[31]

GB1 (**37a**) has drug-like properties, including low molecular weight (<500 g mol^{-1}), and is amenable to rapid synthetic modification. These characteristics increase the translational potential of gatorbulin-based, pharmacologically novel microtubule agents to not just become chemical probes but also drug candidates that complement the arsenal of current clinical and preclinical microtubule agents.

The SAR was systematically investigated (GB2–7, **37b–37g**) at the biochemical and cellular level using GB1 (**37a**)-susceptible ovarian and cervical cancer cells.[31] The hydroxamate moiety in the *N*-methyl-alanine residue is critical for activity. All other structural modifications present in GB1, including C-hydroxylation of asparagine, methylation at C-4 of proline, and sp^2 hybridization in dehydro-alanine, were proven to be functionally relevant.[31] Replacement of the primary amide with a methyl ester also resulted in reduced activity, indicating the intricate scaffold optimization by the GB1-producing cyanobacterium. Inhibition of tubulin polymerization *in vitro* and binding affinities correlated very well, translating into differential cellular efficacy. Using docking and molecular dynamics to evaluate the effects of the chemical simplification at the structural level, any changes resulted in loss of target interactions, although energetically modest. Similar to cevipabulin that targets two different sites on the tubulin dimer,[31,130] GB1 promotes proteasome-mediated tubulin degradation but by an unknown mechanism, presumably distinct from that of cevipabulin.[27] Comparison with GB1 (**37a**) indicated that cevipabulin binds to the same tubulin region although the binding mode is distinct.[130] Cevipabulin almost exclusively interacts with α-tubulin, including nonexchangeable GTP.[130] In contrast, GB1 (**37a**) makes extensive contact and hydrogen bonding with both α- and β-chains of tubulin.[22] GB1–7 (**37a–37g**) showed excellent solubility and much higher than that of paclitaxel.[31] Hepatic microsome stability was shown to be excellent, while

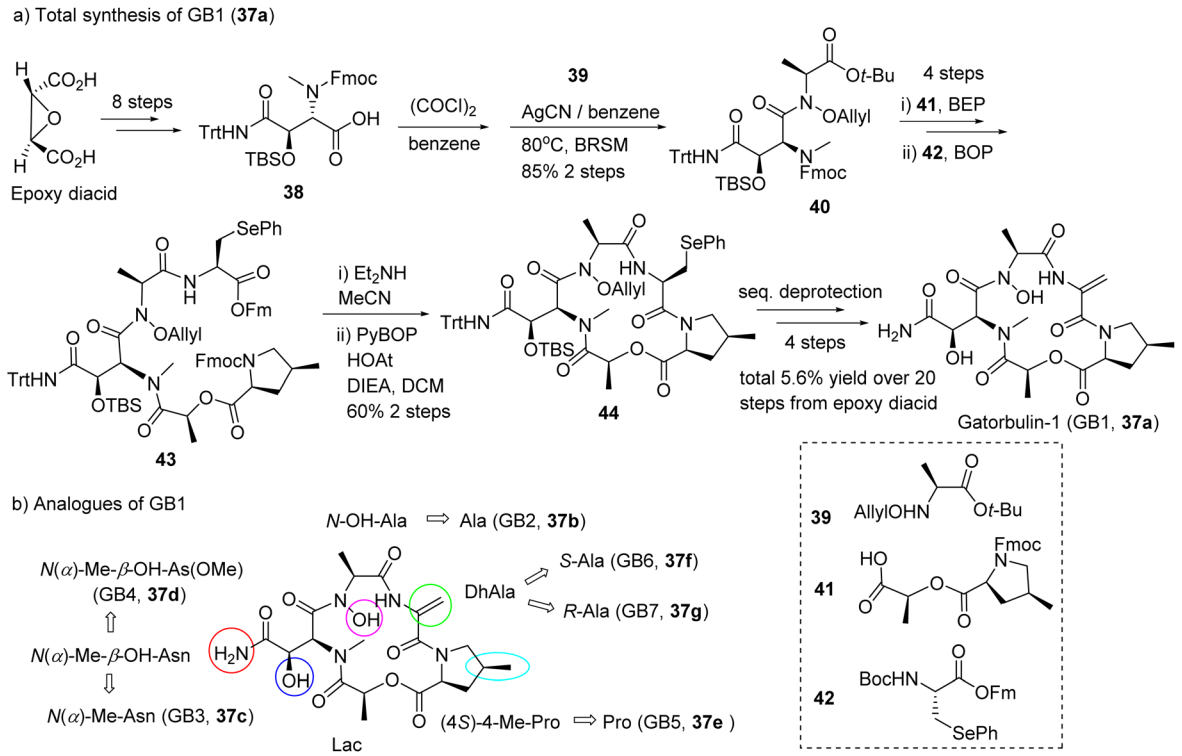

Fig. 10 Abbreviated synthesis (a) of GB1 (**37a**) and (b) the structures of gatorbulin analogues (GB2–7, **37b–37g**) highlighting the structural modifications to the parent molecule.

human cytochrome P450s were not inhibited, and plasma binding was minimal with high free fractions.[31] Passive permeability was predicted to be high based on parallel artificial membrane permeability assay (PAMPA) for GB1–6.[31]

2.6. Repurposing as HIF inhibitors

Dolastatins 10 (**1a**) and 15 (**26a**) as well as gatorbulin-1 (**37a**) were discovered (or re-discovered) as agents with differential antiproliferative activity against hypoxia-inducible factor 1 (HIF-1) containing HCT116 cells, following deconvolution of initial differential selectivity for parental HCT116 cells *versus* dual HCT116$^{HIF-1\alpha-/-HIF-2\alpha-/-}$ knockouts.[25,91,131] The screening system, described in 2016 to aid early-stage drug discovery by providing selectivity already in primary assays, enables the prioritization of agents that have a higher likelihood of activity and selectivity against solid tumors driven and characterized by oncogenic KRAS and hyperactivation of HIF (Fig. 11).[131] It was demonstrated that microtubule agents belonged to the compounds with greatest differential, which was later proven for dolastatin 15 (**26a**) and gatorbulin-1 (**37a**).[25,91] HIF inhibition appears to be a common downstream effect of tubulin-targeting agents as exemplified by multiple studies.[25,91,131–133] The dual effect of tubulin-binding to interfere with tumor vascularization largely in endothelial cells, and HIF-inhibition to downregulate target genes such as VEGFA in growth factor secreting cells suggests that these compounds are also promising anti-angiogenic agents, in addition to its primary utility as antimitotic agents.[134,135] Downregulation of the HIF-target gene, *VEGFA* in parental HCT116 cells was observed in cancer cells for dolastatin 15 (**26a**) and gatorbulin-1 (**37a**) and both were effective in angiogenesis assay *in vitro* model systems using endothelial cells.[25,91] Further, validation of HIF-regulated downstream effects by tubulin agents was demonstrated *in vivo* using a zebrafish model specifically in *vhl* mutants with activated (constitutively active) HIF signaling.[91] Dolastatin 15 showed strong *in vivo* antiangiogenic effects concomitant with HIF target gene downregulation (*Vegf* and *Egln3*) that was revealed by *in situ* hybridization.[91]

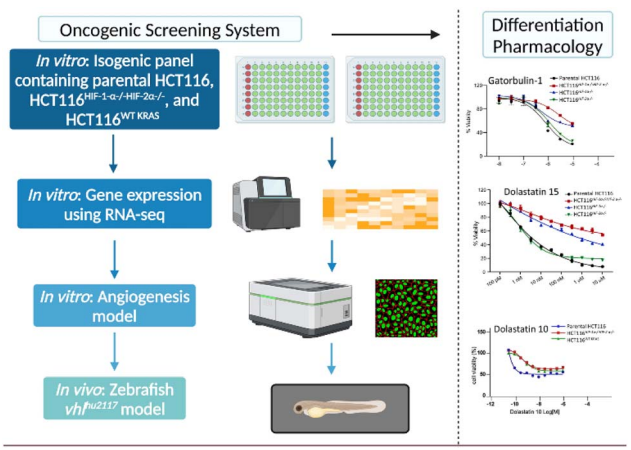

Fig. 11 A multidimensional screening platform designed to identify preferential activity against cells with oncogenic KRAS mutations and downstream HIF hyperactivation in cellular and *in vivo* models.

The specific *in vitro* and *in vivo* effects on HIF signaling provided supportive rationale that these agents are expected to possess activity against solid tumors.[136,137] As described above, dolastatin 10-based ADCs were originally approved for lymphomas but later also for bladder cancer (enfortumab vedotin).[50] Tisotumab vedotin was designed to target tissue factor (TF) which is highly expressed in many solid tumors (ovarian, prostate, bladder, lung) for cervical and ovarian cancers.[58] Ladiratuzumab vedotin was designed for metastatic triple negative/HR+/HER2-breast cancers are in different phases of clinical trials, while dolastatin 10-based ADCs undergo trials for ovarian cancer and other solid tumors (**3a–3e**, Table 1).[74]

3. Inhibitors of cotranslational translocation: Sec61 inhibitors

3.1. Mechanism of action

Cancer cells are usually characterized by overexpression and/or mutation of certain membrane proteins that function as pro-growth signaling receptors, depending on the tissue and cell type, and increased levels of secretion of ligands that act on these receptors.[138,139] Both types of proteins, including receptor tyrosine kinases (RTKs) and growth factors, rely on a functional secretory pathway for proper localization on the cell membrane and extracellular milieu, respectively.[140,141] Synthesis of proteins destined for secretion starts at cytosolic ribosomes and the firstly synthesized *N*-hydrophobic sequence (signal peptide) is recognized by the signal recognition particle (SRP) for subsequent docking at the SRP receptor in the endoplasmic reticulum (ER), where protein synthesis continues (Fig. 12).[142] Cotranslational translocation is the first step in the secretory pathway and is initiated by protein insertion into the lumen of the ER.[143] Insertion of the signal peptide is controlled by Sec61, the central protein translocation channel in the ER (Fig. 12).[144] Targeting Sec61 may ultimately prevent ER translocation of all or a subset of proteins, depending on the specific compound and cellular context, which produces a potent antiproliferative effect.[145] Two anticancer natural product classes from marine cyanobacteria, apratoxins[146,147] and coibamides,[148,149] have been demonstrated to act *via* this mechanism, by targeting Sec61.[150–161] The different binding sites are hypothesized based on differential resistance to Sec61 mutants cells to apratoxin (**45a**) and coibamide A (**52**).[145] (Fig. 13) Recently, high-resolution cryo-EM structures of seven inhibitors bound to chimeric human-yeast Sec61, including apratoxin F (**45d**), were characterized to bind to the lateral gate.[145] These inhibitors have shown to induce different pharmacological fingerprints in the NCI-60 cell line screens.[149,155,159,162,163]

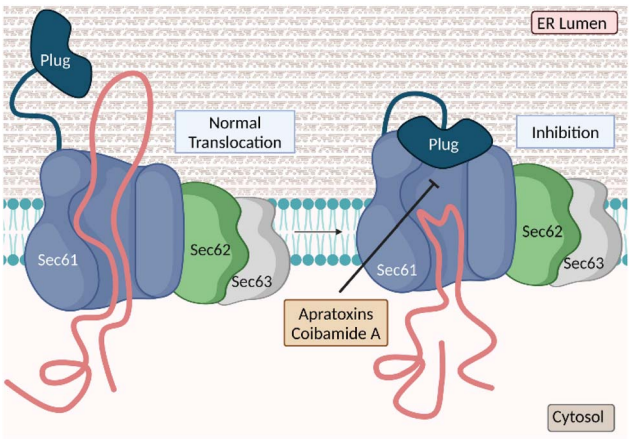

Fig. 12 Cotranslational translocation inhibition into the endoplasmic reticulum using Sec61 inhibitors.

3.2. Apratoxins

Following the discovery of natural apratoxin A (**45a**) the total synthesis was completed before the isolation of subsequent apratoxins, including apratoxins B and C Moore and co-workers,[150] and subsequently apratoxins D–G[151–153] by Gerwick and Luesch groups from *Moorena bouillonii* (recently reclassified as such).[146,154,164] The total synthesis of its oxazoline analogues have been described.[159,160,165,166] So far nine natural analogues have been discovered, with various SAR campaigns conducted to increase potency (Fig. 13). In 2015, Coltart reviewed the isolation, structure determination, and asymmetric total synthesis of natural apratoxins.[167] The real interest in this compound class emerged after the mechanism of action was revealed, demonstrating apratoxin A an inhibitor of cotranslational translocation, a novel strategy to inhibit cancer cell growth at low nanomolar concentrations.[156] The translocon Sec61 was shown to be the direct protein target of apratoxins, exemplified by using apratoxins A (**45a**) and F (**45d**) binding near the luminal plug domain (Fig. 12).[145,157] The cryo-EM structure with F (**45d**) and other (non-cyanobacterial) Sec61 inhibitors suggested a common binding pocket for those Sec61 inhibitors (Fig. 14).[145]

In vivo studies with apratoxin S4 (**45e**) showed potent activity in a HCT116 colorectal cancer xenograft model.[159] Daily dosing with 0.25 mg kg^{-1} produced a pronounced antitumor effect in mice with certain RTKs as pharmacodynamic markers shown to be selectively downregulated in the tumors.[159] Pharmacokinetic studies for apratoxins A and S10 both showed enrichment in the pancreas and a favorable PK profile.[147,168] Apratoxin S10 (**45g**), like apratoxin S4, lacked irreversible toxicity and at low doses apratoxin S10 showed efficacy in an orthotopic patient-derived xenograft (PDX) model for pancreatic cancer, which is the gold standard in the field.[168] At a dosing schedule of 0.25 mg kg^{-1} every other day, apratoxin S10 inhibited the proliferation of pancreatic cancer cells *in vivo*, without inducing cytotoxicity, thus separating antiproliferative from cytotoxic activity.[168] This effect may in part be attributed to the inhibition of growth factor and cytokine secretion from tumor-associated stromal cells that drives pancreatic cancer cell growth, suggesting that apratoxin S10 has an additional indirect effect on pancreatic cancer cells and therefore address a resistance mechanism.[168,169] This finding on other cell types, coupled with the novel mechanism of action, opened up avenues for application beyond cancer.[168,169] Apratoxin S10 was shown to inhibit the secretion of proangiogenic factors, VEGF-A and IL-6, and

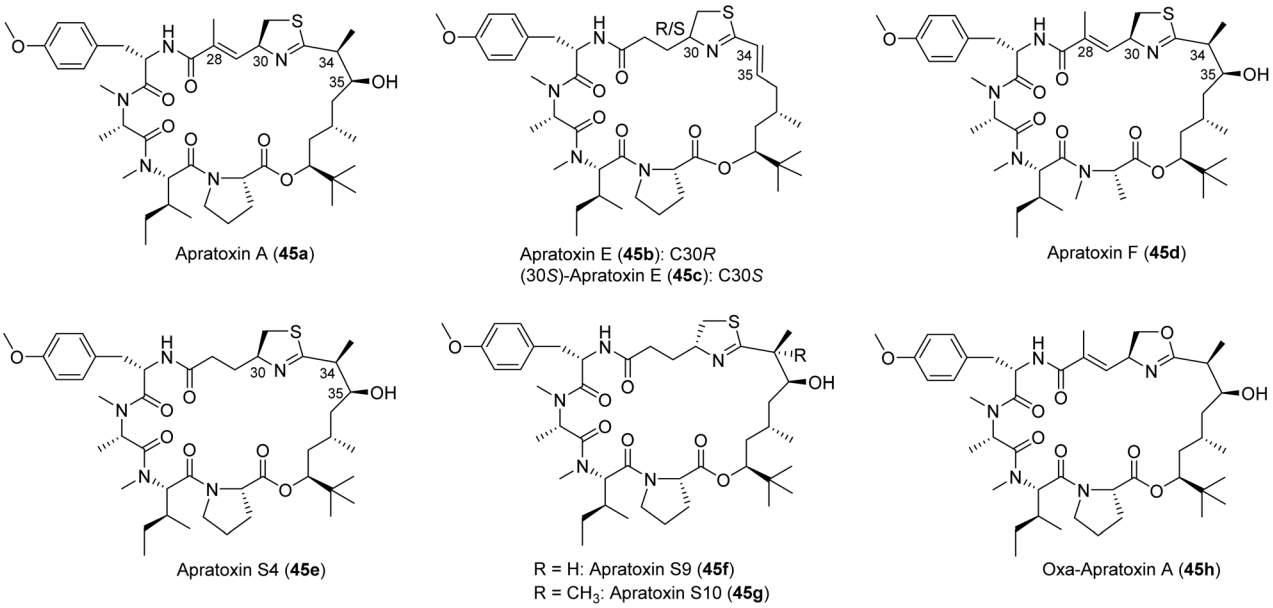

Fig. 13 Structures of selected natural apratoxins A (**45a**), E (**45b**), and F (**45d**), and other synthetic analogues (**45C**, **45e**–**45h**).

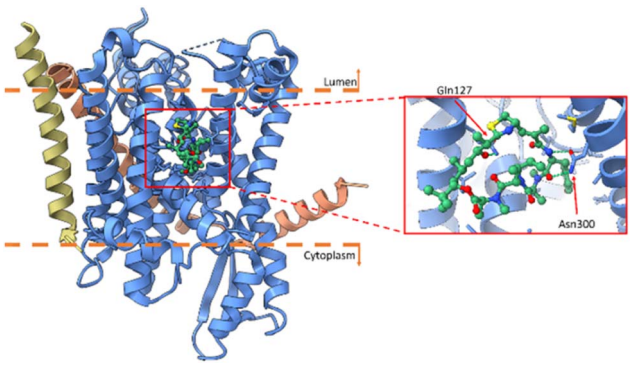

Fig. 14 Cryo-EM structure of apratoxin F (**45d**) with Sec61 in blue (alpha), salmon (gamma) and gold (beta subunit) and apratoxin F in green (PDBID: 8DNZ).

consequently evaluated for activity against cancer cells derived from highly vascularized tumors (renal, colon, neuroendocrine), where the compound showed 2000- to 5000-fold greater activity than FDA approved RTK inhibitors.[169] The dual activity as inherent anticancer and antiangiogenic is particularly intriguing, as the compound may also address the resistance to antiangiogenic therapy through the inhibition of multiple proangiogenic pathways and inhibiting cancer cell growth simultaneously. The antiangiogenic activity *in vitro* has been determined for apratoxins A, S4 and S10 using human umbilical vein endothelial cells (HUVECs).[155,163,169]

To extend the scope of cancers that may be targeted by this compound class, apratoxin S4 (**45e**) was profiled against panels of cancer cells characterized by differential sensitivity to RTK inhibitors due to receptor mutations, oncogenic KRAS mutations, or activation of compensatory pathways.[163] Apratoxin S4 (**45e**) was active at low-nanomolar to sub-nanomolar concentrations against panels of lung, head and neck, bladder, and pancreatic cancer cells, concomitant with downregulation of EGFR and other RTKs.[163] Interestingly, the compound shows a differential substrate selectivity in cellular settings that was not anticipated based on biochemical studies.[157] The selectivity was most pronounced in breast cancer cells, where apratoxin S4 preferentially downregulated HER3 over HER2. The activity of apratoxin S4 was also greater against estrogen receptor positive (ER+) and triple negative breast cancer (TNBC) cells than HER2+ breast cancer cells. The substrate selectivity appears to depend on the cellular context, since apratoxin A was shown previously to strongly downregulate HER2 in U2OS osteosarcoma cells.[163] This apparent coupling or interplay of substrate selectivity and biological context is highly intriguing, and the molecular basis remains to be determined. Importantly, in contrast to known EGFR inhibitors, apratoxin S4 (**45e**) showed antiproliferative activity in mutant KRAS background, extending the application to addressing resistance to these selective targeted therapies.[163]

Apratoxins also differentially modulate cancer-related membrane proteins other than RTKs, including CUB-domain containing protein (CDCP1), a transmembrane protein linked to metastasis and invasion, forming a complex with EGFR to decrease cell adhesion.[163] CDCP1 is also activated by KRAS but strongly downregulated by apratoxin S4 in a breast cancer cell type dependent manner. The fate of CDCP1 was monitored through pulldown experiments followed by proteomics, revealing the expected block in glycosylation by preventing cotranslational translocation and concomitant increase of the chaperone HSP70, presumably recruited due to misfolding of nonglycosylated CDCP1.[163] Additionally, CDCP1 association with HUWE1 was increased in response to apratoxin S4 treatment. HUWE1 functions as an E3 ubiquitin ligase known to target many proteins, including BCL2-related MCL1, histones and DNA polymerases.[170] Apratoxin S4 treatment presumably leads to HUWE1-mediated proteasomal degradation.[163]

SAR studies by alanine scanning pinpointed key amino acid residues, including the Tyr moiety and that the Pro can be replaced by *N*-Me-Ala, and that configurational changes of the Pro (L to D) are detrimental to the activity.[159] Total synthesis led to the reassignment of the thiazoline configuration in apratoxin E (**45b** instead of **45c**), which is different from all other natural apratoxins (Fig. 13). The significantly reduced activity of apratoxin E and dehydrated apratoxin A, indicated the importance of the hydroxy group in the Dtena unit. Importantly, re-engineering of the scaffold to remove the Michael acceptor in the modified cysteine (moCys) unit, further improved potency (apratoxin S4, **45e**), indicating that the conjugated system was not involved in the mechanism of action.[159] Furthermore, the unsaturated amide in apratoxin A was shown by mass spectrometry to be able to undergo conjugate (Michael) addition with thiol nucleophiles, presenting one potential liability and reason for the irreversible toxicity observed for apratoxin A.[159] Collectively, these studies led to the prioritization of apratoxin A/E hybrids S4 (**45e**) and S9 (**45f**), with S9 being slightly more active.[159] To avoid deactivation by dehydration and to improve stability, a *gem*-dimethyl was installed at C34 leading to the apratoxin S8 and S10 (**45g**, Fig. 13).[160,169] All of these synthetic apratoxins demonstrated excellent *in vivo* activity and toxicity was managed through a carefully designed dosing schedule. However, the cytotoxicity of the oxazole analogue (**45h**) is much weaker than that of thiazoline analog.[76]

Among the synthetic analogues, apratoxin S4 and S10 are the promising candidates that have undergone most extensive biological evaluation.[159,160,171] Their synthetic strategy is depicted in Fig. 15.

The moCys precursor units **48a**, **48b** were synthesized from cysteine through the amino aldehyde, Wittig reaction and reduction by $NaBH_4$. However, the product was obtained in only 35% yield.[159] An alternative method to construct moCys fragment was established, starting from glutamic acid derivative, and applied to the total synthesis of apratoxin E and its epimer.[166] This method is straightforward and more efficient.

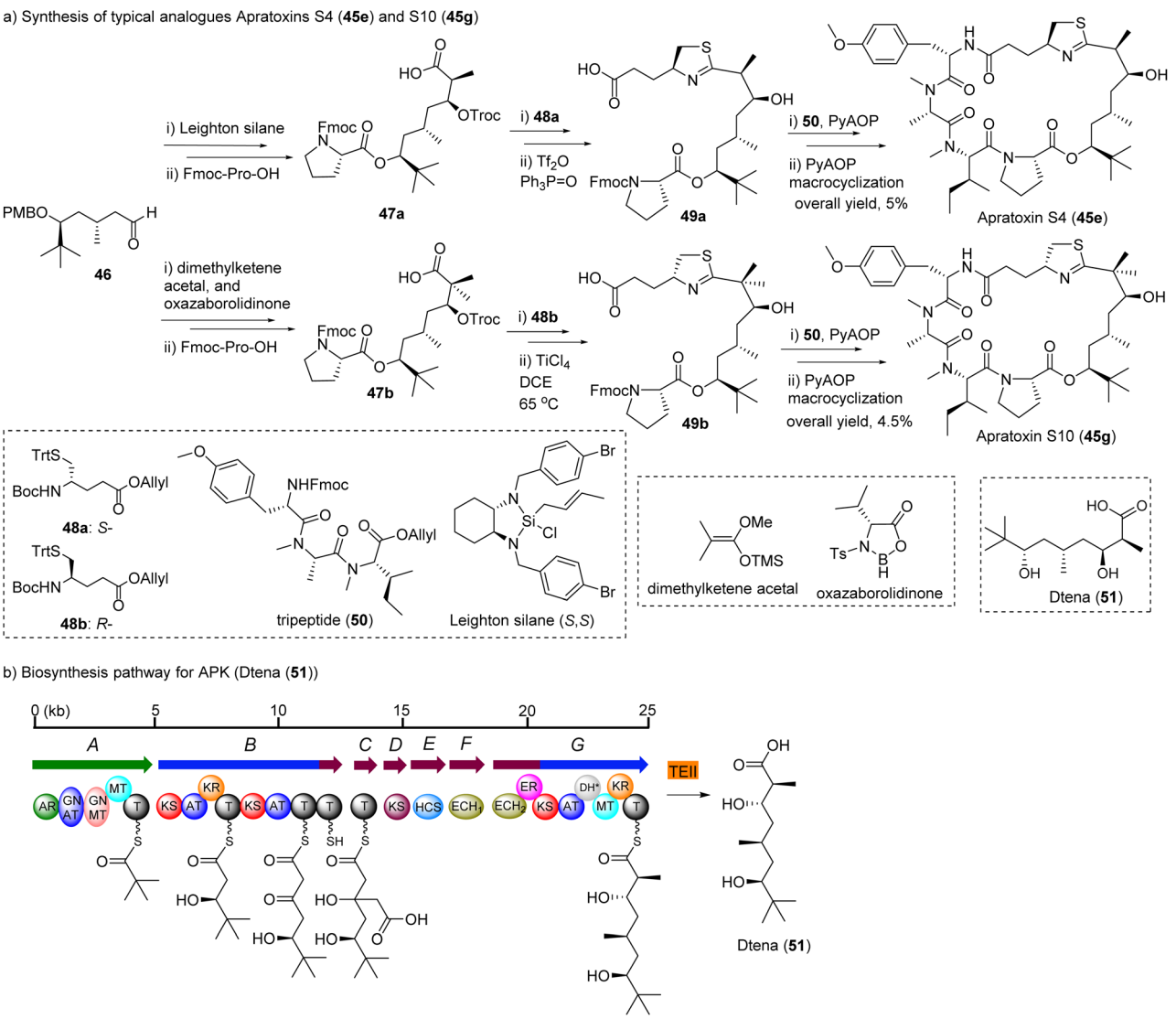

Fig. 15 Abbreviated synthesis (a) of apratoxin S4 (**45e**), S10 (**45g**), and (b) biosynthesis pathway for apratoxin polyketide unit Dtena (**51**).

Aldehyde **46** was a common intermediate for all analogues. It was synthesized from pivalaldehyde by D-proline catalyzed aldol reaction in ten steps.[160] The chiral center of acid **47a** was constructed by crotylation of aldehyde **46** using commercially available material by Leighton's silica (*S*,*S*)-18.[172] The product was easily obtained in high yields with excellent enantiomeric selectivity by simple mixing of both starting materials and keeping the mixture at −20 °C for some time.[160] However, the *gem*-dimethyl acids **47b** were synthesized using Kiyooka reaction through a boron auxiliary, oxazaborolidine.[160,173] The formation of the thiazoline ring in **49a**, and **49b** from its open-chain precursor was a key step and for the mono-methyl (S4) or non-methyl analogues (S7).[160] Kelly method ($Ph_3P(O)/Tf_2O$) provided products in 90% yield, but for *gem*-dimethyl analogues (S8 and S10) were only provided in low yield (5–10%).[160] However, modified Kelly method ($TiCl_4$/1,2-dichloroethane/heating) resulted in satisfactory yields (50–60%). PyAOP was selected as the coupling reagent of acid **49** with tripeptide **50**. PyAOP also was used for final step macrocyclization, and good yields were obtained for all final targets. Other analogues were synthesized by parallel strategy of the total synthesis of apratoxin S4/S10. Each analogue can be synthesized from two fragments, tripeptide **50** and thiazole-containing carboxylic acid **49**. An additional series of apratoxins by replacing the moCys unit with amino acids, has also been described without in-depth biological studies.[174] Towards establishing a convenient hybrid chemistry–synthetic biology to access apratoxins, the key moiety of the apratoxin skeleton, Dtena (**51**, Fig. 15), was heterologously expressed in high yield (9.7 mg L^{-1}).[175]

3.3. Coibamides

In 2008, Gerwick and McPhail isolated coibamide A (**52**, revised structure) a potent cytotoxin with antiproliferative activity against the NCI-60 cancer cell line panel, from the filamentous cyanobacterium *Leptolyngbya* sp.[148] Coibamide A showed cell loss within S phase and increase in the G_1 phase with little change in G_2/M phase of the cell cycle.[148] In 2013, the Ishmael group described coibamide A to possibly induce mTOR-independent autophagy in both mouse embryonic fibroblasts (MEFs) and human glioblastoma cell types, with morphological and biological characteristics of cell death in various cell lines.[176] Coibamide A was more recently found to have a similar mechanism of action as apratoxins and the same molecular target, Sec61. Like apratoxins, coibamide A inhibits VEGFA and decreases expression of VEGFR2, as indicative of Sec61

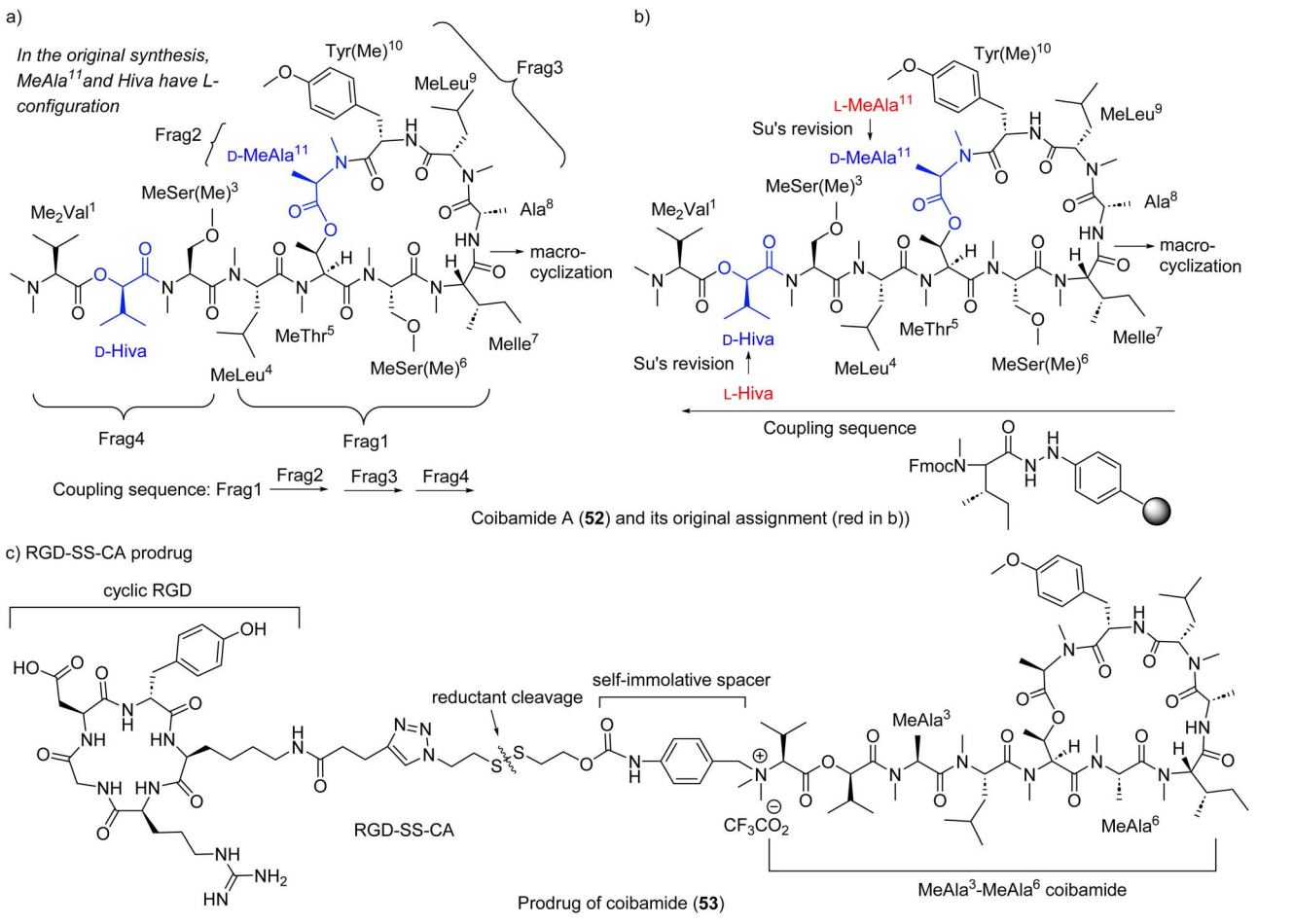

Fig. 16 Synthetic strategies (a and b) for proposed coibamide A (**52**) and (c) for its RGD conjugate, and Su's structure revision as shown in (b): red represents the original assignment and blue the reassignment.

inhibitors.[177] However, as discussed above, comparative analysis of resistance mutations indicated differences in binding and pharmacological consequences, including cell type sensitivities.[176,177] Coibamide A, originally, demonstrated potent cytotoxicity against MDA-MB-231 (GI_{50} 2.8 nM), SNB-75 (GI_{50} 7.6 nM), HL-60(TB) (GI_{50} 7.4 nM), and LOX IMVI (GI_{50} 7.4 nM) with good selectivity for breast, CNS, colon, and ovarian cancer cells.[148] In a more recent study, these lariat depsipeptides demonstrated excellent inhibition of cell growth of six breast cancer cell lines in the nanomolar EC_{50} range, with MDA-MB-231 being the most sensitive (EC_{50} 7.42 nM).[158] In an effort to further define the sensitivity of coibamide A to breast cancer types, including triple negative breast cancer, HER and ErbB proteins indicated the depsipeptide suppressed all four HER protein expression and EGFR, exhibiting cell death as a function of exposure and concentration.[148] However, endogenous HER2 was partially resistant to coibamide A (similarly shown for apratoxins)[163] within the same concentrations of all HER proteins, indicating broad acting Sec61 inhibitors are not equally effective across all HER proteins,[148,178] consistent with data for apratoxins.[163]

Yao group completed the total synthesis of the proposed structure in 2014.[179] Using a liquid-phase and [(4 + 1) + 3 + 3] strategy, they constructed each fragment (Fig. 16a), fusing fragments 1, 2 and 3 sequentially, then preforming macrocyclization between *N*-Me-lle and Ala to obtain the macrocyclic core. Appending fragment 4 to the cyclic core provided the final target molecule. Unfortunately, the NMR spectra of synthetic coibamide were inconsistent with those of natural coibamide A, prompting a structural reassignment. Adopting Fmoc-based SPPS (Fig. 16b), the Su group also synthesized the originally proposed structure of coibamide A, substantiating Yao's result of the mismatch.[180] Synthesis of two diastereomers with highest likelihood of representing natural coibamide A led to the unambiguous structural revision at MeAla (to D-MeAla) and Hiva (to D-Hiva) (Fig. 16b).[180] In Su's SPPS method, the same site between *N*-Me-lle and Ala was chosen for macrocyclization. Starting from *N*-Me-lle on aryl hydrazide resin, they assembled amino acids *via* the sequence as shown in Fig. 16b, starting from *N*-Me-lle to Hiva, then MeAla to Ala to obtain linear precursors. Macrocyclization between *N*-Me-lle and Ala provided final targets.

Su's group accessed a series of coibamide A analogues, as well as the MeAla3-MeAla6 coibamide, replacing Ser hydroxy and amino acids, respectively (Fig. 16c). The MeAla3-MeAla6 coibamide showed almost equal cytotoxicity against breast cancer cell line MDA-MB-231 compared with that of coibamide A.[161] Furthermore, the MeAla3-MeAla6 coibamide exhibited better efficacy against tumor growth than coibamide A *in vivo*.[161] Based on this slightly simplified analogue, authors designed and synthesized a stimuli-responsive peptide-drug conjugate (PDC) RGD-SS-CA as a prodrug (RGD: arginyl-glycyl-aspartic acid), which showed desirable drug release under stimuli and greater or similar cytotoxicity than coibamide A both *in vitro* and *in vivo*.[181] In 2022, Oishi group generated series of analogues of coibamide A at $MeThr^5$-$MeAla^{11}$ site and $Tyr(Me)^{10}$ site using a similar Fmoc-SPPS method and synthetic sequence as Su's method but the amide between $Tyr(Me)^{10}$ and $MeLeu^9$ was selected as the site for macrocyclization.[182] A biphenyl (Bph) mimetic substituting Tyr(Me) was the most potent for the growth inhibition of A549 cells (IC_{50} 0.06 μM).[182]

4. SERCA inhibitors

4.1. Mechanism of action

Calcium regulation intersects various cellular processes, including cancer metastasis and proliferation, and directly induces and regulates cell death.[183] Thus the modulation of organelle Ca^{2+} homeostasis is a key target for treatment against cancer progression.[183] The sarcoplasmic reticulum calcium ATPase (SERCA) is an endoplasmic reticulum 10 transmembrane calcium transporter protein found in all eukaryotic cells.[184] The transporter family consists of SERCA1-3, with SERCA1α being the best characterized, and transfers calcium from the cytosol of the cell to the lumen of the ER.[185] SERCA maintains the majority of calcium homeostasis, therefore potential therapeutic target development is advantageous for diseases with calcium dysregulation.[185] The calcium cascade within the cell is initiated with the entry of calcium into the cell *via* a voltage-gated calcium channel or other calcium transporter, releasing calcium into the cytoplasm. SERCA then uptakes the calcium into the ER in an ATP-dependent manner to regulate the concentration of calcium in the membrane.[184] Calcium concentration is regulated *via* small endogenous molecules and leak channels.[186] When SERCA is inhibited, the concentration of calcium in the ER drops below 500 μM, initiating mitochondrial unfolded protein response (UPR) with the uptake of calcium into the mitochondria. Thus prolonged Ca^{2+} exposure leading to ER stress and subsequent mitochondrial calcium uptake leads to activation of pro-apoptotic signaling as shown (Fig. 17).[187] The two marine natural products, iezoside (**54a**) (IC_{50} 6.7 nM in HeLa; K_i 7.1 nM) and biselyngbyaside (**62a**) (IC_{50} 0.1 μg mL^{-1} in HeLa; K_i 19 nM), were isolated and characterized as potent SERCA1α inhibitors.[188–190]

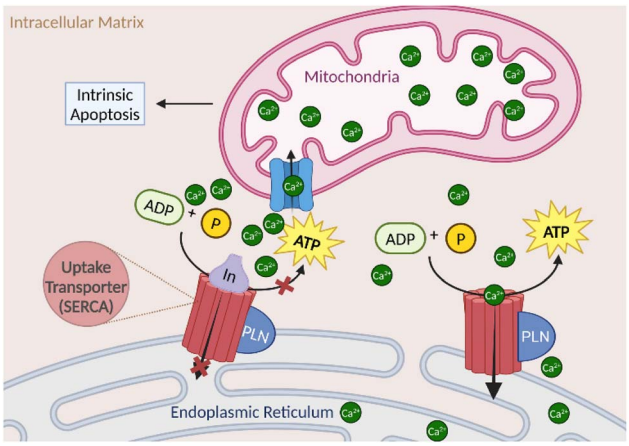

Fig. 17 Mechanism of action of sarcoplasmic reticulum calcium ATPase (SERCA) leading proapoptotic signaling.

4.2. Iezosides

Iezoside (**54a**, Fig. 18) was recently isolated and characterized as a rare peptide-polyketide hybrid glycoside from Ie Island, Okinawa, Japan and identified from the marine cyanobacterium *Leptochromothrix valpauliae* by the Suenaga group.[188] Iezoside features a sugar moiety and multiple double bonds and it also showed strong inhibitory activity against SERCA with comparable Japanese Foundation for Cancer Research 39 (JFCR39) cell lines profiles to the most well-known SERCA inhibitor thapsigargin from *Thapsia* plants and a calcium transporter ionophore A23187 also known as calcimycin.[191–193] Validation of the target was conducted using the morphological changes that thapsigargin and cyclopiazonic (CA) induced upon HeLa cells, as well as the effect of the glycoside on the concentration of cytosolic Ca^{2+} in Fura-2-treated HeLa cells.[188] SERCA1α was confirmed as the target, with K_i of 7.1 nM, making it the most potent marine natural product SERCA1α inhibitor to date.[188] Iezoside (**54a**) exhibited potent antiproliferative activity against HeLa cells in cytotoxicity studies (IC_{50} 6.8 ± 0.3 nM *vs.* 650 ± 82 nM) with an increase in G_1 phase and a decrease in S phase cells at 10 nM, reflecting a cell cycle delay rather than cell cycle arrest due to moderate cell cycle distribution variation.[188] More recently, iezoside (**54a**) and the demethylated analogue iezoside B (**54b**), were isolated by the Luesch group from Loggerhead Key in Florida from a marine cyanobacteria mixture composed of mainly *Dichothrix* sp. and *Lyngbya* sp.[194] Additional validation of the bioactivity of iezoside and biological characterization of iezoside B were conducted showing cytotoxicity against non-small cell lung cancer cell line A549 (IC_{50} 1.5 and 3.0 μM) and cervical cancer cell line HeLa (IC_{50} 1.0 and 2.4 μM), providing preliminary SAR.[155]

The synthetic strategy of iezoside (**54a**) is depicted in Fig. 18, in which it was detached into two primary building blocks **55** and **56**. Amine **55** is a thiazole-containing dipeptide. The alcohol **57** was glycosylated to afford **56** successfully in the presence of carbonyl group. From known aldehyde **56**, *via* a series of sequential reactions including Wittig reaction, aldol reaction, Grignard reactions, oxidative rearrangement, and Horner–Wadsworth–Emmons (HWE) reaction, compound **57** was synthesized.[188]

4.3. Biselyngbyasides

Biselyngbyaside (**62a**, BLS), an 18-membered ring macrolide, was isolated from *Lyngbya* sp. in 2009 by the Suenaga group.[190] Similar to iezosides, structural features include sugar moieties and multiple double bonds. The macrolide exhibited cytotoxicity against HeLa S_3 (IC_{50} 100 ng mL^{-1}) and an average GI_{50} of 600 nM against the JFCR39 human cancer cell line panel, with specific selectivity to glioblastoma SNB-78 cell line (GI_{50} 36 nM) and the non-small cell lung cancer cell line NCI H522 (GI_{50} 67 nM).[189,190] The JFCR39 profile was similar to that of known SERCA inhibitors, with enzyme assays against SERCA1 and 2 confirming biselyngbyaside strongly inhibited SERCA1α (K_i ∼ 10 nM).[189] Later studies described the isolation and biological activity of biselyngbyaside B (**62b**), which is less potent than BLS.[195] Additional natural analogues (C–F) were isolated from the *Lyngbya* sp. and tested for potency against HeLa and HL60 cell lines.[195,196]

The Suenaga group reported the first total synthesis of BLS (**62a**, Fig. 19) in 2017 based on their successful total synthesis of biselyngbyolide (**63**) in 2016.[197,198] They found that direct glycosylation of biselyngbyolide (**63**) at a late-stage failed to produce BLS (**62**) and proposed to install the sugar moiety before the carbonyl group was formed (Fig. 19). For the macrocycle formation, building blocks **64** and **65** were conjoined *via* Mitsunobu reaction, and then a Stille coupling between stannane of **65** and vinyl iodide of **64** closed the linear precursor. The glycosylation of free *sec*-OH of **66** was completed by trichloroacetimidate-activated glycoside donor, differing from the installation of a sugar moiety of iezoside. Further two-step oxidation of primary alcohol of **66** provided **64**. The coupling reaction of **67** with **68**, and then stereoselective reduction with $BH_3 \cdot SMe$ in the presence of chiral boron auxiliary (*R*)-Me-CBS (Corey-Bakshi-Shibata), followed by oxidation and Takai olefination to provide **66**. Wittig reaction and Aldol reaction were involved when used building blocks **73**, **72**, and **71** to construct **67**. For the construction of building block **65**, the Ando's type phosphonate **70** with nitrile group was selected for HWE olefination, which afforded good yield and selectivity for *E*-configuration.

While SERCA inhibitors may have gained momentum as potential agents against cancer, the major practical concern has

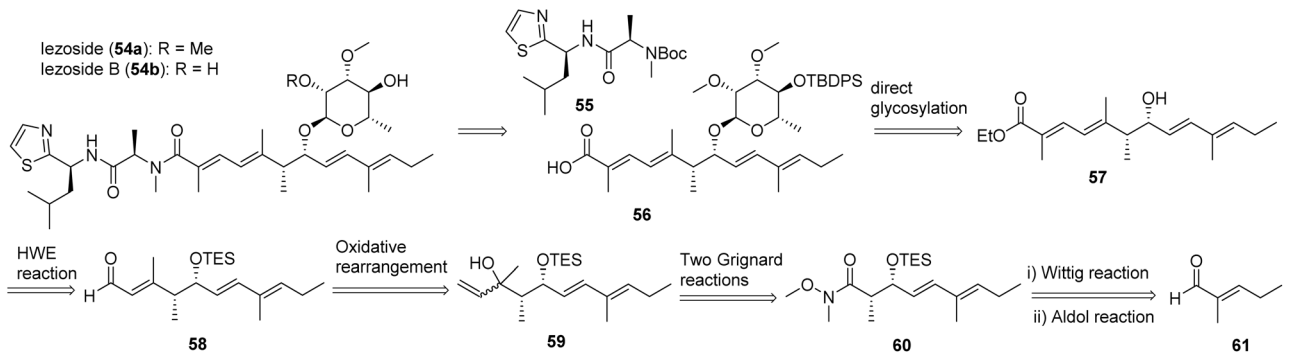

Fig. 18 The structures of iezoside (**54a**) and iezoside B (**54b**), and synthetic strategy for iezoside.

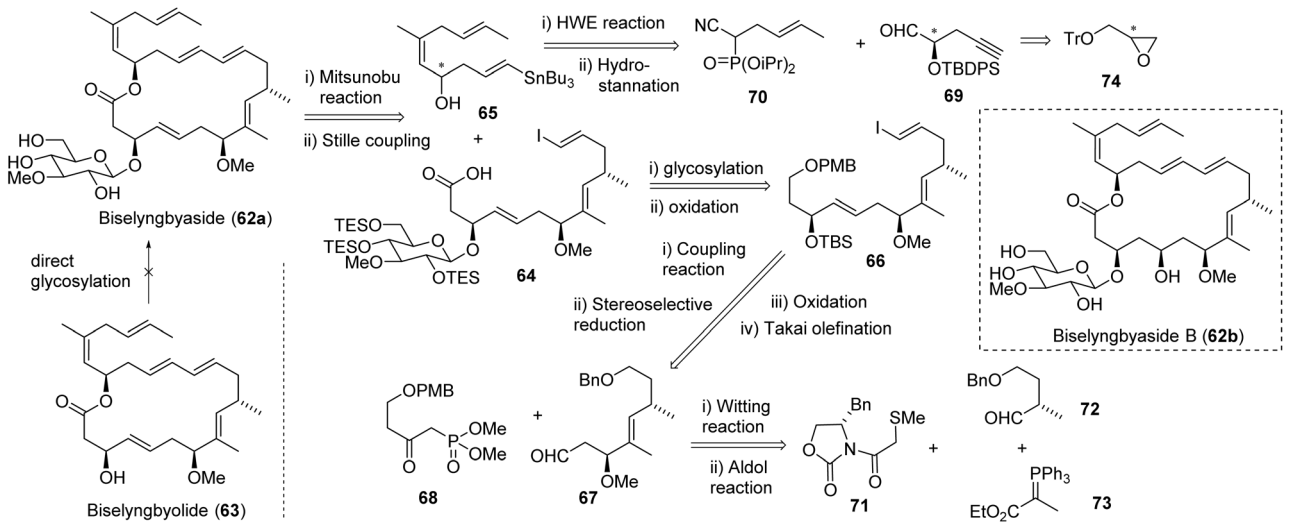

Fig. 19 The synthetic strategy for biselyngbyaside (**62a**).

been the difficulties associated with the synthesis of their complex structures for large scale synthesis. The synthesis of BLS still remains a laborious multistep methodology, while the lack of diversity in the structure scaffold with target specific inhibitory activity remains a challenge. The recent discovery of the potent cyanobacterial iezosides provides more feasibility in addressing both of these challenges.

5. Mitochondrial cytotoxins and extrinsic apoptosis inducers

5.1. Mechanism of action

As the mitochondria are responsible for several critical cell functions, such as apoptosis regulation and oxidative phosphorylation, cancer pathology involving the organelle is a prime target for therapeutics.[199,200] Mitochondrial cytotoxins target functional pathways resulting in the induction of tumor cell apoptosis (Fig. 20). Apoptosis is guided by the intrinsic and extrinsic pathways, both involving the activation of caspases.[201] The intrinsic pathway is mediated by intracellular signals from an array of positive or negative non-receptor-mediated catalysts, producing a cascade effect to lose mitochondrial membrane potential and initiate the release of pro-apoptotic enzymes to execute the caspase cascade.[202,203] Oxidative stress through various enhancers, like lagunamides (**75a–e**), increases signaling to induce an accelerated effect on caspase cascade induction.[204] In contrast, the extrinsic pathway often involves pro-death signaling from outside of the cell *via* CD8-positive cytotoxic T or Natural Killer lymphocytes to death receptors on the cell membrane, including TNF-related apoptosis-inducing ligand (TRAIL), tumor necrosis factor (TNF), and Fas receptors.[205] Caspase-8 is a gateway inducer of both intrinsic and extrinsic apoptotic pathways as a mediator of cell death and inflammation, which is targeted by the somocystinamide compound class (**106b**).[206,207] Caspase-mediated mitochondrial cytotoxins can disrupt the membrane potential and cause overexpression of radical oxygen species, as well as upregulate/downregulate pro/anti-apoptotic signaling.[208] This includes respiratory chain inhibitors targeting oxidative phosphorylation *via* interrupting glycolysis, terminating the austerity of tumor cell lines, such as caldorazole (**90**).[209–211] Targeting apoptosis is one of the most successful non-surgical remedies and recognized as an effective universal target for treatment.[201]

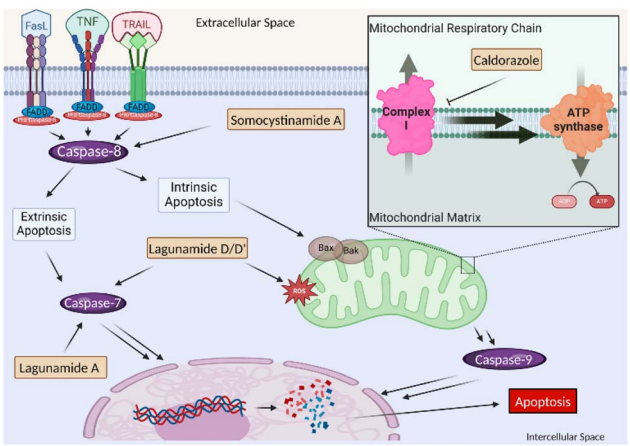

Fig. 20 Mitochondrial cytotoxins within the cell and the downstream affects, including the caspases of the intrinsic apoptotic pathways and various signaling proteins to induce arrest or oxidative stress.

5.2. Lagunamides and odoamide

The lagunamides are cyclic dipeptides that were isolated from the cyanobacterium *Lyngbya majuscula* by the Tan and Luesch groups.[212–214] The compounds are structurally related to aurilides and kulokekahilide-2.[212,215–217] Lagunamide A (**75a**) induced morphological changes to A549 cells after a 24 h treatment, including shrinkage, pseudopodia retraction, karyopyknosis, and chromatin condensation, as well as nuclear cracking and DNA released into the cytoplasm *via* transmission

electron microscopy (TEM).[208] Further biological characterization of lagunamide A (**75a**) indicated the overproduction of ROS and mitochondrial membrane potential disruption, as well as upregulation of pro-apoptotic Bcl-2 proteins and downregulation of the anti-apoptotic Bcl-2 proteins, specifically Mcl-1.[208] Lagunamide C (**75c**) was isolated in 2011 by the Tan group and indicated nanomolar cytotoxic potency against murine leukemia (P388; IC_{50} 2.24 nM), lung carcinoma (A549; IC_{50} 2.4 nM), prostate cancer (PC3; IC_{50} 2.6 nM), ileocecal colorectal adenocarcinoma (HCT8; IC_{50} 2.1 nM), and ovarian (SK-OV; IC_{50} 4.5 nM) cancer cell lines.[214] Recently, the structural revision of lagunamide C (**75c**) by the Kigoshi group revealed the lagunamide C is the identical to odoamide.[218] Odoamide (**75c**) is structurally similar to lagunamide A (**75a**), differing only by a single methylene, and was isolated from the Okinawan cyanobacterium *Okeania* sp. by the Teruya group in 2016.[219] Biological characterization of lagunamide D (**75d**), and D′ (**75e**, Fig. 21) indicated activation of caspases-3/7 within 6 h of treatment as well as mitochondrial rearrangement without fragmentation, exhibiting effects of both apoptotic pathways.[204] The exact mechanism in which lagunamide D affects the mitochondria is yet to be elucidated, despite their ability to induce apoptosis.[208,213,220] However, as a member of the aurilide class, the likely target could be prohibitin-1 (PHB1).[221] PHB1 has a role in cell proliferation as a negative regulator and is localized to the inner membrane of the mitochondria.[222] This is mediated through the stimulation of optic atrophy 1 (OPA1), which leads to the induction of mitochondrial fragmentation and cell death *via* apoptosis.[221] However, a functional genomics driven approach using lagunamide D revealed that the depsipeptide might exert its affects through proteostasis modulation or having a chemical genetic interaction with the proteasome pathway.[204] This was revealed through an unbiased chemogenomic RNAi screening. A targeted approach indicated the mechanism worked through mitochondrial network rearrangement, not mitochondrial fragmentation.[204] Preliminary biological studies indicated potent cytotoxicity against HeLa S3 cells (IC_{50} 26.3 nM). The later synthesized odoamide exhibited nanomolar potency against A549 cells (IC_{50} 2.1 nM).[219,223,224]

Ye and Xu finished the first total synthesis of lagunamide A (**75a**, Fig. 21) in 2012.[225] In 2013, Wei achieved the synthesis using different strategies for the generation of the α-hydroxy acid unit and macrocyclization.[226] In 2018, Kazmaier applied Matteson homologation as the major tool to finish the total synthesis of lagunamide A (**75a**).[227] Oishi completed the total synthesis of odoamide (**75c**) in 2016 and then synthesized a series of analogues in 2018.[223,224] The emphasis of the total synthesis of lagunamide or odoamide has been the construction of α-hydroxy acid fragment and macrocyclization (Fig. 21).

Fig. 22 shows the different strategies for the synthesis of the hydroxy acid fragment. In the synthesis of the proposed lagunamide A, Ye group found the configurational assignment for C39 and C40 was problematic and used the known chiral olefin as a starting point to furnish chiral carbons C37 and C38.[225] Its aldehyde derivative, obtained by oxidative cleavage, afforded chiral carbon C39(*S*) and C40(*S*) through Brown anticrotylation in which *E*-2-butene/(−)-Ipc_2BOMe assembly was used (Fig. 22a).[225] Another two C40 epimers (C39(*R*)-C40(*S*) and C39(*S*)-C40(*R*)) were also synthesized using different assembly of butene and Ipc_2BOMe (Fig. 22a). From these three parallel building blocks, they generated the corresponding diester fragments *via* HWE reaction and esterification and completed three analogues of lagunamides. By comparison, the correct structure of natural lagunamide A was determined to be the C39(*R*)-C40(*S*) isomer; however, the original assignment was C39(*S*)-C40(*S*).

Generally, Wei applied Evans's selective aldol reaction of Evans (*R*)-oxazolidinone and (*S*)-2-methylbutanal to establish

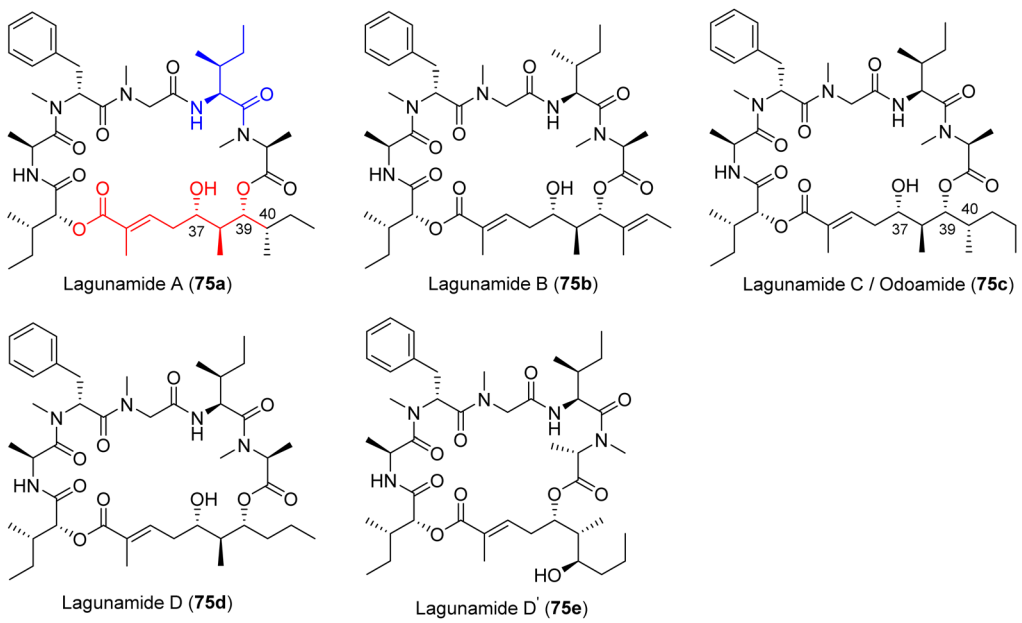

Fig. 21 Mitochondrial cytotoxins from marine cyanobacteria structures of lagunamides (**75a–e**) and odamide (**75c**).

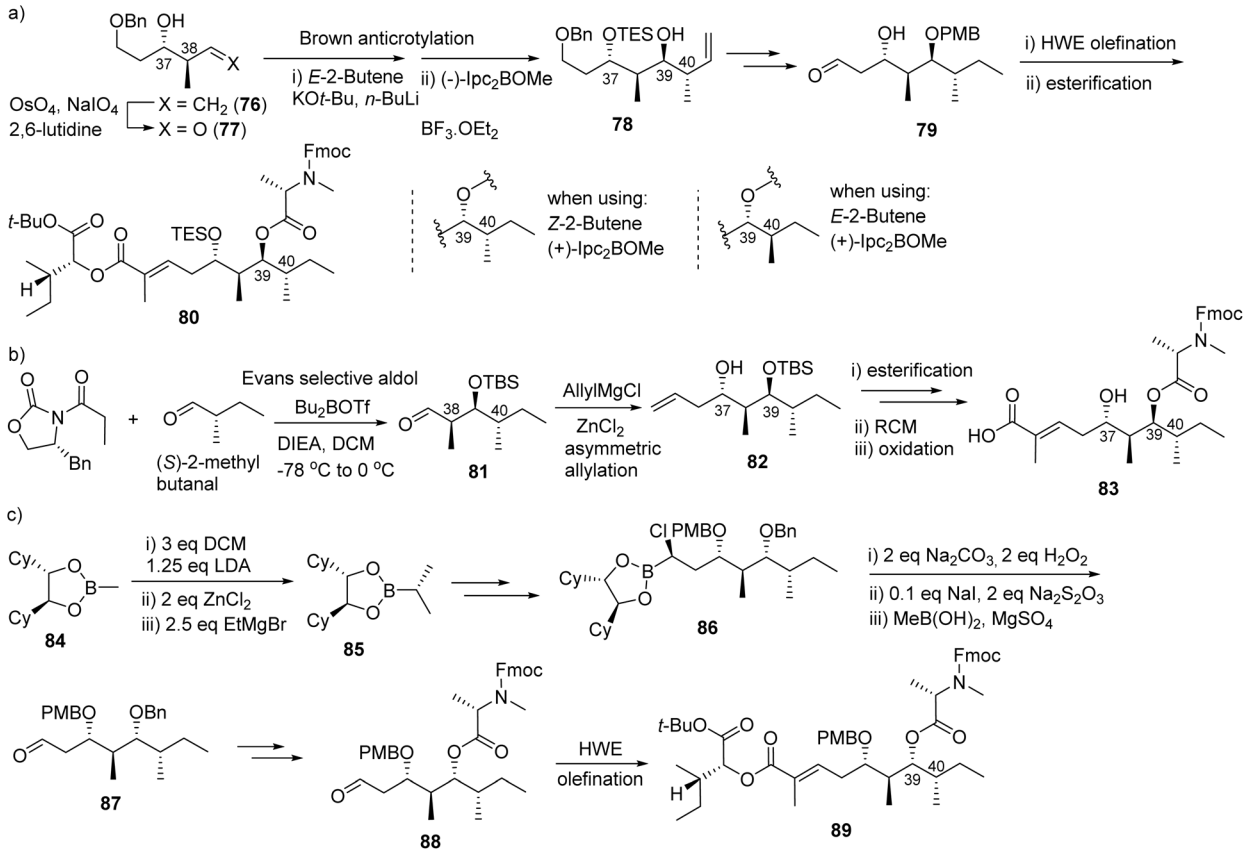

Fig. 22 Comparison of different strategies (a–c) for the synthesis of hydroxy acid fragment.

the three chiral centers, C38-40, of the hydroxy acid building block (Fig. 22b), similar to the strategy Ye used in the primary effort.[225,226] Asymmetric allylation with allylmagnesium chloride generated the chiral carbon C37, in which the diastereoselectivity was improved to 90 : 10 when $ZnCl_2$ was selected as an additive (Fig. 22b). Furthermore, Wei applied the ring closing metathesis (RCM) reaction to furnish the unsaturated acid side chain for this fragment. Creatively, Kazmaier applied Matteson homologation to establish the four chiral centers of the hydroxy acid fragment (Fig. 22c).[227] For the macrolactamization, it seems that the site between Ala and Hmpa (2-hydroxy-3-methylpentanoic acid) provided better cyclization efficiency than the site between Gly and Ile.

Oishi achieved the total synthesis of odoamide (**75c**) and some analogues by establishing the stereogenic center, C38–C39, using a method similar to that of Ye's and Wei's.[223–226] Instead of Evans selective aldol reaction, Oishi used Mukaiyama aldol reaction to generate the chiral center at C37.[223]

Oishi chose the site between Ala and Hmpa as macrocyclization site. However, serious epimerization problems at isoleucine were encountered because isoleucine was installed prior to the tetrapeptide.

5.3. Caldorazole

Caldorazole (**90**, Fig. 23) was isolated from *Caldora* sp. off the coast of Tomuruzaki in Ishigaki Island, Japan in 2022 by the Suenaga group.[228] The polyketide contains two thiazole rings, a terminal olefin and an *O*-methylenolpyruvamide moiety (**90**, Fig. 23). The compound showed potent cytotoxic activity (IC50 < 100 nM) against several solid tumor cell lines (HeLa IC_{50} 23 nM; CaSki IC_{50} 68 nM; HT1080 IC_{50} 74 nM).[228] The potential as a phosphoenolpyruvate mimic was confirmed *via* selectivity in the presence of 2-deoxy-D-glucose (2DG), which suppresses glycolysis in the mitochondrial respiratory chain complex 1.[228] Selectivity for glucose-suppressed conditions in tumor cells was confirmed with caldorazole showing no toxicity against the normal cell line WI38 in the presence of 2DG. Caldorazole did not show selectivity against HeLa S3Mer$^-$ cells, which are highly selective for DNA alkylating agents; thus the mechanism of cytotoxicity *via* DNA alkylation was not relevant to caldorazole.[228] Biakamides, a sponge isolated natural products, are a similar structure class with similar mechanism to caldorazole in inhibition of mitochondrial respiration making them both attractive agents for developing therapies that can potentially cause "nutrient starvation" in cancer cells.[229,230]

The Suenaga group and their co-workers completed the total synthesis of caldorazole (**90**) in 2023 as depicted in Fig. 23.[211] The authors' preliminary convergent synthetic strategy is to disassemble the molecule into three parts at the sites of amide and middle keto and the ketone will be formed by sulfone coupling. The synthesis of the left side building block was started with Swern oxidation of iodide alcohol **91**. The aldehyde

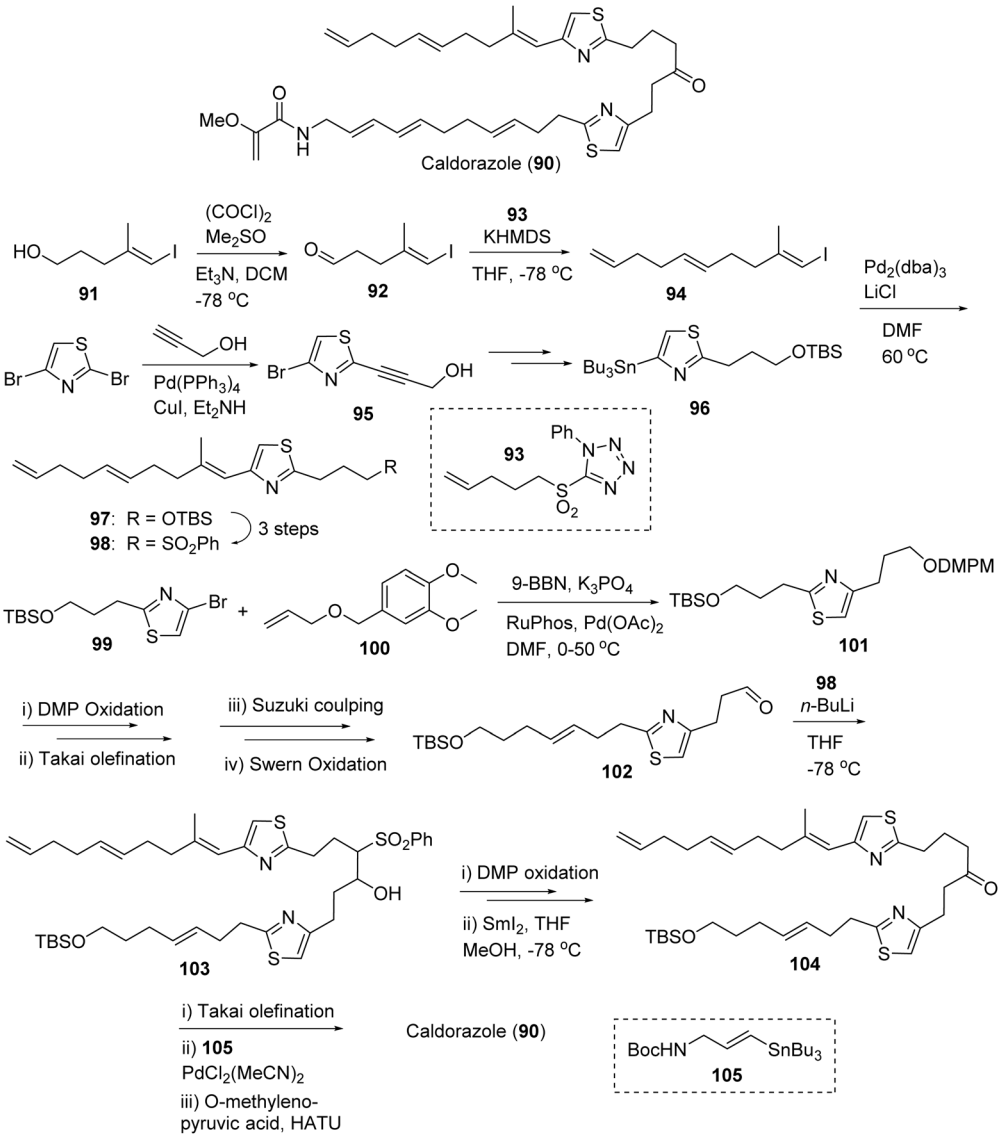

Fig. 23 Structures and total synthesis of caldorazole (**90**).

was subjected to Julia-Kocienski olefination with sulfone **93** to afford vinyl iodide **94** (*E*/*Z* 4 : 1). The selective alkynylation of 2,4-dibromothiazole with Sonogashira cross-coupling to provide alkyne **95**, which was transformed into stannane **96** *via* reduction of alkyne by $TsNHNH_2$ and stannylation by Bu_3SnCl. Stille coupling between **94** and **96** gave TBS ether **97**. Then its sulfide (by PhSSPh/*n*-Bu_3P) was oxidized to sulfone **98**. Suzuki–Miyaura cross coupling of **99** with the hydroboration product of allyl ether **100** afforded protected ether **101**. The elongation of the TBS ether side of **101** was completed by sequential deprotection, DMP oxidation, Takai olefination and Suzuki coupling with the corresponding product being converted into aldehyde **102** by Swern oxidation. It is noteworthy that a 10 : 1 *E*/*Z* olefination ratio was achieved. Sulfone coupling of **102** and **98** produced β-OH sulfone **103**, which was subjected to oxidation and desulfonylation to provide keto compound **104**. The sequential deprotection of TBS group of **104**, oxidation, Takai olefination, Suzuki coupling (with **105**) and the coupling with *O*-methylenolpyruvic acid afforded the final product caldorazole **90** in 0.47% overall yield.[211]

5.4. Somocystinamide A and laucysteinamide A

Somocystinamide A (**106b**, Fig. 24) was isolated by the Gerwick group from a cyanobacteria mixture *Lyngbya majuscula*/*Schizothrix* sp. in 2002 from Somosomo, Fiji.[231] This novel lipopeptide of mixed PKS/NRPS biosynthetic origin was mildly cytotoxic to mouse neuro-2a neuroblastoma cells (IC_{50} 1.4 μg mL^{-1}) originally,[231] then later revealed potent cytotoxicity against leukemia (Jurkat IC_{50} 3 nM; CEM IC_{50} 14 nM) and lung carcinoma (A549 IC_{50} 46 nM) and good cytotoxicity against breast carcinoma (MCF-7 IC_{50} 210 nM), neuroblastoma (NB7 IC50 819 nM), and prostate carcinoma (PC3 IC_{50} 970 nM).[206] Further characterization revealed somocystinamide A activates programmed cell death *via* caspase-8 as well as apoptotic activity in tumors

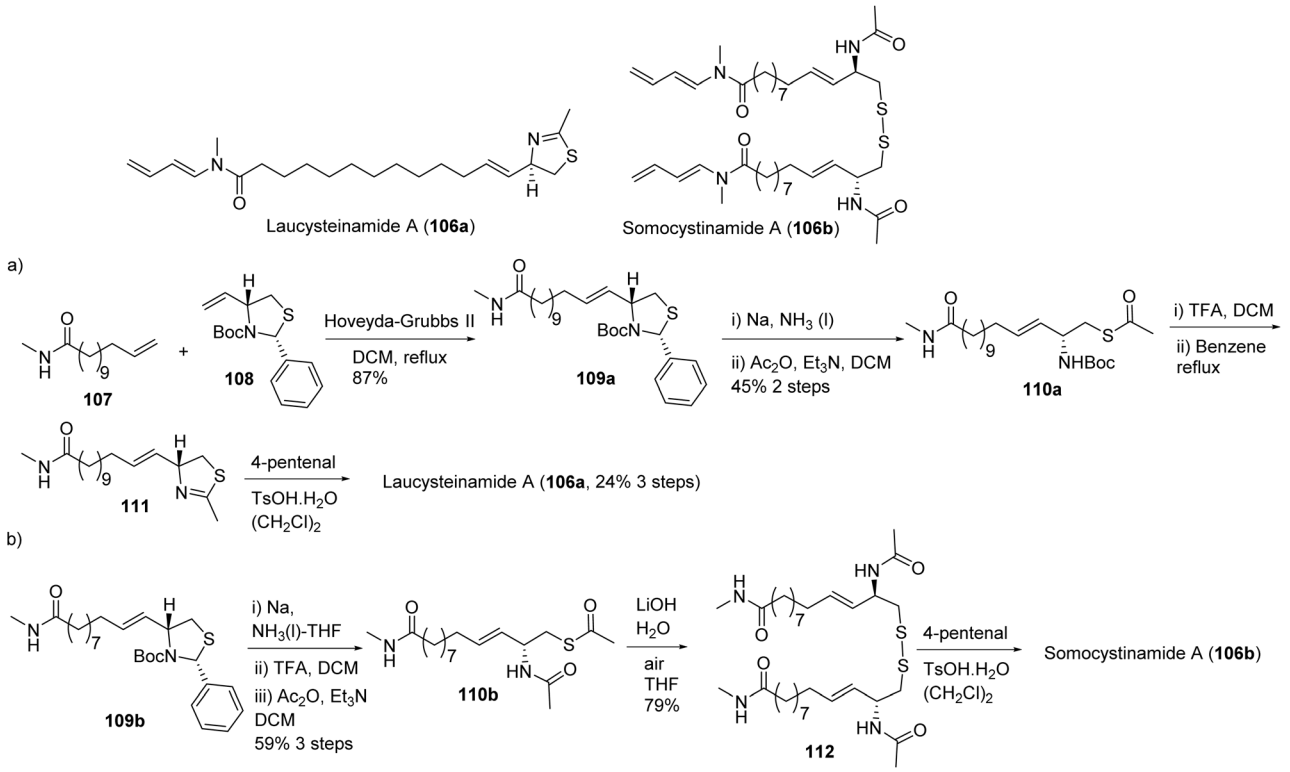

Fig. 24 Structures of laucysteinamide A (106a) and somocystinamide A (106b) and the synthetic strategies (a and b) for the two compounds.

resistant to death receptor-mediated killing and Fas-mediated apoptosis *via* plasma membrane lipid compartment modifications.[206] Together, the mechanistic studies revealed the unique method in which ScA exhibits both an angiogenetic effect and inhibition of tumor cell progression. (Fig. 24, **106b**).[206]

Laucysteinamide A (**106a**, Fig. 24), monomeric analogue of somocystinamide A, was isolated from *Caldora penicillata* in the Northern Mariana Islands by the Gerwick group.[232] The lipopeptide exhibited weak cytotoxicity, compared to somocystinamide A, against lung cell carcinoma (H460) with an IC_{50} of 11 μM, with the synthetic equivalent of laucysteinamide A exhibiting cytotoxicity against H460 at 20 μM.[233]

Using the their improved protocols for the total synthesis of somocystinamide (**106b**), Gerwick and co-workers completed the total synthesis of laucysteinamide A (**106a**) in 2021 (Fig. 24, **b**).[233,234] The available unsaturated compound **107** and **108** were subjected to olefin cross metathesis catalyzed by Hoveyda-Grubbs II catalyst to afford thiazolidine **109a**. Birch reduction followed by acylation of **109a** provided thioester **110a**. The thiazoline compound **111** was prepared by reflux to induce dehydrative cyclization of the Boc-cleaved **110a**. The condensation of **111** with 4-pentenal using TsOH as a catalyst afforded the final product laucysteinamide A (**106a**) in 9.4% overall yield. The authors applied the improved protocols to the total synthesis of somocystinamide (**106b**, Fig. 24) and obtained a better overall yield. The thioester **110a** was prepared from **109a** using the same protocols for **110a**. The basic hydrolysis of thioester of **110b** in the presence of air made the dimerization provided somocystinamide A (**106b**) with an overall yield of 16.1%.[233,234]

6. Epigenetic modulators

6.1. Mechanism of action

Inhibition of histone deacetylases (HDACs) is a validated anticancer strategy. Several drugs that target zinc-dependent isoforms (HDAC1–11) with different selectivity profiles have been approved for the treatment of various lymphomas (T-cell lymphomas, multiple myeloma) but have not shown significant clinical efficacy against solid tumors.[235,236] HDAC inhibition leads to hyperacetylation of histones, open chromatin structure and activation of gene expression, including genes encoding cell cycle inhibitors and pro-apoptotic proteins, which mainly or at least partially account for the anticancer activities of pharmacological HDAC inhibitors.[237] Recent reviews have highlighted the importance of these targets for therapeutic applications.[235,238] (Fig. 25) To date, two HDAC inhibitors have been identified from marine cyanobacteria: (1) largazole (**122a**, Fig. 26), a thioester prodrug that liberates a zinc-binding thiol group upon activation, and (2) santacruzamate A (**130**, Fig. 30), containing a hydroxamate functionality as the moiety with Zn^{2+} affinity.[239–242]

6.2. Largazole

In 2012, Hong and Luesch reviewed the discovery, general synthetic strategies, cytotoxicity, HDAC isoform selectivity

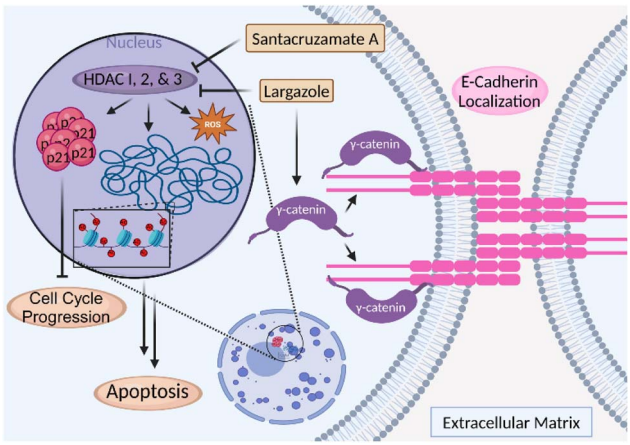

Fig. 25 Class I HDAC inhibitors regulate histone deacetylation through HDAC 1, 2, and 3, therefore activating gene expression, but also possess cytoplasmic (non-nuclear) targets that promote anti-cancer activity, including modulation of the E-cadherin complex and consequent cell–cell adhesion.

profile, HDAC8-largazole thiol crystal structure, mechanism of action, and SAR for largazole (**113a**).[243] Initial biological evaluation indicated nanomolar potency on human bone cancer (U2Os IC_{50} 55 nM) and mouse normal breast/fibroblast cells (NMuMG IC_{50} 122 nM/NIH3T3 IC_{50} 480 nM), with superior potency for the breast cancer cell line MDA-MB-231 (IC_{50} 7.7 nM).[241] Bowers *et. al.* characterized the HDAC selectivity as HDACs 1, 2, and 3 selective over HDAC6.[239] Importantly, largazole (**113a**) showed solid tumor activity in a HCT116 colorectal cancer xenograft mouse model at 5 mg kg^{-1}, correlating with

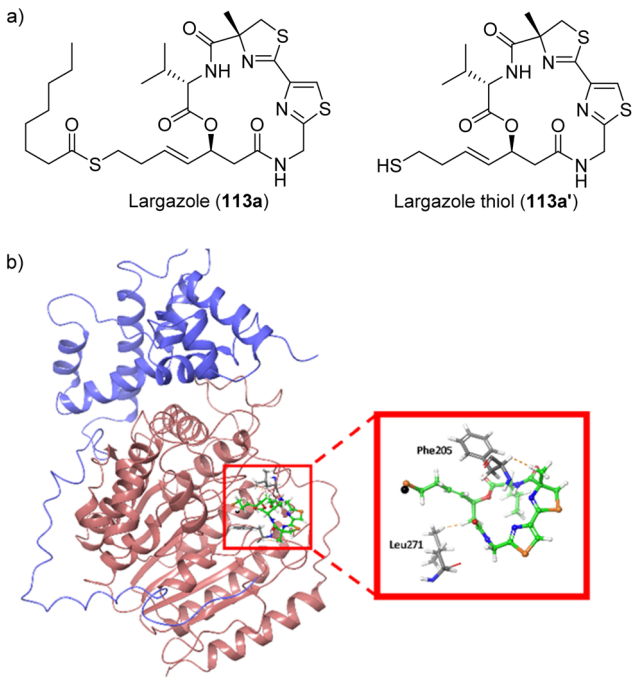

Fig. 26 (a) Structures of largazole (prodrug) and its active species (largazole thiol) and (b) molecular docking of largazole thiol (**113a′**) to HDAC1 crystal structure (PBDID: 5ICN).

the histone hyperacetylation status at that dose, so that the antitumor effect was attributed to gene expression changes due to HDAC inhibition.[244] Although to a lesser extent than tubulin agents dolastatins 10 and 15 (Sections 2.2, and 2.3), largazole also showed greater efficacy in HCT116 cells containing oncogenic KRAS and selectivity for HCT116 cells containing functional HIF transcription factors.[131] Largazole phenocopied the *colgate* 1 zebrafish mutant and inhibited HIF-induced angiogenesis *in vivo* in *vhl* mutant zebrafish, but also to a lesser degree than dolastatin 15 (Section 2.3).[131]

Largazole (**113a**) is a prodrug that is activated by protein-assisted hydrolysis to generate largazole thiol (**113a′**) that is optimized to access the zinc within the active site of the HDAC to give its potent inhibitory effect, similar to the active (reduced) form of FDA approved drug FK228 (romidepsin).[245] Largazole thiol (**113a′**) exhibited potent, sub-nM activity against class I isoforms HDAC 1, 2, and 3 (K_i of 0.07, 0.07, 0.17 nM), and to a much lesser extent class IIb isoform HDAC6 (K_i 25 nM).[239] For comparison, FK288 exhibited K_i values of 0.12, 0.14, 0.28, and 35 nM against HDAC1, 2, 3, and 6, crowning largazole thiol (**113a′**) as the more potent HDAC inhibitor.[239] The molecular docking of largazole thiol to HDAC1 crystal structure has provided a foundation in which these inhibitors interact with HDAC (Fig. 26). The largazole thiol binds to the zinc deep within the active cleft of the zinc finger, forcing the overall metal coordination geometry to be almost tetrahedral.[243] Additionally, the macrocyclic portion exists outside of the convergent region of all HDACs, providing a base to induce isoform selectivity *via* SAR of the amino acid residues on the ring.[243] Comprehensive profiling against all eleven zinc-dependent HDAC isoforms underscored the HDAC1–3 selectivity.[243] Largazole (**113a**) exhibits greater antineoplastic effects than largazole thiol (**113a′**) on malignant melanoma cells (IC_{50} 45 nM–315 nM *vs.* IC_{50} 360 nM–2600 nM), highlighting the importance of the prodrug for cellular efficacy.[239]

Largazole (**113a**) was shown to both induce the expression of the tumor suppressor E-cadherin and also to modulate the composition of the E-cadherin complex in triple negative breast cancer cells (TNBCs) by increasing the content of γ-catenin, promoting transport of E-cadherin to the cell surface to mediate cell–cell interaction and reduce invasion.[246,247] Reduced or lack of E-cadherin expression and improper cytoplasmic localization (if expressed) are characteristic feature and causative for the invasiveness of TNBCs, and largazole reversed both TNBC features to "normalize" the cellular phenotype to a less invasive state.[246,248] This dual effect of largazole on gene expression and modulation of protein–protein interaction translated into mouse models.[246] TNBC line tumors ectopically expressing GFP-tagged E-cadherin demonstrated the proper cell surface localization upon treatment with largazole *ex vivo* using excised tumors or by systemic administration *in vivo* (10 mg kg^{-1}).[246] The activity was enhanced in combination with dexamethasone which acts by preventing CDCP1 cleavage and formation of the invasive cleaved (cCDCP1) form.[246] The cooperative effects with glucocorticoids indicated that largazole (**113a**), or HDAC inhibitors in general, could be effective in this biological

context, potentially providing the basis for combination therapy clinical trials for TNBC.[246]

Largazole (**113a**) was shown to demonstrate potent and selective cytotoxicity towards a number of lung cancer cell lines, inhibiting cell proliferation within an IC_{50} range of 0.077 to 0.57 μM in wild type or mutant EGFR cell lines. The 16-HBE normal human bronchial epithelial cells exhibited less potency at more than 10 μM.[249] Largazole was shown to arrest the cell cycle at G1 phase with high concentrations of treatment causing activation of caspase 9 with the downregulation of pro-caspase 9, indicating a role in the intrinsic apoptotic pathway with the cleavage of PARP using Annexin V/PI staining and flow cytometry analysis.[249] The upregulation of p21 as demonstrated in A549 cells further supports the conclusion that largazole induces G1 phase arrest.[249]

More recently, largazole (**113a**) was found to be bioavailable in the brain and can reach *in vivo* concentrations sufficient to inhibit glioblastoma cell proliferation *in vitro*.[250] At 50 mg per kg ip, largazole treatment for 12 h induced neuroprotective and cancer-related gene expression changes, extending the applicability of largazole to neurodegenerative diseases and brain cancers.[250] Global gene expression profiling of largazole and Ingenuity Pathway Analysis (IPA) of RNA sequencing data sets revealed upregulation of neuronal transcription factor *Pax6* and *Oprm1*.[250] In addition to its role in neurogenesis and neuronal plasticity, Pax6 is known to suppress proliferation, invasion and colony formation of glioblastoma cells.[251] Pax6 expression also inversely correlates with tumor grade. The data implicates Pax6 as a relevant indirect largazole target to mediate both beneficial activities. Oprm1 is a μ-opioid receptor shown to induce neuroprotective activity *via* the mTOR signaling against β-amyloid peptide neurotoxicity and is the target for morphine.[252]

The therapeutic potential of largazole (**113a**, Fig. 27) to treat cancer and other diseases triggered the synthesis of analogues, including different prodrugs like hydroxamates, ketones and disulfides (**113b–113n**, Fig. 27)[247,253–263] The pyridyl "IN" analogue (**113b**) showed similar potency against 797 NUT midline carcinoma cell line.[264] Bipyridine analogue (**113c**), series of C7 and thiazole analogues (**113d–113h**), and the fluoroolefin analogue (**113i**) exhibited similar potency against HDAC1 or HDAC8.[259,265,266] Zinc-binding group analogues (**113j–113m**), including different disulfide prodrugs (**113m**), were also synthesized to modulate activity profiles and change the modes and timing of activation, providing opportunities for conjugation to targeting agents, and to address potential liabilities or efficacy issues due to the rapid protein-assisted thioester hydrolysis observed for largazole during extensive pharmacokinetic studies in rats.[244,247,260,262,267] The disulfide homodimer (**113n**) generates two equivalents of largazole thiol and therefore has superior *in vitro* potency on a molar basis. Other structural modifications were aimed at tuning the class I HDAC isoform

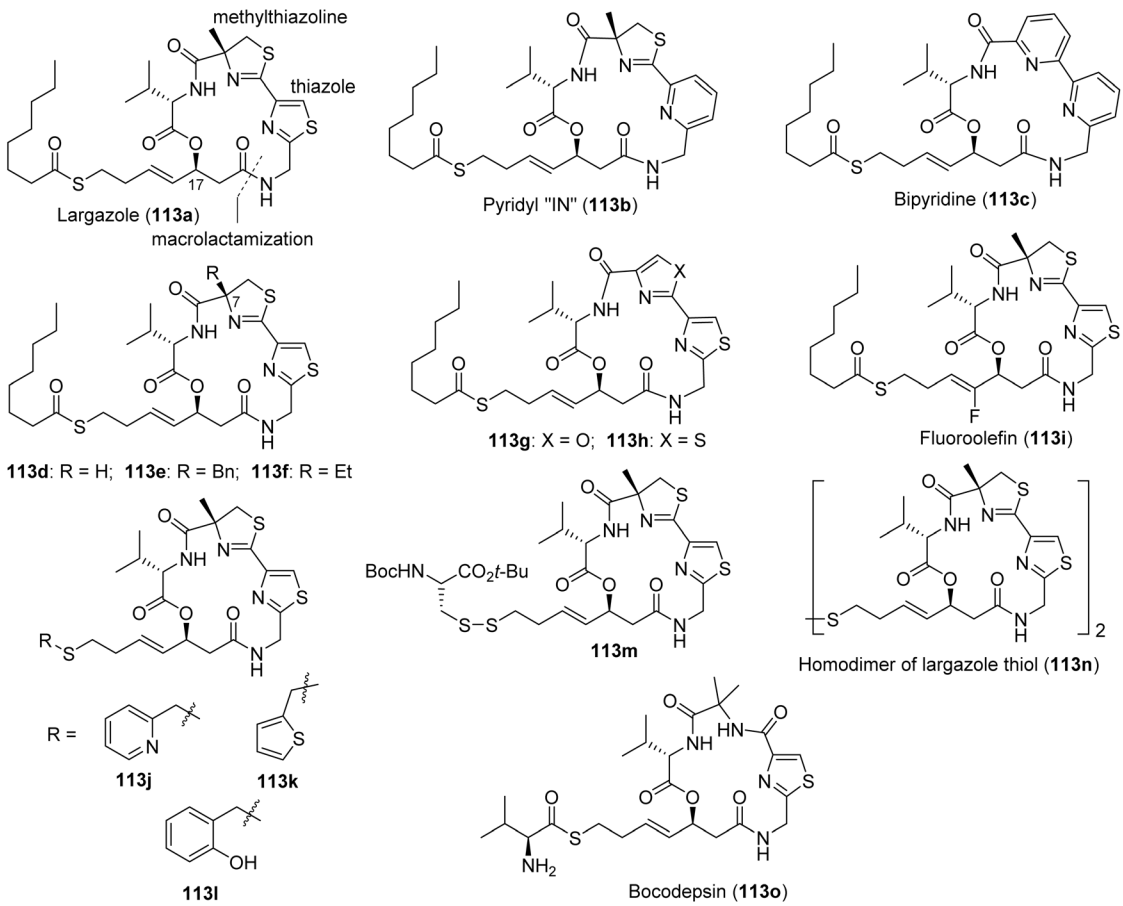

Fig. 27 Structures of selected largazole analogues (**113a–o**) designed and synthesized for SAR studies.

selectivity profiles (HDACs 1–3, 8), which was achieved by replacing the valine residue with other amino acids (Phe, Tyr, His, Asp, and lower homologues of Lys). These efforts led to largazole analogues without significant HDAC8 inhibition and where HDAC2 activity was dialed down (Phe), resulting in an HDAC1,3 inhibitor with 5.9-fold selectivity for HDAC1 over HDAC2. Replacing Val with His resulted in the most HDAC1-selective isoform inhibitor with 7.0- and 5.5-fold selectivity over HDAC2 and HDAC3, respectively.[257] This data suggests that the largazole scaffold can be a template for the design of next-generation isoform selective inhibitors. One largazole-based thioester prodrug with simplified core structure, bocodepsin (OKI-179, **113o**), has reached the clinic so far. Designed through a lead candidate optimization program to enhance isoform selectivity and oral bioavailability, its thiol retained class I selectivity HDACs (IC_{50} 1.2 nM for, HDAC1; 2.4 nM for HDAC2, 2.0 nM for HDAC3, and 47 nM for HDAC8) over class IIb HDACs, including HDAC6 and 10 (IC_{50} 47 nM, 2.8 nM); and class IV HDAC11 (IC_{50} 2.3 nM).[268,269] Recently, a first-in-human phase 1b/2 trial was conducted using bocodepsin (**113o**) as a treatment for advanced solid tumors and concluded in prolonged disease stabilization as the first orally bioavailable, Class I targeting HDAC inhibitor.[270,271]

For the synthesis of largazole (**113a**), most groups chose the site between β-hydroxy acid and thiazole fragment for macrocyclization, which offers less steric hindrance. Two main convergent strategies were developed for the total synthesis of largazole (**113a**). The major difference between these two strategies is the timing of incorporation of the pendant side chain and pharmacophore. In one strategy (Fig. 28), the allylic cyclic core **119** was synthesized first from vinyl hydroxy acid **114**, valine, thiazolyl nitrile **116** and α-methylcysteine **117**.[264,272–274] Then thiol **120** was fused to the cyclic core using a cross metathesis reaction to complete the final target. This strategy is amenable to the synthesis of diverse analogues using various building blocks, **114**, **116**, **117**, Val and **120**. However, in the second strategy (Fig. 28b), the trityl-masked thiol (**121**) was first esterified with Fmoc-protected valine.[239,275,276] Subsequently, the cyclic core was synthesized from this fragment, the valine and thiazoyl-thiazoline moiety (**118**). The *n*-octanoyl chloride was coupled with unmasked thiol group to provide final product (**113a**). Strategy depicted in Fig. 28a is suitable for the late-stage diversification of the side chain and installation of various prodrugs.

Hydroxy acid (**114**, Fig. 28) is the key building block in both synthetic strategies (Fig. 28a and b). The Nagao auxiliary masked hydroxy acid (**126**, Fig. 29b) induced a direct reaction without the cleavage of the auxiliary.[240] Aldol reaction between acrolein and enolate from *t*-butyl acetate provided a racemic allylic hydroxy ester (*RS*)-**114** (Fig. 29a).[265,272,273,275] The (*S*)-enantiomer of **114** could be separated from the (*R*)-**114** when the (*S*)-**114** was selectively protected by allyl acetate under enzymatic resolution (amano lipase). Base-catalyzed deacetylation afforded (*S*)-hydroxy acid (**114**). However, the hydroxy acid **114** is sensitive to basic condition and prone to dehydration. From this point of view, the asymmetric selective aldol reactions (Fig. 29b and c) using Nagao auxiliaries (**125a–c**) has advantages over the method in Fig. 28a.[240]

In the process chemistry study, the Luesch group adopted the method from Fig. 29a, with notable critical modifications.[277] Only 0.5 eq. K_2CO_3 was used in the large-scale preparation and the dehydration was alleviated significantly. When the thioester (**120**) was installed at the late-stage, the final product largazole (**113a**) was contaminated with catalyst (brownish product). This problem was solved by the assembly separation using normal-phase and reversed-phase C18 chromatography. For the synthesis of the thiazoline-thiazole moiety (**118**), most groups proceeded in a similar manner.

6.3. Santacruzamate A

Santacruzamate A (**130**, Fig. 30) is an achiral cytotoxin isolated from the cyanobacterium *Symploca* sp. collected in Coiba National Park off the Pacific coast of Panama by the Gerwick and Balunas groups. The compound possesses structural

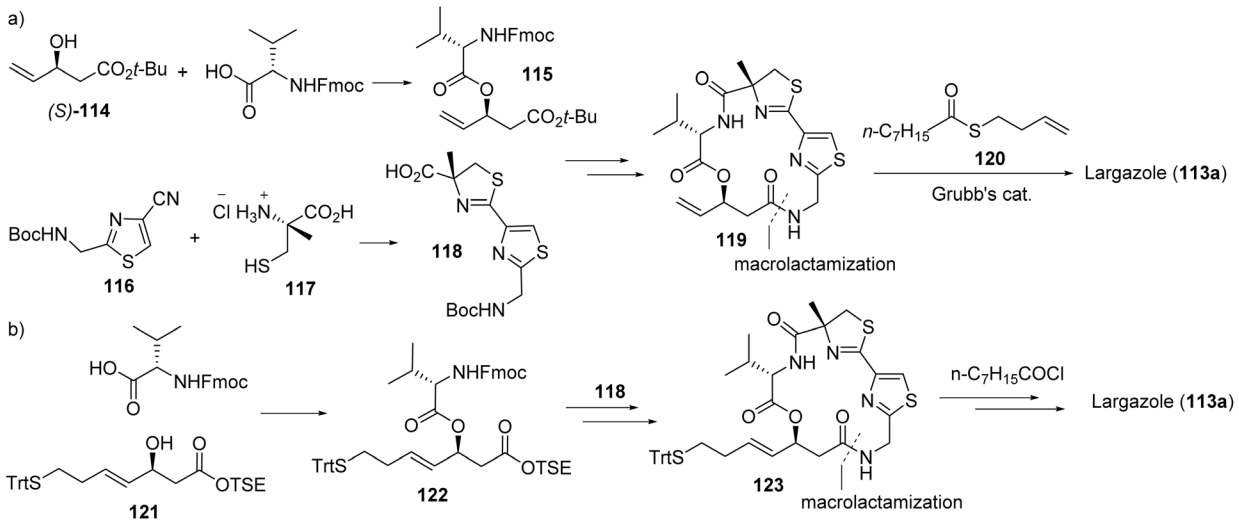

Fig. 28 Two main strategies (a and b) for the total synthesis of largazole (**113a**).

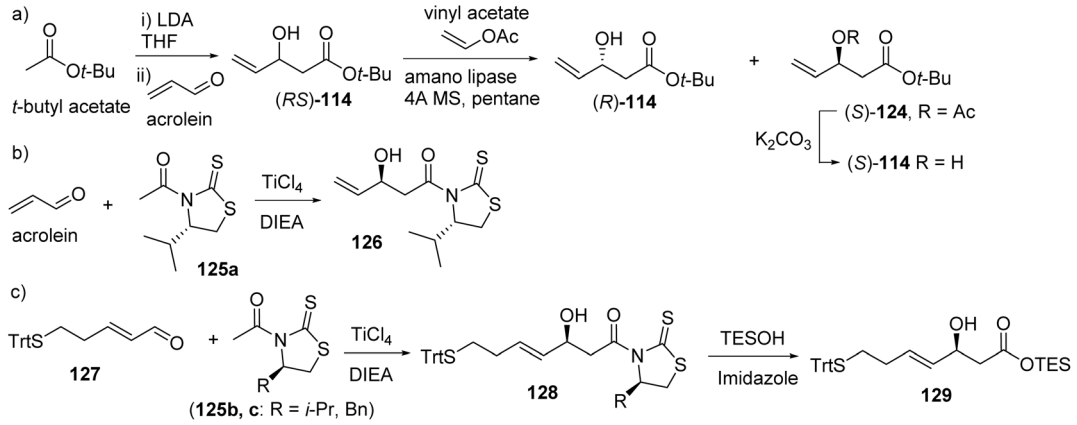

Fig. 29 The synthesis of hydroxy acid moiety ((*S*)-**114**) using different strategies (a–c).

similarities to the clinically approved HDAC inhibitor suberoylanilide hydroxamic acid (SAHA, vorinostat).[242] Preliminary bioactivity indicated selectivity for HDAC2 at an IC_{50} of 0.119 nM and cytostatic activity against cutaneous T-cell lymphoma (Hut-78 GI_{50} 1.4 μM) and colorectal cancer (HCT116 GI_{50} 29.4 μM).[242] In an independent study, the HDAC2 inhibitory activity of santacruzamate A (**130**) was found to block nuclear translocation of PD-L1, presumably by enhancing the acetylation status of Lys263, leading to reprogramming of the expression of immune-response related genes.[242] Consequently, santacruzamate A was found to enhance the antitumor activity of PD-1 blockage using anti-PD-1 antibodies in a MC38 syngeneic mouse tumor model.[278] This effect was not observed in immunocompromised nude mice, supporting the hypothesis of T-cell dependent combinatorial effect, opening up new therapeutic opportunities for HDAC2 inhibitors.[9]

The chemical structure of santacruzamate A (SCA, **130**, Fig. 30a) is simple and consists of three sections: an ethyl carbamate (EC) terminus, a γ-aminobutyric acid (GABA) linker and a phenethylamine (PEA) cap. The original total synthesis of SCA was reported by Balunas, alongside the isolation work.[242] As shown in Fig. 30a, coupling of the N-terminal and C-terminal of GABA with the ethyl chloroformate and PEA, respectively, provided product SCA (**130**). Starting from monomethyl glutarate, Balunas also synthesized the SCA-SAHA hybrid (**131**, Fig. 30b). In 2016, following similar protocols, Balunas synthesized 40 analogues of SCA by alteration of EC, GABA and PEA with different moieties, respectively.[279] Unfortunately, all analogues, including the SCA (both natural and synthetic) and SCA-SAHA hybrid (**131**), were inactive against HDAC2 enzyme as well as HCT116 cells. Only two PEA-altered analogues **132a**, **132b** showed moderate to weak activity against MCF-7 with micromolar GI_{50}. However, using similar synthetic strategy as Balunas, Wen and Rodriquez developed more potent analogues of SCA in 2015 and 2017 against HCT116 cell line with IC_{50} values in the micromolar range at 48 h and 72 h (**133**, **134a,b** and **135**, Fig. 30b).[280,281]

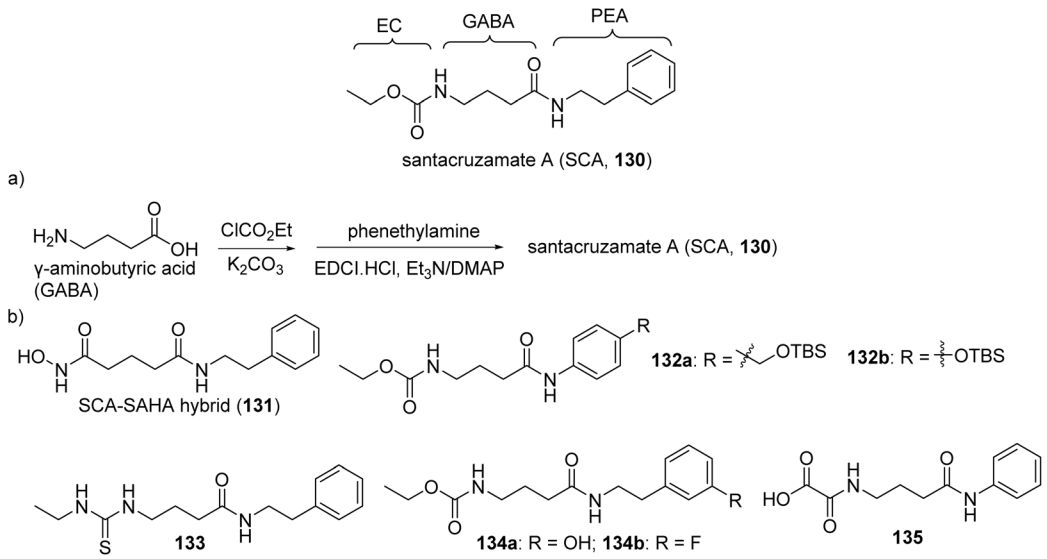

Fig. 30 Parent structure of santacruzamate A (**130**), (a) synthesis and (b) analogues.

7. Proteasome inhibitors

7.1. Mechanism of action

Multiple myeloma (MM) is malignant plasma cells that metastasize as osteolytic bone legions without the formation of new bone, with proteasome inhibitors as typical treatment for the incurable disease.[282] Proteasomes are large protein complexes working with polymerized ubiquitin to degrade mutated or misfolded intracellular proteins in a metabolic depleting fashion. Ubiquitin targets damaged proteins, initiates a 3-step cascade to produce a tagged protein with a polyubiquitin chain, in which the proteasome then passes the protein through its 20S core to be degraded into small oligopeptides (Fig. 31).[283] Inhibition of proteasomes are generally well received for clinical use with minimal side effects, with the FDA approval of bortezomib in 2003 for multiple myeloma and later the semi-synthetic carfilzomib, derived from epoxomicin, for refractory multiple myeloma in 2012.[283] Both inhibit the chymotrypsin-like, trypsin-like, and caspase-like subunits of the 20S proteasome (β5, β2, β1) and are given in triple combination therapy with an immunomodulatory drug and dexamethasone. Other therapies, like the γ-lactam-β-lactone natural product salinosporamide A, target the 20S proteasome as well and is currently in a phase III trial under the name marizomib as a treatment for patients with recently diagnosed glioblastoma.[284] However, the plasma cells of MM are highly resistant, leading to patient serial relapse post treatment with no clear resistant mechanism defined.[285] Precision therapy *via* ADCs are the imminent treatment for resistant cells, with the FDA approval of the B-cell maturation antigen (BCMA) targeted ADC belantamab mafodotin (Bela) in 2020. The marine cyanobacterial natural product carmaphycin is in development by linking carmaphycin B analogues with the antibody trastuzumab (Fig. 32).[286–288]

7.2. Carmaphycins

Carmaphycins A and B (**136a,b**, Fig. 32) were first isolated from *Symploca* sp. from Curacao in 2012 by the Gerwick group and feature an α,β-epoxyketone warhead with potential for ADC preparation *via* a methionine sulfoxide or methionine sulfone (A and B).[287] Both target the β5 subunit of the 20S proteasome with an IC_{50} of 2.5 and 2.6 nM, respectively.[287] Cytotoxicity assays for carmaphycin A (**136a**) and B (**136b**) initially resulted in strong potency against H-460 (EC_{50} 9 and 6 nM) and HCT116 (IC_{50} 19 and 43 nM) cancer cell lines. In the NCI 60 cell-line panel, most GI_{50} values ranged between 1 and 50 nM, with specific antiproliferative effects in CNS, lung, and colon tumor cell lines with specific sensitivities to mutants of KRAS or p53 cell lines.[287] With little effect on total growth inhibition at higher concentrations, the α,β-epoxyketones signify the need for modification to the natural product warhead for drug development, as was done for the approved drugs carfilzomib and epoxomicin with similar warheads.[289]

The key feature of carmaphycins is the α,β-epoxyketone and the key issue in the total synthesis was the construction of this fragment (Fig. 33). The Gerwick group completed the first total synthesis and reported it along with the isolation and structure determination.[287] In their initial work, Gerwick used the typical procedure (straight way) for the synthesis of the epoxyketone fragment (**139**): the combination of a Grignard reaction of Leu Weinreb amide and oxidation with oxone provided the α,β-epoxyketone fragment **139** as major product (Fig. 33, route a).[287] The yield for these two steps was 26% and the diastereomeric selectivity was 1.7 : 1.[290] For ADC preparation, a different protocol was followed for the synthesis of epoxyketone **139**, through alcohol intermediates **140**, **141** (route b), and the total yield for these three steps was 60–80%.[288,291] However, only 27% yield for this three-step reaction was reported by Zhou.[291] With epoxyketone **139** in hand, general peptide coupling with dipeptide **142** (commercially available) gave carmaphycin A (**136a**), which was further oxidized to carmaphycin B (**136b**) with oxone. Similar to published synthetic routes, a series of analogues were synthesized as well as ADCs of carmaphycin A.[288,292,293] Development of carmaphycin ADCs resulted in the coupling of a cleavable and non-cleavable payload of DBCO-C6-acid to carmaphycin B analogues with the eventual conjugation to the antibody trastuzumab (**137b** and **137a**, respectively, Fig. 32).[287] The synthesis of a novel ADC with the natural product scaffold was successful, but biological evaluation revealed decreased potency compared to the antibody itself and significantly less potency than the payload MMAE.[288]

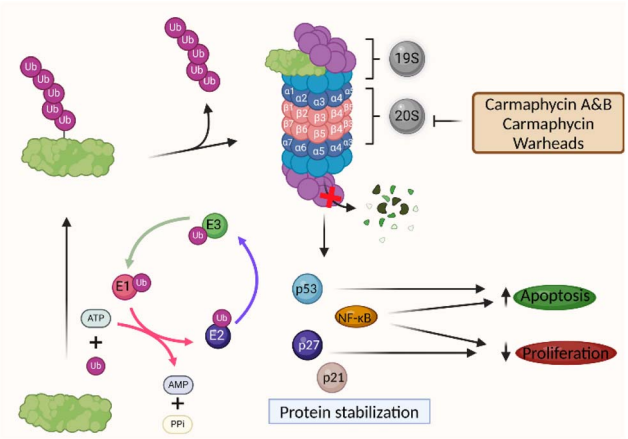

Fig. 31 Proteasome degradation mechanism with inhibitors acting on 20S, stabilizing proteins that upregulate apoptotic signals and downregulate proteins that induce cell proliferation.

8. Macrocyclic membrane-targeting agents

8.1. Mechanism of action

Therapeutics targeting membranes dominate the druggable sphere as more than 60% of targets are membrane proteins, with macrocyclic agents as an exciting class of druggable entities.[294] But targets are not necessarily proteins. Bacterial membrane inhibitors, such as the soil bacteria metabolites lysocin E and daptomycin, target predominantly phospholipid classes like menaquinone and phosphatidylglycerol, respectively.[295] The eukaryotic lipid membrane targets include ergosterol (fungi) and cholesterol (mammalian cells), with various

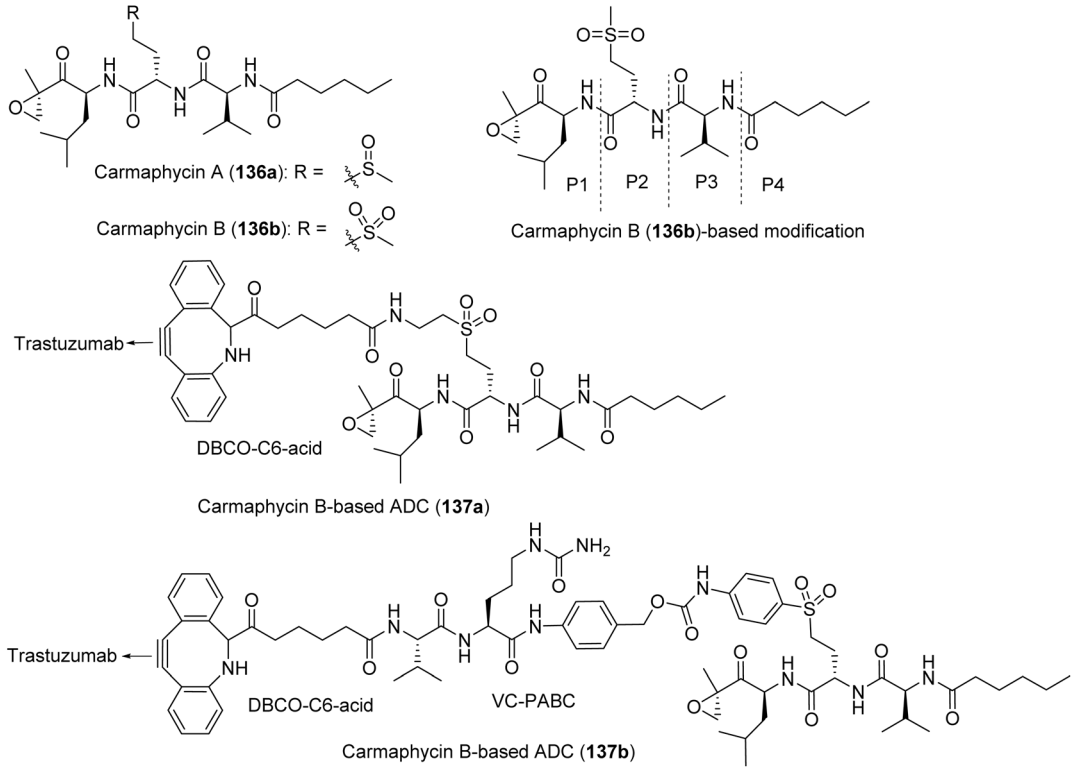

Fig. 32 Structures of the natural products carmaphycin A (136a) and B (136b) and two ADCs containing a carmaphycin B-based payload (137a–b).

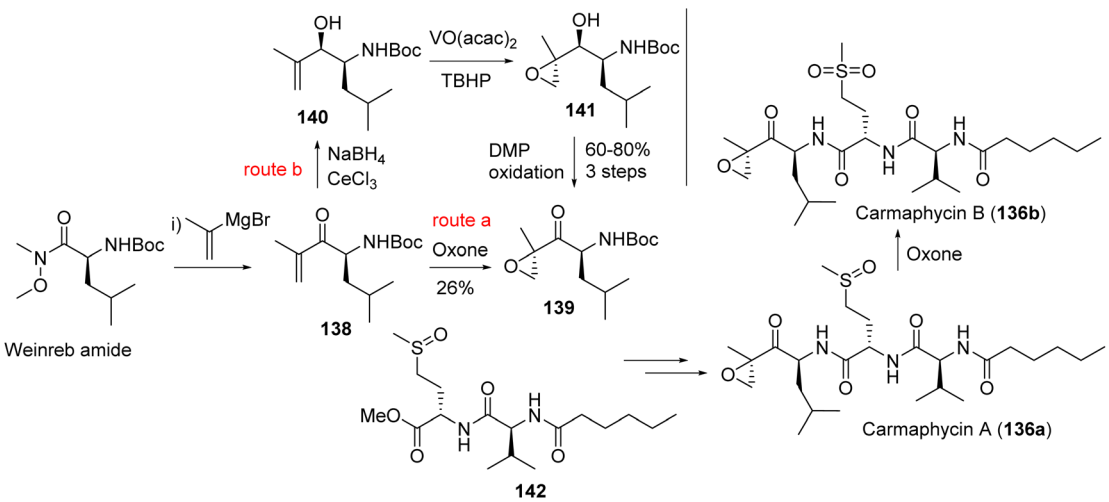

Fig. 33 Abbreviated synthesis of carmaphycins (136a–b) and analogue 142 for SAR studies.

natural product inhibitors with a wide structure diversity as described by Nishimura and Matsumori in a 2020 review.[296] The frontline defense of polyene antifungal agents, like amphotericin B, complex ergosterol in the plasma membrane, disrupting membrane fluidity and integrity by permeabilizing the fungal membrane to inhibit cellular functions.[297] The marine cyanobacterial polyhydroxylated macrolide amantelide A (143a) has a similar mechanism to polyene antifungals, with the additional ability to promote the polymerization of actin in cell-free systems.[298,299] The marine sponge helix forming product polytheonamide B works as an ion channel and methyl-β-cyclodextrin as an acute cholesterol depleting agent, and the natural product theonellamides, the bicyclic peptide, targets both ergosterol and cholesterol. Cholesterol plays an essential role in the mechanical stability of the membrane during division and reduces shear force stress in cell separation. It thus could represent a prime target for cancer therapeutics as cancer cells restructure their membrane to avoid apoptosis, ensure proliferation, and resist treatment[300,301] (Fig. 34).

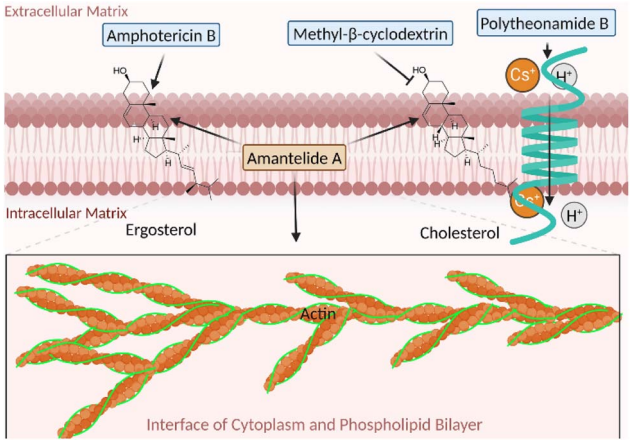

Fig. 34 Natural macrocyclic agents targeting eukaryotic sterol containing membranes.

8.2. Amantelides and other polydroxylated macrolides

The isolation of amantelides A and B were described by the Luesch group from a gray cyanobacterium collected from Tumon Bay, Guam.[298] The mode of action of amantelide A (**143a**, Fig. 35) has been studied through a combination of yeast knockout mutants and chemogenomics, as well as targeted biophysical and biochemical methods.[299] Amantelide A preferentially binds to sterol-containing membranes based on 1-palmitoyl-2-oleoyl-*sn*-glycero-3-phosphatidylcholine(POPC)-based liposome studies, although the interaction is not completely dependent on sterols; however, the binding affinity increased with sterols compared with POPC liposomes alone.[299] In contrast to other sterol-targeting compounds, amantelide A does not require β-configuration of the 33-OH group; binding occurred equally to cholesterol and epi-cholesterol containing POPC membranes.[299] Interaction with cholesterol-containing membranes is the likely cause of rapid cell death of mammalian cells. In yeast, the (ergosterol-containing) membrane was determined to be the major functionally relevant target, causing pore formation and cell death.[299] The mode of interaction and lipid recognition on the molecular level remains to be investigated. Interestingly, C33-acetyl analogue, amantelide B (**143b**, Fig. 35), also binds to POPC and the presence of sterols decreased binding, providing clear SAR based on only two compounds.[298] The lack of activity of amantelide B (**143b**) suggests that acylation might serve as a self-protective mechanism of the native organism.

Other related macrolides from marine cyanobacteria such as bastimolide A (**144a**), and B (**144b**), palstimolide A (**146**), and caylobolides (**145a**, **145b**) with similar structural scaffold (Fig. 35) may have a comparable, membrane-mediated mechanism of action with to-be-determined affinity for membrane components.[302–307] It has been challenging to deduce the absolute configuration of the stereocenters, also hampering

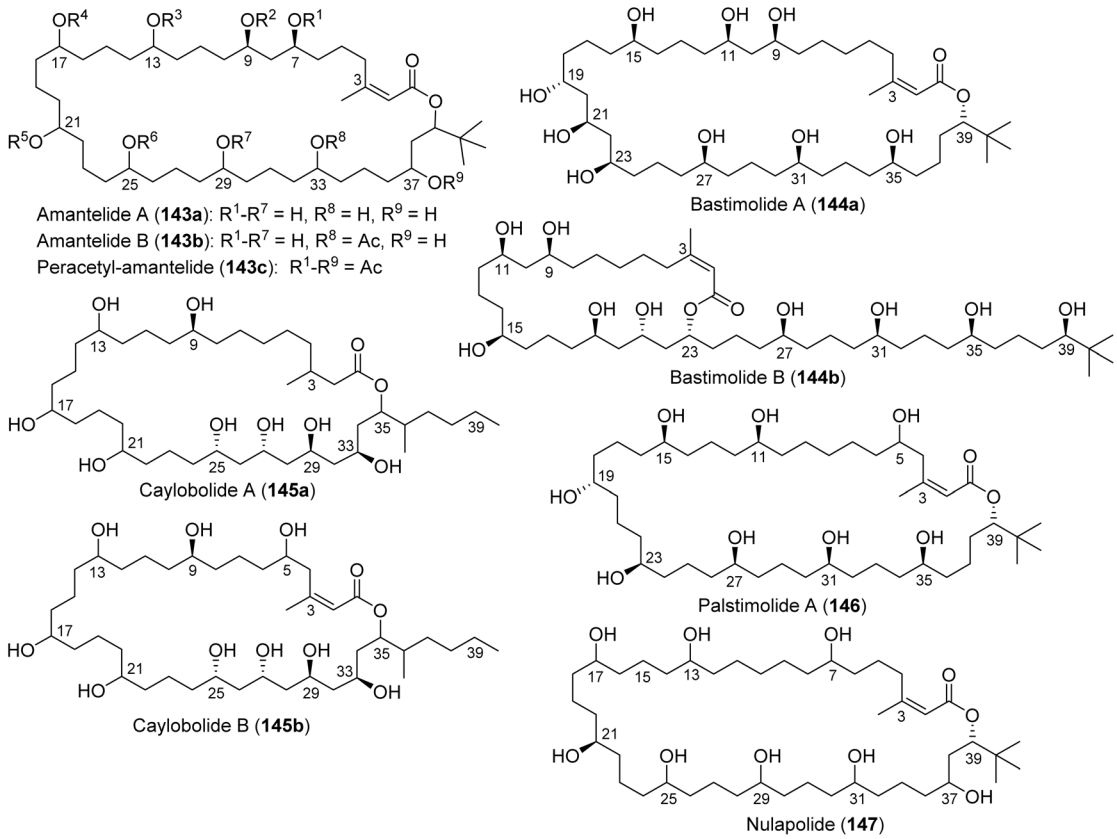

Fig. 35 Structures of amantelides (**143a–c**) and the related cyanobacterial macrolides, bastimolides (**144a,b**), caylobolides (**145a,b**), palstimolide A (**146**) and nulapolide (**147**).

synthetic accessibility so far. Preliminary SAR for amantelide A (**143a**) and B (**143b**) suggests that minor changes drastically influence recognition and binding, indicating selectivity can likely be tuned. However, amantelides also bind to membranes in a sterol-independent manner.[298]

In addition, chemogenomic profiling has suggested that actin modulation might also play a role in the mechanism of action of amantelide A.[299] Amantelides A (**143a**) and B (**143b**) both appeared to directly affect actin dynamics, promoting polymerization to a minor extent *in vitro*. Since both compounds have the same effect in biochemical assays and membrane integrity is quickly compromised in cells treated amantelide A (**143a**) before actin interaction can occur, (1) actin binding is most likely not functionally relevant and may not occur in cells, and (2) the direct effects on sterol-membranes and actin can be separated, as is the case for amantelide B (**143b**). Compound activity, however, could potentially be modulated by actin as the cytoskeleton is associated with the membrane.[299]

To serve as an antifungal agent, amantelide A (**143a**) is too non-selectively cytotoxic against fungi and mammalian cells (HT29 IC_{50} 870 nM; HeLa IC_{50} 870 nM). However, the modulation of sterol-selectivity might lead to an antifungal if cholesterol affinity can be dialled out.[298] For cancer applications, it may require targeted delivery to cancer cells to spare normal cells, or the differential biological context for cancer and normal cells beyond sterols can be exploited. Nevertheless, target identification has provided the basis for further evaluation of this compound class.

There are several publications about the total synthesis of polydroxylated macrolides, but selectively constructing multiple chiral centers in this type of molecules is very challenging. Achieving an excellent stereochemical control by enantioselective organocatalytic halogenation, Quintard group completed the synthesis of the C15–C27 fragment of bastimolide A (**144a**, Fig. 36).[308] The total synthesis of bastimolide B (**144b**, Fig. 36) was completed by Aggarwal group in 2022 as showed in Fig. 36.[309] The key strategy for success was the combined application of iterative boronic ester homologation with metal carbenoids and metal catalyzed alkene hydroboration and diboration. Excellent remote stereocenter control was achieved in the construction of acyclic backbone of bastimolide B (**144b**). Fig. 36 depicts the retrosynthetic analysis and stepwise synthesis of the authors' work.

9. Chemosensitizing agents

Resistance to chemotherapeutic agents in cancer treatment has been reported for most drugs used to treat lethal cancers and contributes to the failure of therapy and the cause of tumor recurrence.[310] Typical drug resistance involve the tumor microenvironment (hypoxia, vascular viscosity, and reduced glucose supply), progression pathways (PI3K/Akt, MAPK, and Wnt pathways), drug influx and efflux throughout the cell (acidic pH and limited solute carrier transporters), and impaired apoptosis (enhanced DNA repair *via* Wnt signaling).[310] Chemosensitizing agents discussed here fall into two groups: (1) inherently cytotoxic but do not display the requisite selectivity or inappropriately used, including compounds that act on actin dynamics grassypeptolide A (**165**), lyngbyabellin A (**166**) and dolastatin 12 (**167**), and (2) compounds that are weakly or non-cytotoxic but enhance the sensitivity to cytotoxins and to inducers of apoptosis (doscadenamides (**175a,b**; **176a,b**)).[311–315]

9.1. Overcoming Nrf2-mediated drug resistance: actin agents and grassypeptolides

Similar to microtubules, the actin cytoskeleton is critical for many processes, including cell division and migration.[21] However, actin agents, including promoters of G-actin polymerization into F-actin or microfilament depolymerizers, have not been successful as stand-alone agents which can likely be due to cardiac and respiratory toxicities associated with non-specific binding to actin.[311,316,317] However, nuances including different binding sites exist that might lead to distinct pharmacological consequences.[318] Actin also influences signaling pathways and actin related protein suggested by the identification of ACTR10 in a genomic siRNA screen for Nrf2 inhibitors.[319,320] In a small molecule screen, the cyanobacterial actin agents lyngbyabellin A (**166**) and dolastatin 12 (**167**) were also identified as inhibitors of Nrf2 signaling, a stress response pathway that is linked to drug resistance (Fig. 37).[311,313,320] Nrf2 is an important regulator of detoxification and electron exchange *via* antioxidant response elements (ARE) gene expression and Phase II detoxification enzyme regulation, critical for cell survival and suppression of carcinogenesis in early stage cancer diagnosis.[318,321] However, overactivation of Nrf2 within cancer cells can induce the overexpression of metabolic enzymes, contributing to the metabolic reprogramming to avoid apoptosis, thus installing a cancer resistance mechanism.[318,321] Grassypeptolide A (**165**) was identified in the same screen as an Nrf2 inhibitor and also sensitized cancer cells to chemotherapeutic tubulin agent vinblastine, revealing a potential opportunity for combination therapy at low doses.[314,320] Grassypeptolide A (**165**) isolated from the marine cyanobacterium *Lyngbya confervoides* has modest (low micromolar) antiproliferative activity and induces p21 and p27 and decreases cyclin D1 expression, presumably leading to the observed G1 cell cycle arrest.[314] These compound classes with unrelated mechanisms would probably benefit from detailed mechanistic studies and could be resurrected for use as agents for combination therapy (Fig. 38).

The total synthesis of grassypeptolide A (**165**) is depicted in Fig. 39.[322,323] The precursors of thiazoline ring, thioacylating agents **169**, and **170** were activated by nitrobenzotriazole and fused into peptide chain (**168**) to afford subunit **171**. The installation of *O*-TBS-Ser was mediated by PyAOP and achieved in 88% yield, but yields were low when other coupling reagents were used (EDCI, HATU, BOPCl, CMPI). A similar problem was encountered in the synthesis of fragment **172**. The esterification of Maba to Pla residue (alcohol) resulted in low yields when mediated by EDCI (DCC)/DMAP and CMPI. However, the acyl chloride method provided 90% yield. The convergent synthesis in which subunits **172** and **171** were jointed between Maba and Thr through

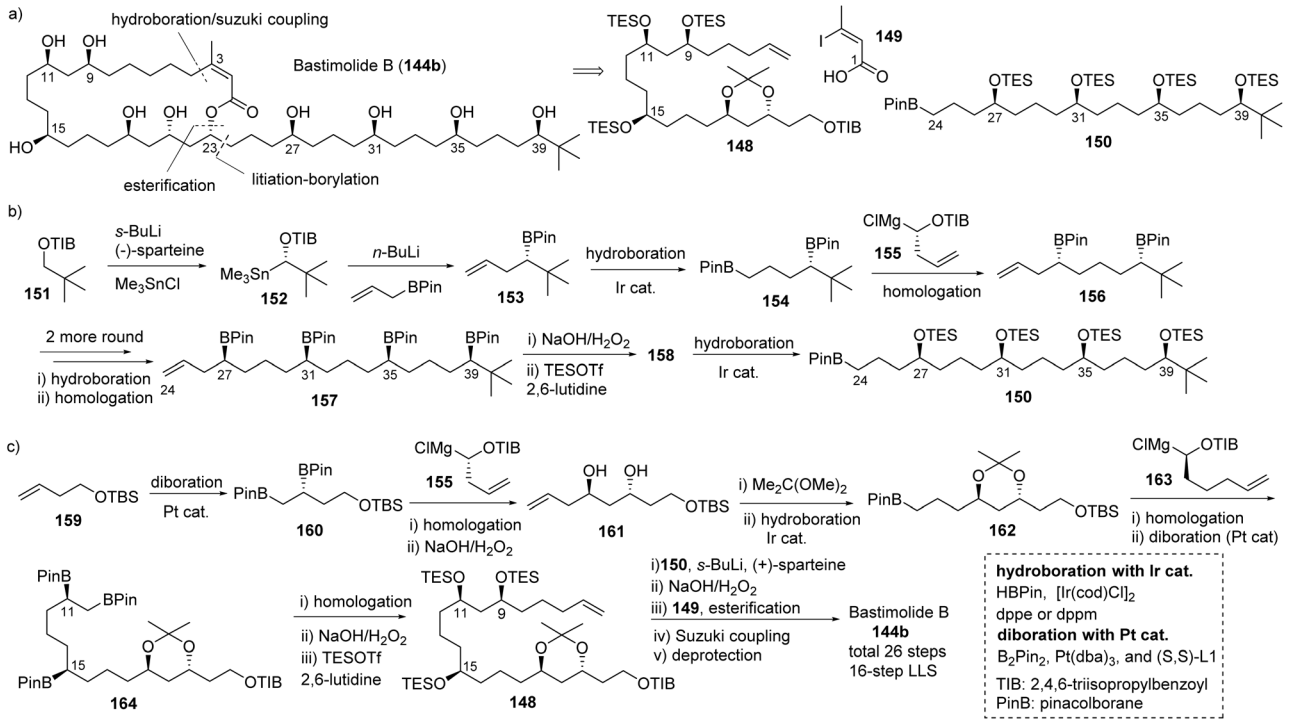

Fig. 36 Total synthesis of bastimolide B (**144b**) with the (a) retrosynthetic analysis, (b) synthesis of the tail, and (c) synthesis of the macrocyclic core and coupling of the two fragments.

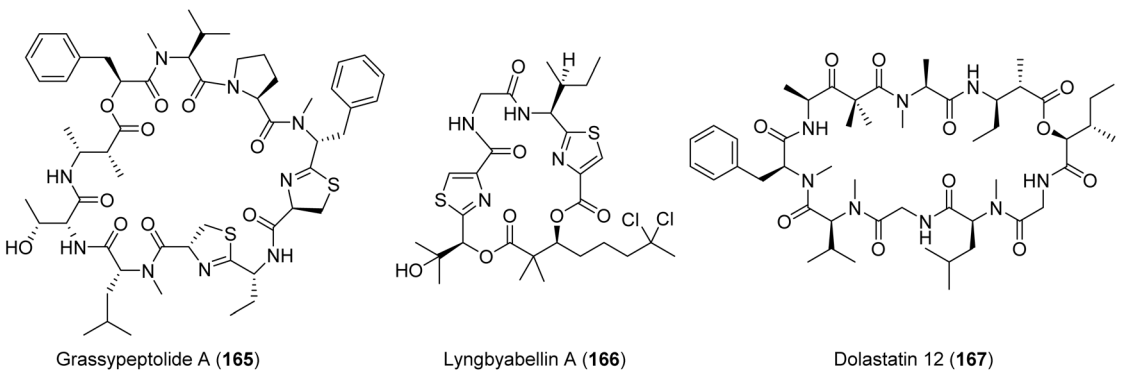

Fig. 37 Structures of grassypeptolide A (**165**), lyngbyabellin A (**166**), and dolastatin 12 (**167**).

amidation, and the site between Pro and *N*-Me-Phe-thn-ca was chosen for macrolactamization, which proceeded smoothly. However, the macrolactonization failed between Maba and Pla and initiated intramolecular cyclization between the Pro and *N*-Me-Phe-thn-ca to form the hydroxy acid. The two thiazoline rings were formed simultaneously when the primary alcohols of thioamide were activated with DAST, following TBS deprotection. However, the secondary alcohol of Thr must be protected (by Troc) in the reaction of bis(thiazoline) ring formation as the free hydroxy would react to form the oxazoline at Thr.

9.2. Synergy with TRAIL: doscadenamides

Tumor necrosis factor-related apoptosis-inducing ligand (TRAIL) binds to death receptors DR4 and DR5, leading to selective cancer cell death.[324] However, recombinant TRAIL protein and agents targeting the TRAIL pathway lacked sufficient efficacy in the clinic due to developing resistance to TRAIL.[325] Quorum sensing (QS) activators in Gram-negative bacteria also have eukaryotic targets with cancer relevance.[326] Mutant studies revealed that doscadenamide A (**175a**, Fig. 40b) binds to LasR to activate quorum sensing in *Pseudomonas aeruginosa*, similar to *N*-(3-oxododecanoyl)-L-homoserine lactone (C12) that was reported to synergize with TRAIL to induce apoptosis in cancer cells.[315] Doscadenamides were first reported from the marine cyanobacterium *Moorena bouillonii* by the Luesch group.[315] Similarly, the doscadenamide scaffold (Fig. 40a) can act as a non-homoserine lactone template for combination with TRAIL or TRAIL pathway activators based on

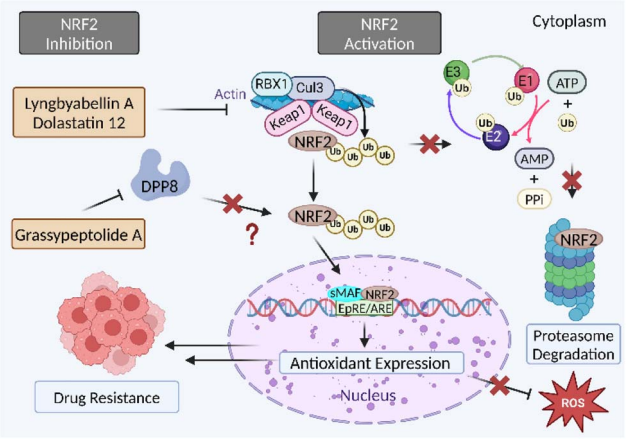

Fig. 38 NRF2 pathway and indirect inhibition to overcome drug resistance.

model studies in triple negative MDA-MB-231 breast cancer cells at 50 μM for most analogues.[327] Synthesis of the natural doscadenamides (**175a**) and a strategic set of analogues (**175b–c**, **175b**) (Fig. 40a and b) solved the supply problem and enabled the rigorous probing of the SAR.[315,327]

Biological testing using various Gram-negative bacteria and TNBC cells (MDA-MB-231) revealed that side chain Moya2 (see **175a** in Fig. 40b) is predominantly responsible for both QS and TRAIL-sensitizing activity.[327] Specifically, doscadenamides F (**175b**, natural product) and S4 (**175c**, synthetic) with partial or complete saturation of the two acyl side chains, respectively, and doscadenamides S10–S12 (synthetic), lacking one of the acyl chains (Moya1), were most effective in sensitizing to TRAIL.[327] These compounds reduced the MDA-MB-231 cancer cell viability and induced PARP cleavage as an indicator of apoptosis. The data suggest that the scaffold may be further tuned to enhance the activity and, with the synthetic method in hand, further rapid diversification can be achieved rather easily.[327]

The total synthesis of doscadenamide A is depicted in Fig. 40c. 7-octynoic acid (Oya) was regio- and stereo-selectively methylated *via* its oxazolidinone derivative (*R*-**177**) to afford (2*R*)-methyl-7-octynoic acid (Moya, *R*-**178**). The (5*S*)-pyrrolinone **180** was synthesized by the condensation of *N*-Fmoc-L-Lyn(Boc)-OH with Meldrum's acid, followed by thermolysis and methylation.[328] The key step for this total synthesis was the acylation of **180**, which was accomplished by treatment of the PFP ester of **178** (**179**) with *n*-BuLi as base at −50 °C to afford intermediate **176a** (doscadenamide S10).[315] Using standard deprotection and coupling protocols, final product doscadenamide A (**175a**) was successfully synthesized from **176** and **178**. Using a parallel strategy, a series of analogues was created to determine the effect of the saturation status of both acyl chains or the necessity of the presence to have one or the other chain (Fig. 40a).

Although the eukaryotic target has not yet been elucidated, the fact that the L-homoserine lactone (C12) and doscadenamides target the same receptor in bacteria and exhibit similar effects in human cancer cells suggest that they may share the same target and/or mechanism in eukaryotic systems, which might provide opportunities to explore cancer vulnerabilities for rational combination therapy. However, the potency of doscadenamides is very low (25 to 50 μM) hence these agents are merely proof-of-concept compounds at this stage.[327]

10. Antimetastatic agents

Several cyanobacterial compounds that do not have inherent cytotoxic anticancer effects have shown to inhibit proteases and modulate GPCRs that mediate cell migration and invasion.[329,330] The cellular effects, mainly assessed in invasive breast cancer cells, suggest their potential as antimetastatic

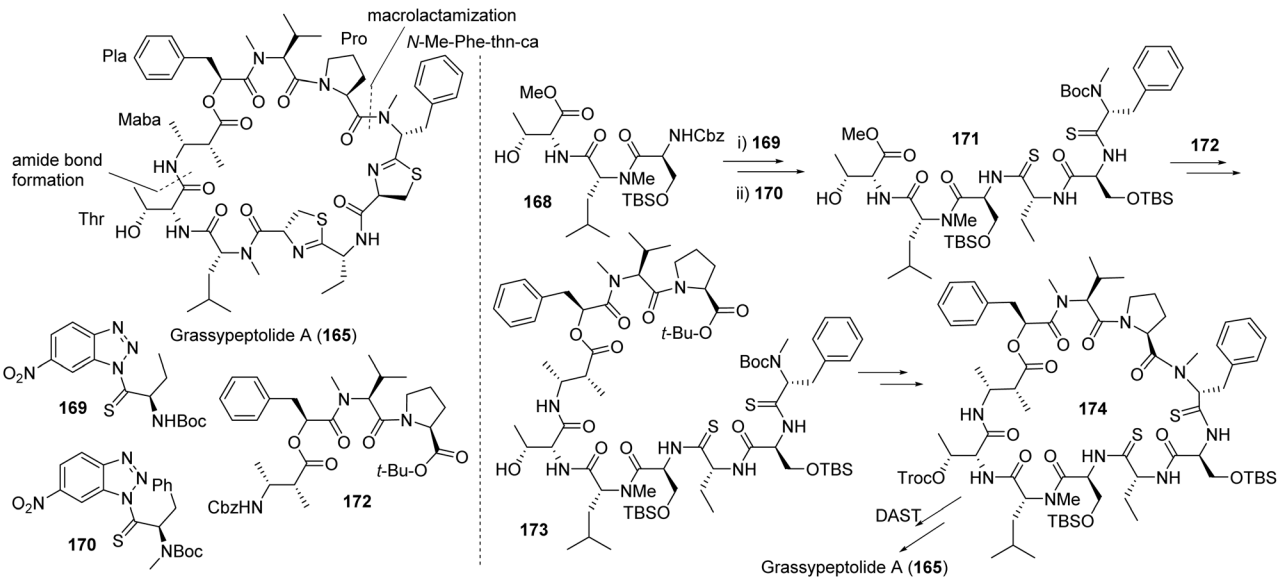

Fig. 39 Total synthesis of grassypeptolide A (**165**).

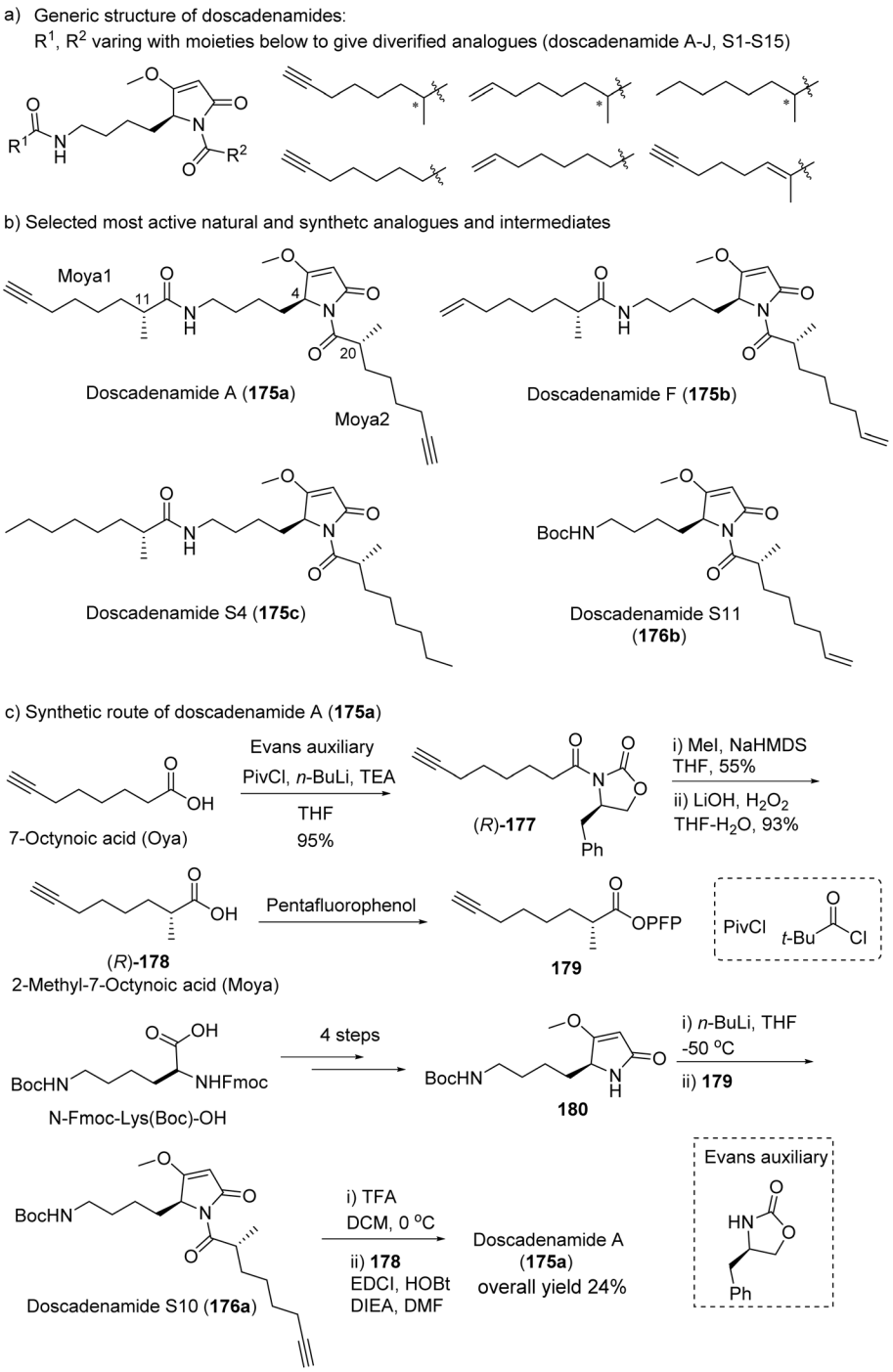

Fig. 40 Natural and synthetic doscadenamides (a) showing generic structure with side chains and (b) structures of selected key analogues with enhanced activity and (c) synthetic route for doscadenamide A (175a).

agents.[331] Proteases are also components of the tumor microenvironment and protease inhibitors might also indirectly affect cancer cells through inhibition of aberrant protein processing in different cell types. As described in Section 3.2, apratoxins also modulate the tumor microenvironment; however, they also have inherent antiproliferative effects that are not observed with the compounds discussed in this section (Fig. 41).

10.1. Protease inhibitors

Drug development efforts for protease inhibitors based on natural products, including those of marine cyanobacterial origin, was recently reviewed.[332] While the focus has been mainly on pulmonary diseases, certain serine proteases play a role in cancer progression and metastasis and are targeted by marine cyanobacterial compounds.[9,332] One such protease is human neutrophil elastase (HNE) which has mainly been

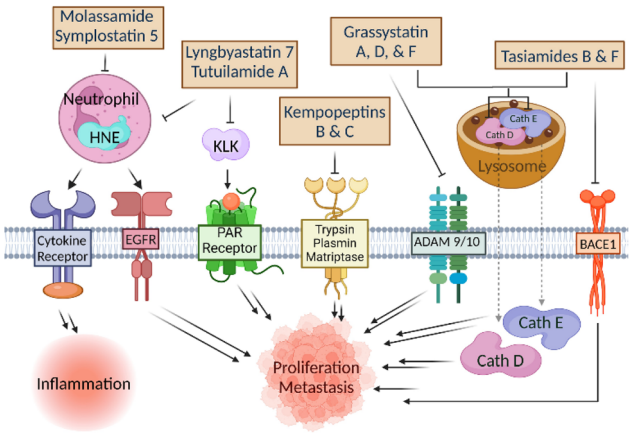

Fig. 41 Protease inhibitors with various targets.

linked to pulmonary inflammatory conditions, but also cancer progression, cell migration and metastasis.[333] HNE has broad substrate specificity and overactivity leads to degradation of extracellular matrix, cleavage of inflammatory mediators and induction of cytokines and growth factors. Dysfunction of kallikreins (KLKs), a group of 15 family members, has also been impacted in cancer and many other disorders.[334] Among them, KLK7 was recently shown to be targeted by the same class of cyclodepsipeptides as HNE inhibitors.[335]

The serine proteases, chymotrypsin-like human neutrophil elastase (HNE), kallikreins (KLK), and trypsin-like enzymes are broad spectrum mediators of biological processes with multiple targets, including cytokine receptors and EGFR for HNE, PAR receptors for KLK, and trypsin, plasmin, and matriptase for trypsin-like proteases.[336] The aspartic proteases include cathepsin D and E which are both biomarkers of cancer (particularly cathepsin D) and induce downstream proliferation of cancer cells after entered the cell from the lysosomes.[337,338] BACE1 is an aspartic protease involved with poor prognosis and overexpression in tumor progression.[339] ADAM9 and 10 are metalloproteases that promote tumor progression and metastasis, with effect on therapeutic resistance and poor diagnosis *via* ADAM9 (Fig. 41).[340]

10.2. Chymotrypsin-like serine protease inhibitors: symplostatin 5, molassamide, lyngbyastatin 7, and tutuilamide A

Among the over 100 members of the 3-amino-6-hydroxy-2-piperidone (Ahp)-containing cyclodepsipeptides with 19-membered core ring structure, only a few have been rigorously characterized and evaluated for potential therapeutic applications (Fig. 42), including symplostatin 5 (**181d**), molassamide (**181b**), lyngbyastatin 7 (Lbs7, **181a**) and tutuilamide A (TtaA, **181i**).[341] While Ahp unit is the classical pharmacophore for the serine protease-inhibitory activity, the adjacent 2-amino-2-butenoic acid (Abu) drives the selectivity towards chymotrypsin-like enzymes (elastase), especially HNE and KLK7, leading to nanomolar to sub-nanomolar activity at the enzyme level (IC_{50}). Selectivity is presumably determined by hydrogen bonding of the Abu unit, as previously seen with the stabilization of the ethylidene unit of Abu *via* CH/π interactions and the interaction of the Abu-containing inhibitor FR901277 towards the porcine pancreatic elastase.[342,343] Specifically, under identical conditions, lyngbyastatin 7 (**181a**) and tutuilamide A (**181i**) inhibited HNE with IC_{50} of 0.85 nM and 0.73 nM, respectively, and human KLK7 with IC_{50} of 3.1 nM and 5.0 nM, respectively.[335] Docking studies of lyngbyastatin 7 (**181a**) and tutuilamide A (**181i**) to HNE showed that both interact with the enzymes similar to other Ahp-Abu elastase inhibitors (Fig. 43).[335] Additionally, docking models of lyngbyastatin 7 and tutuilamide A against KLK7 revealed the presence of key interactions between Asn192 and Phe218, amino acids that are not conserved between other KLK homologues.[335] This could indicate the reason for the observed selectivity of KLK7 by both compounds.

Molassamide (**181b**) first reported from the assemblages of *Dichothrix utahensis*, by the Luesch group, as a representative member of the Ahp-Abu cyclodepsipeptide family was shown to prevent CD40 proteolytic processing in biochemical assays at 1 μM and in MDA-MB-231 breast cancer cells at 10 μM, when exogenously adding 100 nM HNE.[344] CD40 is a membrane protein and member of the tumor necrosis factor receptor family that is a known extracellular HNE substrate, which regulates NF-κB signaling to promote expression of genes encoding breast cancer cell migratory factors, including ICAM-1, which is a cell surface receptor that regulates cell–cell adhesion.[345] Molassamide (**181b**) not only attenuated *ICAM1* gene expression but also inhibited HNE-induced membrane-bound ICAM-1 protein cleavage, therefore preventing soluble ICAM-1 (sICAM-1) release from the cell surface receptor. These molecular changes translated into phenotypic effects, *i.e.*, inhibition of migration specifically of HNE-induced MDA-MB-231 cells but not basal migration.[346]

Lyngbyastatin 7 and tutuilamide A have been synthesized and the side chain diversified, using a different strategy than that previously used for the generation of somamide A (**181c**).[335] The new strategy allowed the late-stage modulation of drug-like properties by introducing changes in the pendant side chain (Fig. 44). The Shioiri group completed the total synthesis of somamide A (**181c**, Fig. 44a) in 2002, as the first member of this Abu-containing Ahp-cyclodepsipeptides.[347] The Ahp unit was viewed as glutamate-derived alcohol and Abu was derived from Thr. Considering the risk of epimerization, they chose the site at Abu/norvaline; in their synthetic strategy, the precursor **182a** was composed of three fragments **184a**, **185a** and **186** and the side chain was installed into fragment **184a** in advance (Fig. 44a). Abu was synthesized from Thr through oxidation by Martin's sulfurane and Ahp was synthesized by biomimetic strategy from 5-OH norvaline *via* its aldehyde (Fig. 44b). In order to build a macrocyclic core-based library for SAR studies, the Luesch group developed a new strategy, constructing the macrocyclic core first and installing the side chain at late-stage (Fig. 44c).[348,349] This new strategy made it is possible to synthesize a small library of lyngbyastatin 7 (**181a**) with diverse side chains (Fig. 44a). In the same

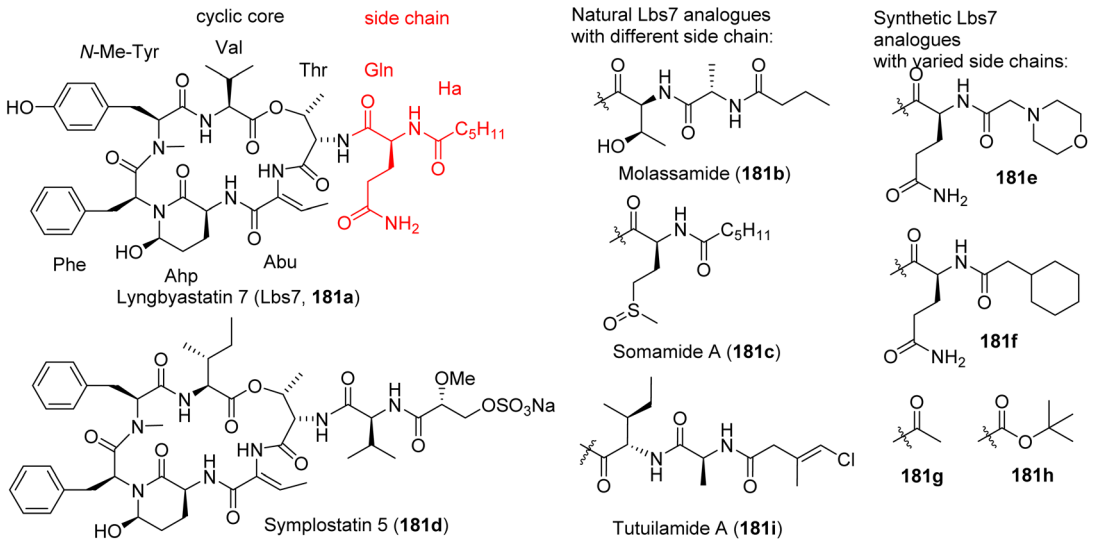

Fig. 42 Structures of lyngbyastatin 7 (**181a**), and symplostatin 5 (**181d**) and naturally occurring and synthetic analogues of lyngbyastatin 7 with side chain modifications.

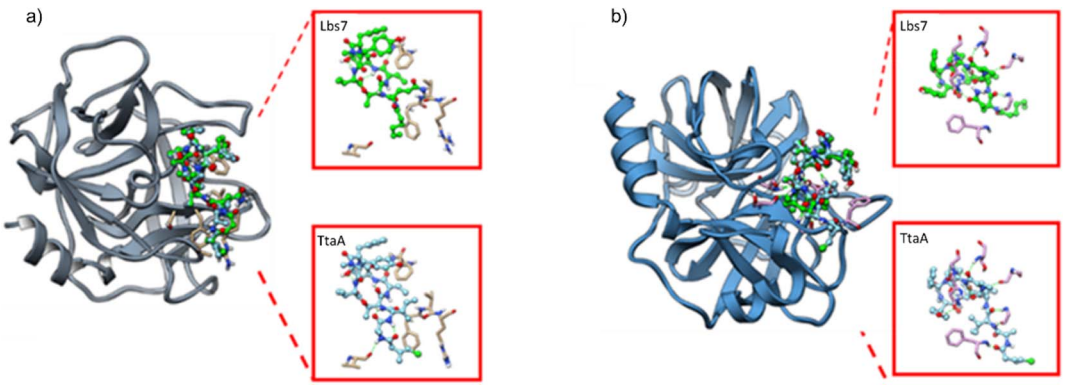

Fig. 43 Molecular docking of lyngbyastatin 7 (**181a**) (Lbs7: green) and tutuilamide A (**181i**) (TtaA: blue) to (a) HNE (PDBID: 3Q76) and (b) KLK7 (PDBID: 2QXI).

fashion, the Luesch group accomplished the total synthesis of tutuilamide A (**181i**) using this convergent approach *via* only five steps from the macrocycle **183** (Fig. 44c).[335]

10.3. Trypsin-like serine protease inhibitors: kempopeptins

The serine protease inhibitors kempopeptins are also Ahp-containing cyclodepsipeptides produced from a tentative *Lyngbya* species, compared with those in Section 10.2, favoring trypsin-like enzymes. The Lys-bearing kempopeptins B and C (**188a,b**, Fig. 45) discovered from a cyanobacterium in the Florida Keys differ only by the nature of the halogen atom (Br *vs.* Cl) at the *N*,*O*-diMe-Tyr moiety.[350,351] Kempopeptin C (**188b**, chlorinated) showed 3- to 7-fold higher potency at the enzyme level in direct comparison to kempopeptin B with IC_{50} values of 0.19 μM (trypsin), 0.36 μM (plasmin) and 0.28 μM (matriptase).[351] Differences in potency might not only be attributed to steric hindrance within the binding pocket from the Br atom, reducing binding affinity, but also to differential electronic effects. Binding of kempopeptin C (**188b**) to the active site of matriptase (Fig. 45) at 1 to 10 μM prevented the cleavage of membrane targets of matriptase, including CDCP1 and desmoglein-2 (Dsg-2), as shown *in vitro* using human recombinant proteins.[351] Kempopeptin C (**188b**, 10 μM) also attenuated CDCP1 cleavage in MDA-MB-231 cells upon exogenous addition of recombinant human matriptase. At the same concentration, a significant inhibitory effect on cell migration was detected, presumably due to inhibition of trypsin-like serine proteases.

When the Abu unit is replaced with a basic residue (Lys, Arg), then the selectivity of the scaffold changes to preferentially inhibit trypsin, plasmin and matriptase, which recognize the X–Y–Z-sequence in substrates. Particularly plasmin and matriptase have been implicated in cancer progression and metastasis because of their processing of cancer-relevant membrane proteins. Despite the wealth of known cyanobacterial serine protease inhibitors specifically targeting these enzymes as

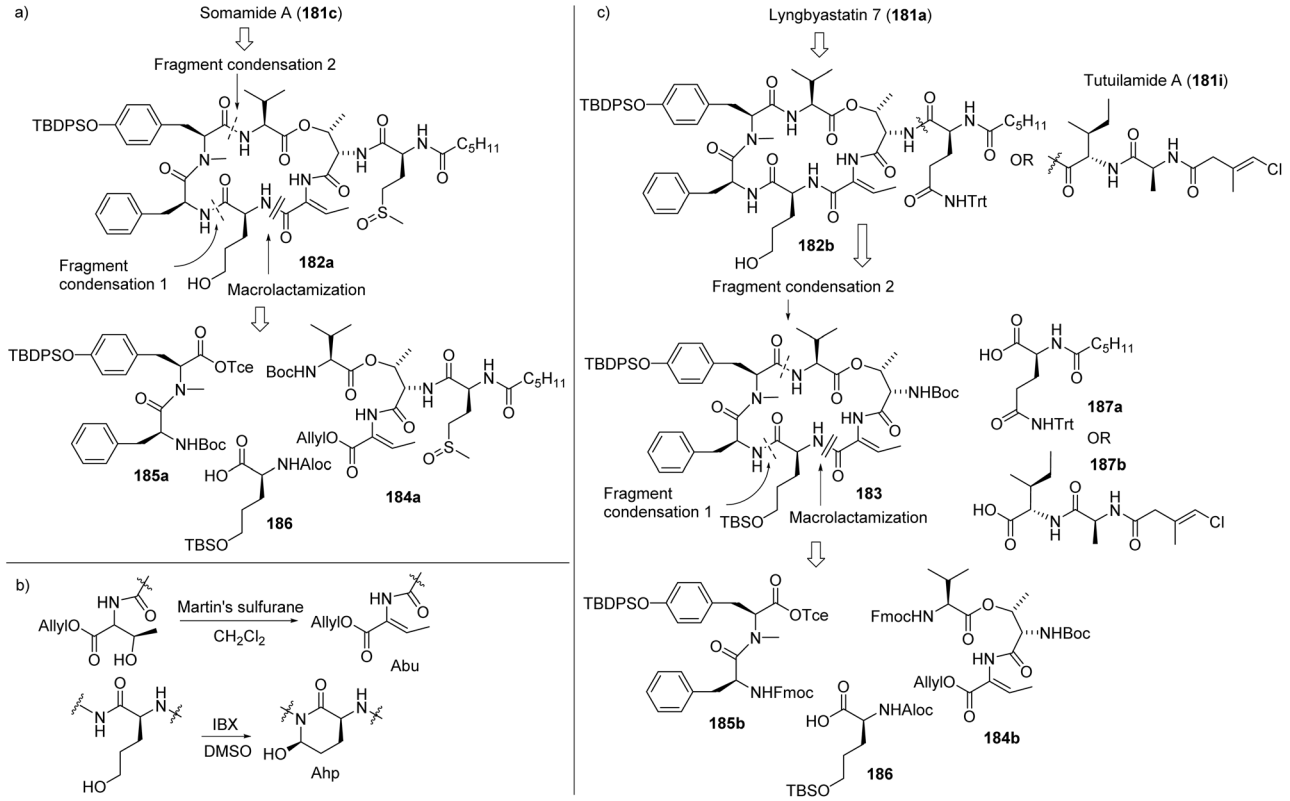

Fig. 44 The different synthetic strategies for (a) somamide (**181c**), (b) the Abu/Ahp unit, and (c) lyngbyastatin 7 (**181a**) and tutuilamide A (**181i**).

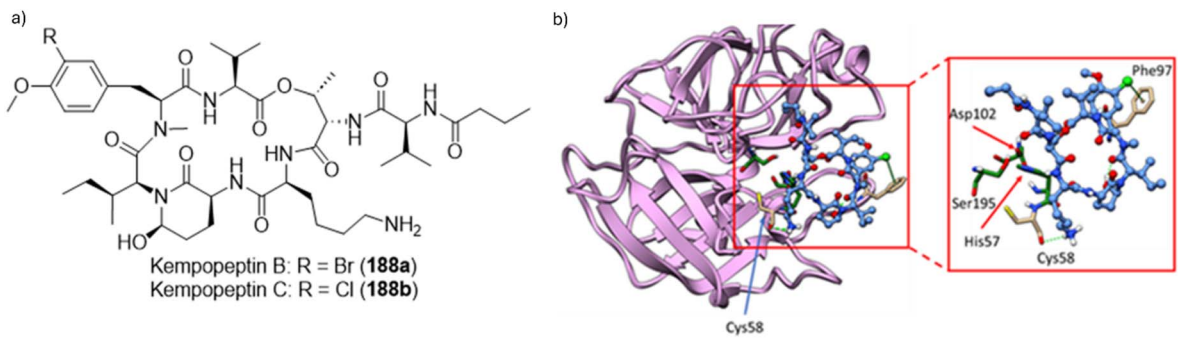

Fig. 45 (a) Structures of kempopeptins B (**188a**) and C (**188b**) and (b) docking of kempopeptin C into matriptase (PDBID: 2GV7).

substrate mimics, including micropeptins,[352,353] there have been limited studies to probe cellular activity and phenotypic consequences in the context of cancer.[354]

10.4. Aspartic protease inhibitors: grassystatins

Among aspartic proteases, particularly cathepsin D has been linked to cancer, as a biomarker for aggressive breast cancer with poor prognosis but also therapeutic target.[337] Cathepsin D controls several signaling cascades, including plasminogen activators and cysteine cathepsins B and L that lead to metastasis and invasion. Specifically, plasminogen activators are inhibited by PAI-1 which is one target of cathepsin D, while another proteolytic cathepsin D target, cystatin C (Cys-C), inhibits cysteine proteases that play a role in cancer progression.[355]

The pepstatin-like aspartic protease inhibitors of the grassystatin class (**189a**, **189b**, Fig. 46) and certain tasiamides, are linear peptides with the statin or statin-derived pharmacophore that potently inhibit cathepsin D and related proteases with differential selectivity for cathepsin E.[356–359] A small subset has been investigated for cellular activity against cathepsin D-mediated molecular changes and migration using MDA-MB-231 breast cancer cells, which are characterized by high levels of cathepsin D and secreted PAI-1 and Cys-C.[357] Grassystatin A (**189a**, Fig. 46) was the most potent cathepsin D inhibitor, while grassystatin F (**189c**) was used in proof-of-concept studies and inhibited migration, in contrast to grassystatin D (**189b**, Fig. 46),

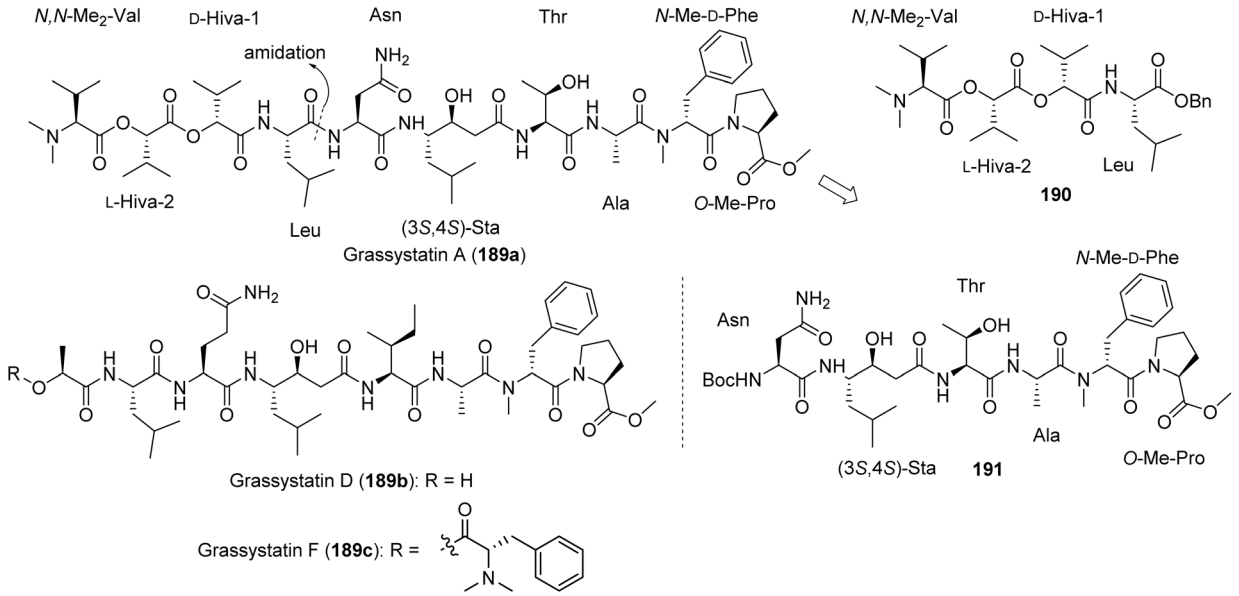

Fig. 46 Chemical structures of grassystatins A (**189a**), D (**189b**) and F (**189c**) with retrosynthetic strategy.

supporting *in vitro* SAR results that underscore the importance of the N-terminal, *N*,*N*-diMe amino acid.[356,357] Selectivity for cathepsin D over cathepsin E may be enhanced by phenyl-statin-containing pharmacophore as in tasiamides B and F and further tuning in other sites based on molecular modeling results (Fig. 47).[358,359]

The first total synthesis of grassystatin A (**189a**, Fig. 46) was reported in 2012.[360] In the retrosynthetic strategy, grassystatin A was disassembled into two sub-fragments at the site Leu/Asn site (**190**, **191**, Fig. 46).[360] Choosing amidation for fragment coupling provided versatility with respect to analogue generation through building different sub-fragments **190** and **191**. Purification by silica gel chromatography led to decomposition; however, the pure final product **189a** was obtained in 45% yield by directly submitting the crude product to HPLC for purification. More recently, the Hunter group designed and synthesized a series of fluorinated analogues of grassystatin A using SPPS.[361]

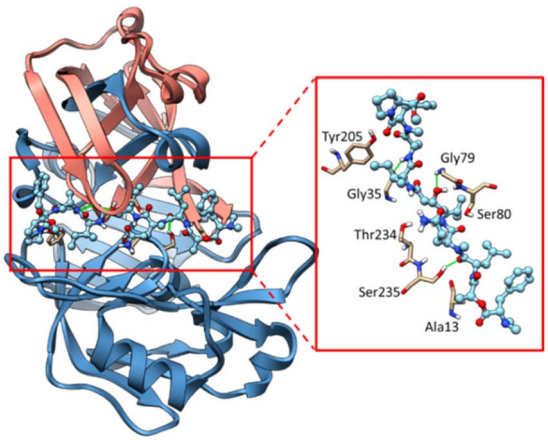

Fig. 47 Molecular docking of grassystatin A (**189a**) into cathepsin E (PDBID: 4PEP).

11. GPCR modulators

G-Protein Coupled Receptors (GPCRs) are a diverse group of membrane receptors that function within most physiological processes across the body. This includes regulation, growth, and homeostasis, with multiple avenues for dysregulation, such as causing an assortment of neurodegenerative disorders, cardiovascular diseases and cancer.[362] Due to the vast effect of the proteins within the physiological functions as well as their downstream affects, GPCRs can affect tumor cell invasion and metastasis, promote favorable conditions for tumor survival by enhancing the tumor microenvironment, and affect abnormal cell growth and survival.[363] Recently, cellular profiling of marine cyanobacterial natural products identified selective GPCR agonists and antagonists, including modulators of cancer-relevant GPCRs.[364]

11.1. Brintonamides

Brintonamides were isolated by the Luesch group from intertidal cyanobacterial mats mainly from Oscillatoriaceae and characterized as modified peptides with dual activity targeting protease and GPCRs (Fig. 48).[365] Using functional, β-arrestin assays, brintonamides C–E (**192c–e**, Fig. 49) have been found to target CCR10, OXTR, SSTR3, TACR2 (antagonism) and CXCR7 (agonism) with differential selectivity profiles depending on the nature of the N-terminal residue that confers the depsipeptide character.[365] Only brintonamide D (**192d**, Fig. 48) exhibited sub-micromolar activity against one of the GPCRs, namely CCR10, while others were in the micromolar range.[365] The C–C motif chemokine receptor 10 (CCR10) selectivity and link of CCR10 to

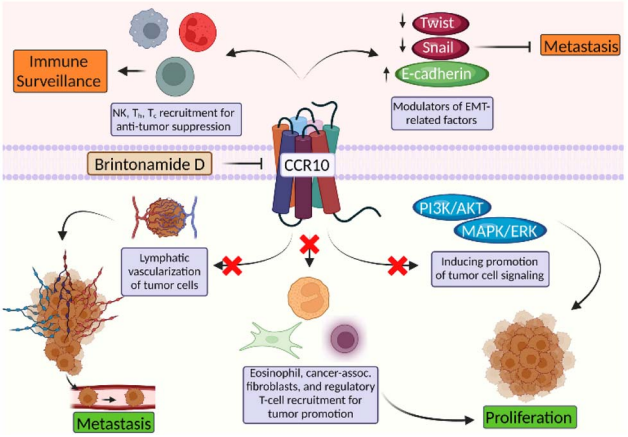

Fig. 48 Activity of brintonamide D (**192d**) as a CCR10 antagonist and potential downstream effects. Only effects on proliferation and on migration as an indicator of metastasis have been studied so far.

metastasis prompted targeted studies to assess the anti-metastatic potential of brintonamides A–E (**192a–e**, Fig. 49) along with synthetic analogues that were accessible through standard methodology.[365]

CCR10 is associated with cutaneous T-cell lymphoma, T-cell mediate skin inflammation and metastasis. A putative binding model for the interaction of brintonamide D with CCR10 is depicted in Fig. 50. CCR10 is the receptor for ligand CCL27. Since the invasive MDA-MB-231 breast cancer cells are TNBCs with high CCR10 expression, the antimetastatic potential was assessed in this cell type using cell proliferation and migration assays upon stimulation with CCL27 under serum-starved condition.[366] Brintonamide D dose-dependently inhibited specifically the CCL-27 induced proliferation (10% viability reduction) and more pronouncedly inhibited migration, which was functionally linked to CCR10 antagonism because the compound phenocopied effects of an siRNA targeting CCR10 but not other GPCRs.[365]

Interestingly, all brintonamides were also inhibitors of the serine protease KLK7, although in high micromolar range and without appreciable SAR and cellular activity against this target.

The total synthesis of brintonamide A (**192a**, Fig. 49b) was accomplished by general SPPS protocol (Fig. 49), in which Fmoc-L-Pro was attached to CTC resin first, and then other amino acids were attached sequentially (C → N). The cleavage from the CTC resin, followed by sequential methylation of the C-terminal Pro and acylation of the other Pro by Hmpa provided the final product, brintonamide A (**192a**). Further esterification of brintonamide A by cinnamide acid using Yamaguchi method afforded brintonamide D (**192d**).[365] Other analogues were synthesized using same protocol and provided critical insight into the SAR.

12. Perspective & conclusion

Marine cyanobacteria are a promising source of new drug candidates, particular for cancer, as validated by the approval of several ADCs with cyanobacteria-based cytotoxic payloads. As

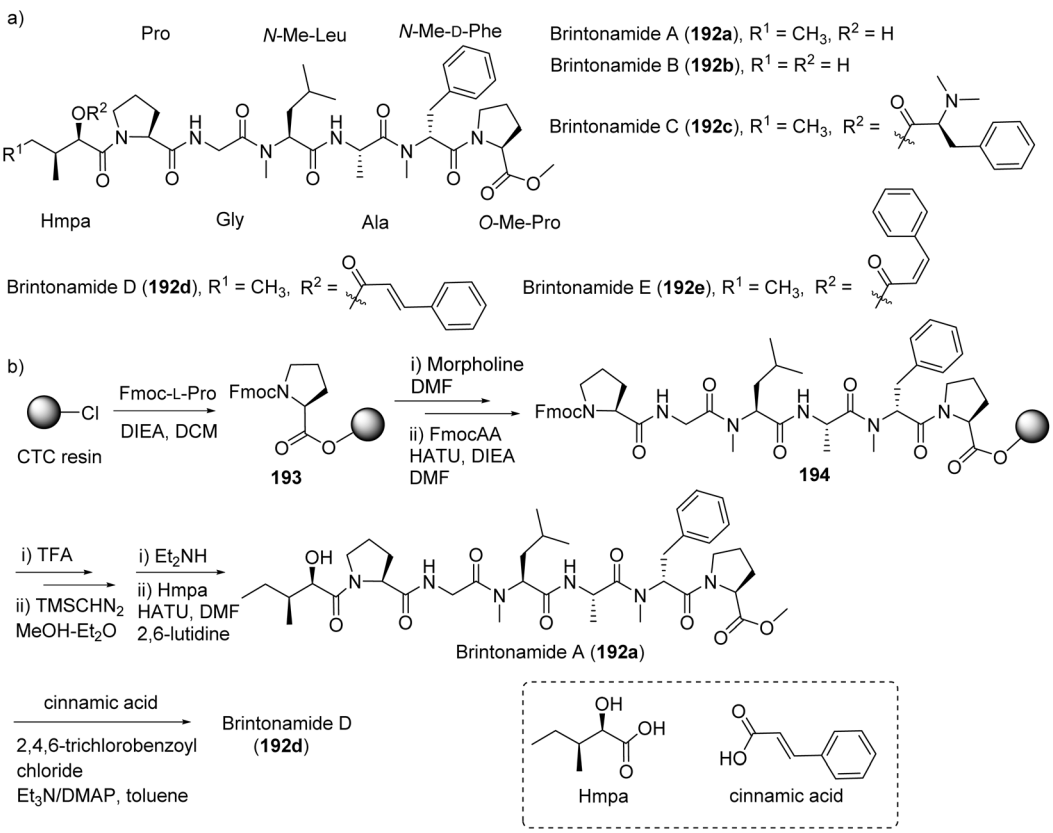

Fig. 49 Brintonamides A–D (**192a–d**) (a) chemical structures and (b) synthesis.

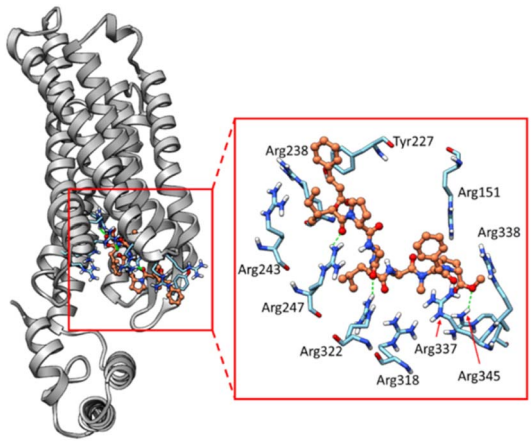

Fig. 50 Molecular docking of brintonamide D (**192d**) into CCR10 homology model (PDBIDs: 5LWE, 5UIW, 4MBS, 4RWD, 4N6H, 3OE9).

demonstrated in the review, many compounds from these sources represent new chemical scaffolds that target novel pharmacological space (Fig. 51). In other cases, biological targets may be identical to those of compounds from other microbial, including terrestrial sources; however, the potency is oftentimes superior or binding sites differ. Even though the pharmacophore may be similar to those from other sources, the specific decoration or modifications modulate selectivity profiles. Cyanobacterial protecting group chemistry that keeps compounds in a latent condition may also be unique or characteristic. Natural products research oftentimes leads to the elucidation of a structurally intriguing compound. However, the structural beauty (to a natural product chemist) is not enough to trigger developmental efforts. Translating the chemical diversity into therapeutic potential requires target identification, rigorous pharmacological profiling, and mechanistic studies, which can guide towards suitable biomedical applications. The identification of novel biology ultimately justifies and drives the tedious and sometimes seemingly brute-de-force chemistry, which should never be the major hurdle given the expense of drug development at other stages that is larger by magnitudes. The medicinal chemistry campaigns are not as elaborate as for non-natural products due to the structural complexity. They may also not have to be as extensive since compounds are already fairly optimized by nature for physiologically relevant targets. Adaption to human targets and physiology may require tweaking selectivity or dialing out liabilities that may lead to off-target toxicity. Oftentimes the starting point provided by nature is good enough, assuming intellectual property protection concerns can be addressed to ensure development.[367]

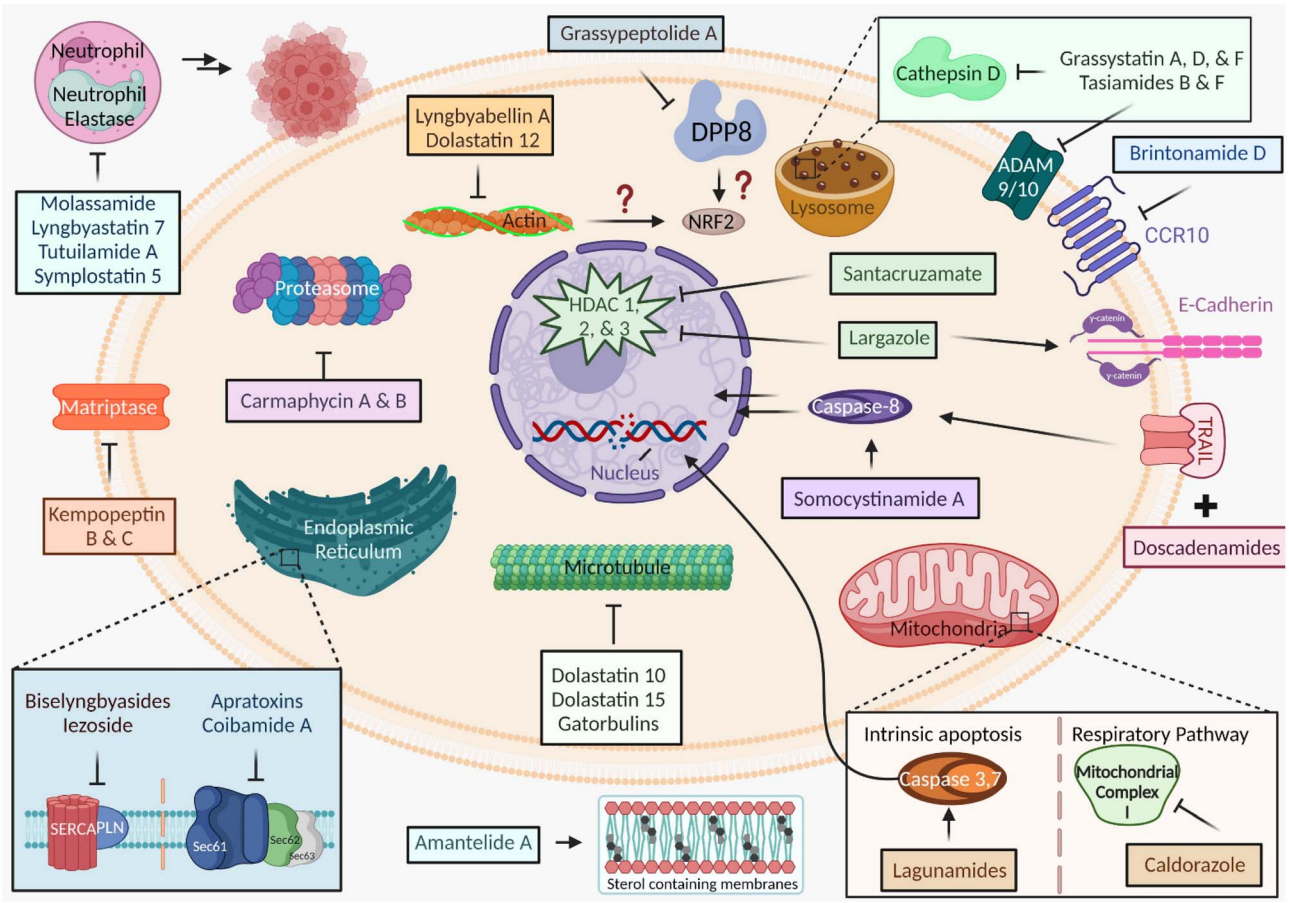

Fig. 51 Overview of marine cyanobacterial anticancer agents and their various targets.

Fundamentally, both the supply problem and novel pharmacological action need to be addressed in order to differentiate the compounds from other agents in development or in the clinic. For almost all compounds discussed in this review, the key biology (target) and chemistry (supply) issues have been solved. Some compounds may not have drug-like properties; however, they could provide the basis for the design of compounds with similar pharmacology that are more amenable for development. The target space of cyanobacterial agents is tremendously broad for cancer alone. While this review has focused on cancer, the same approach can be applied to other disease indications, particularly infectious diseases, where natural products always have been playing and will continue to play a dominant role.[368]

Lastly, we have only seen the tip of the iceberg of specialized metabolites from marine cyanobacteria, as genome or metagenome sequencing suggest that the biosynthetic potential is oftentimes 10-fold higher than what is observed at the chemical level.[369] Translating biosynthetic potential into screenable and therefore actionable compounds through synthetic biology is another exciting avenue in the field and for drug discovery.[353,370,371] Furthermore, enabling technologies such as antibody conjugation and other emerging technologies will guarantee that we maximize the potential of these evolutionarily optimized compounds.[372–374]

13. Conflicts of interest

H. L. is cofounder of Oceanyx Pharmaceuticals, Inc. that has licensed patents and patent applications related to apratoxins and optioned patents based on largazole.

14 Acknowledgements

Anticancer drug discovery from marine cyanobacteria in the authors' laboratory is supported by the NIH grant R01CA172310 (H. L.), and the Debbie and Sylvia DeSantis Chair professorship (H. L.). E. K. E. is supported by NIGMS grant T32GM136583: Chemistry–Biology Interface Training Program at the University of Florida. We thank Gustavo Seabra (University of Florida) for preparing docking figures. Pathway figures were created using BioRender.

15 References

1 A. G. Atanasov, S. B. Zotchev, V. M. Dirsch and C. T. Supuran, *Nat. Rev. Drug Discovery*, 2021, **20**, 200–216.
2 J. A. Beutler, *Curr. Protoc. Pharmacol.*, 2019, **86**, e67.
3 D. J. Newman and G. M. Cragg, *J. Nat. Prod.*, 2020, **83**, 770–803.
4 X. Liang, D. Luo and H. Luesch, *Pharmacol. Res.*, 2019, **147**, 104373.
5 L. Wan, G. Kong, M. Liu, M. Jiang, D. Cheng and F. Chen, *Green Synth. Catal.*, 2022, **3**, 243–258.
6 G. Li, X. Peng, Y. Guo, S. Gong, S. Cao and F. Qiu, *Front. Chem.*, 2021, **9**, 761609.
7 K. C. Nicolaou, S. Pan, Y. Shelke, S. Rigol, R. Bao, D. Das and Q. Ye, *Proc. Natl. Acad. Sci. U. S. A.*, 2022, **119**, e2208938119.
8 Approved Marine Drugs, **https://www.marinepharmacology.org/approved**, accessed December 15, 2023.
9 L. T. Tan and M. Y. Phyo, *Molecules*, 2020, **25**, 2197.
10 R. Carpine and S. Sieber, *Curr. Res. Biotechnol.*, 2021, **3**, 65–81.
11 N. Haque, S. Parveen, T. Tang, J. Wei and Z. Huang, *Mar. Drugs*, 2022, **20**, 528.
12 L. A. Salvador-Reyes and H. Luesch, *Nat. Prod. Rep.*, 2015, **32**, 478–503.
13 B. Robles-Bañuelos, L. M. Durán-Riveroll, E. Rangel-López, H. I. Pérez-López and L. González-Maya, *Molecules*, 2022, **27**, 4814.
14 J. Xu, T. Zhang, J. Yao, J. Lu, Z. Liu and L. Ding, *Eur. J. Med. Chem.*, 2020, **201**, 112473.
15 T. Nawaz, L. Gu, S. Fahad, S. Saud, Z. Jiang, S. Hassan, M. T. Harrison, K. Liu, M. A. Khan, H. Liu, K. El-Kahtany, C. Wu, M. Zhu and R. Zhou, *Food Energy Secur.*, 2023, **12**, e495.
16 P. M. D'Agostino, *Nat. Prod. Rep.*, 2023, **40**, 1701–1717.
17 R. Kaul, A. L. Risinger and S. L. Mooberry, *J. Nat. Prod.*, 2019, **82**, 680–685.
18 S. Dall'Acqua, *Curr. Top. Med. Chem.*, 2014, **14**, 2272–2285.
19 A. Akhmanova and M. O. Steinmetz, *Nat. Rev. Mol. Cell Biol.*, 2015, **16**, 711–726.
20 T. Mühlethaler, D. Gioia, A. E. Prota, M. E. Sharpe, A. Cavalli and M. O. Steinmetz, *Angew. Chem., Int. Ed.*, 2021, **60**, 13331–13342.
21 M. Dogterom and G. H. Koenderink, *Nat. Rev. Mol. Cell Biol.*, 2019, **20**, 38–54.
22 B. Kumar, R. Kumar, I. Skvortsova and V. Kumar, *Curr. Cancer Drug Targets*, 2017, **17**, 357–375.
23 A. V. Blokhin, H. D. Yoo, R. S. Geralds, D. G. Nagle, W. H. Gerwick and E. Hamel, *Mol. Pharmacol.*, 1995, **48**, 523–531.
24 M. O. Steinmetz and A. E. Prota, *Trends Cell Biol.*, 2018, **28**, 776–792.
25 S. Matthew, Q.-Y. Chen, R. Ratnayake, C. S. Fermaintt, D. Lucena-Agell, F. Bonato, A. E. Prota, S. T. Lim, X. Wang, J. F. Díaz, A. L. Risinger, V. J. Paul, M. Á. Oliva and H. Luesch, *Proc. Natl. Acad. Sci. U. S. A.*, 2021, **118**, e2021847118.
26 H. Pérez-Peña, A.-C. Abel, M. Shevelev, A. E. Prota, S. Pieraccini and D. Horvath, *Biomolecules*, 2023, **13**, 285.
27 D. Panda, R. H. Himes, R. E. Moore, L. Wilson and M. A. Jordan, *Biochemistry*, 1997, **36**, 12948–12953.
28 R. Bai, G. R. Petit and E. Hamel, *Biochem. Pharmacol.*, 1990, **39**, 1941–1949.
29 R. Bai, S. J. Friedman, G. R. Pettit and E. Hamel, *Biochem. Pharmacol.*, 1992, **43**, 2637–2645.
30 E. Eren, N. R. Watts, D. L. Sackett and P. T. Wingfield, *J. Biol. Chem.*, 2021, **297**, 101138.
31 Q.-Y. Chen, R. Ratnayake, R. Hortigüela, G. M. Seabra, M. D. Cameron, J. Fernando Díaz, M. Ángela Oliva and H. Luesch, *Bioorg. Med. Chem.*, 2023, **95**, 117506.

32 L. Wordeman and J. J. Vicente, *Cancers*, 2021, **13**, 5650.
33 S. L. Holbeck, J. M. Collins and J. H. Doroshow, *Mol. Cancer Ther.*, 2010, **9**, 1451–1460.
34 G. R. Pettit, Y. Kamano, C. L. Herald, A. A. Tuinman, F. E. Boettner, H. Kizu, J. M. Schmidt, L. Baczynskyj, K. B. Tomer and R. J. Bontems, *J. Am. Chem. Soc.*, 1987, **109**, 6883–6885.
35 H. Luesch, R. E. Moore, V. J. Paul, S. L. Mooberry and T. H. Corbett, *J. Nat. Prod.*, 2001, **64**, 907–910.
36 N. Engene, A. Tronholm, L. A. Salvador-Reyes, H. Luesch and V. J. Paul, *J. Phycol.*, 2015, **51**, 670–681.
37 G. R. Pettit, Y. Kamano, C. L. Herald, Y. Fujii, H. Kizu, M. R. Boyd, F. E. Boettner, D. L. Doubek, J. M. Schmidt, J.-C. Chapuis and C. Michel, *Tetrahedron*, 1993, **49**, 9151–9170.
38 A. Maki, R. Mohammad, S. Raza, M. Saleh, K. D. Govindaraju, G. R. Pettit and A. Al-Katib, *Anticancer Drugs*, 1996, **7**, 344–350.
39 T. Turner, W. H. Jackson, G. R. Pettit, A. Wells and A. S. Kraft, *Prostate*, 1998, **34**, 175–181.
40 G. P. Kalemkerian, X. Ou, M. R. Adil, R. Rosati, M. M. Khoulani, S. K. Madan and G. R. Pettit, *Cancer Chemother. Pharmacol.*, 1999, **43**, 507–515.
41 S. B. Singh, *J. Nat. Prod.*, 2022, **85**, 666–687.
42 K. Tomioka, M. Kanai and K. Koga, *Tetrahedron Lett.*, 1991, **32**, 2395–2398.
43 K. Miyazaki, M. Kobayashi, T. Natsume, M. Gondo, T. Mikami, K. Sakakibara and S. Tsukagoshi, *Chem. Pharm. Bull.*, 1995, **43**, 1706–1718.
44 A. Maderna, M. Doroski, C. Subramanyam, A. Porte, C. A. Leverett, B. C. Vetelino, Z. Chen, H. Risley, K. Parris, J. Pandit, A. H. Varghese, S. Shanker, C. Song, S. C. K. Sukuru, K. A. Farley, M. M. Wagenaar, M. J. Shapiro, S. Musto, M.-H. Lam, F. Loganzo and C. J. O'Donnell, *J. Med. Chem.*, 2014, **57**, 10527–10543.
45 P. D. Senter and E. L. Sievers, *Nat. Biotechnol.*, 2012, **30**, 631–637.
46 G. Gao, Y. Wang, H. Hua, D. Li and C. Tang, *Mar. Drugs*, 2021, **19**, 363.
47 Y.-T. Tai, P. A. Mayes, C. Acharya, M. Y. Zhong, M. Cea, A. Cagnetta, J. Craigen, J. Yates, L. Gliddon, W. Fieles, B. Hoang, J. Tunstead, A. L. Christie, A. L. Kung, P. Richardson, N. C. Munshi and K. C. Anderson, *Blood*, 2014, **123**, 3128–3138.
48 J. A. Francisco, C. G. Cerveny, D. L. Meyer, B. J. Mixan, K. Klussman, D. F. Chace, S. X. Rejniak, K. A. Gordon, R. DeBlanc, B. E. Toki, C.-L. Law, S. O. Doronina, C. B. Siegall, P. D. Senter and A. F. Wahl, *Blood*, 2003, **102**, 1458–1465.
49 D. Dornan, F. Bennett, Y. Chen, M. Dennis, D. Eaton, K. Elkins, D. French, M. A. T. Go, A. Jack, J. R. Junutula, H. Koeppen, J. Lau, J. McBride, A. Rawstron, X. Shi, N. Yu, S.-F. Yu, P. Yue, B. Zheng, A. Ebens and A. G. Polson, *Blood*, 2009, **114**, 2721–2729.
50 P. M. Challita-Eid, D. Satpayev, P. Yang, Z. An, K. Morrison, Y. Shostak, A. Raitano, R. Nadell, W. Liu, D. R. Lortie, L. Capo, A. Verlinsky, M. Leavitt, F. Malik, H. Aviña, C. I. Guevara, N. Dinh, S. Karki, B. S. Anand, D. S. Pereira, I. B. J. Joseph, F. Doñate, K. Morrison and D. R. Stover, *Cancer Res.*, 2016, **76**, 3003–3013.
51 A. López de Sá, C. Díaz-Tejeiro, E. Poyatos-Racionero, C. Nieto-Jiménez, L. Paniagua-Herranz, A. Sanvicente, E. Calvo, P. Pérez-Segura, V. Moreno, F. Moris and A. Ocana, *J. Hematol. Oncol.*, 2023, **16**, 118.
52 *Center for Drug Evaluation and Research (CDER)*, FDA, accessed March 13, 2024.
53 S. Trudel, N. Lendvai, R. Popat, P. M. Voorhees, B. Reeves, E. N. Libby, P. G. Richardson, L. D. Anderson, H. J. Sutherland, K. Yong, A. Hoos, M. M. Gorczyca, S. Lahiri, Z. He, D. J. Austin, J. B. Opalinska and A. D. Cohen, *Lancet Oncol.*, 2018, **19**, 1641–1653.
54 J. T. W. Tong, P. W. R. Harris, M. A. Brimble and I. Kavianinia, *Molecules*, 2021, **26**, 5847.
55 M. A. Dimopoulos, V. T. M. Hungria, A. Radinoff, S. Delimpasi, G. Mikala, T. Masszi, J. Li, M. Capra, A. Maiolino, V. Pappa, D. Chraniuk, I. Osipov, X. Leleu, M. Low, M. Matsumoto, N. Sule, M. Li, A. McKeown, W. He, S. Bright, B. Currie, S. Perera, J. Boyle, S. Roy-Ghanta, J. Opalinska and K. Weisel, *Lancet Haematol.*, 2023, **10**, e801–e812.
56 GSK provides an update on Blenrep (belantamab mafodotin-blmf) US marketing authorization | GSK US, **https://us.gsk.com/en-us/media/press-releases/gsk-provides-an-update-on-blenrep-belantamab-mafodotin-blmf-us-marketing-authorization/**, accessed September 20, 2024.
57 L. H. Sehn, A. F. Herrera, C. R. Flowers, M. K. Kamdar, A. McMillan, M. Hertzberg, S. Assouline, T. M. Kim, W. S. Kim, M. Ozcan, J. Hirata, E. Penuel, J. N. Paulson, J. Cheng, G. Ku and M. J. Matasar, *J. Clin. Oncol.*, 2020, **38**(2), 155–165.
58 Seagen Inc., *Open Label Phase 2 Study of Tisotumab Vedotin for Locally Advanced or Metastatic Disease in Solid Tumors*, **https://clinicaltrials.gov/**, accessed March 13, 2024.
59 E. D. Deeks, *Drugs*, 2021, **81**, 1929–1935.
60 J. W. Goldman, H. Horinouchi, B. C. Cho, P. Tomasini, M. Dunbar, D. Hoffman, A. Parikh, V. Blot and D. R. Camidge, *J. Clin. Oncol.*, 2022, **40**, 9013.
61 W. Yu, M. P. Ramprasad, M. Pal, C. Chen, S. Paruchuri, L. Skidmore, N. Knudsen, M. Allen and Y. Buechler, *PLoS One*, 2023, **18**, e0284198.
62 G. E. Mudd, H. Scott, L. Chen, K. van Rietschoten, G. Ivanova-Berndt, K. Dzionek, A. Brown, S. Watcham, L. White, P. U. Park, P. Jeffrey, M. Rigby and P. Beswick, *J. Med. Chem.*, 2022, **65**, 14337–14347.
63 G. Bennett, A. Brown, G. Mudd, P. Huxley, K. Van Rietschoten, S. Pavan, L. Chen, S. Watcham, J. Lahdenranta and N. Keen, *Mol. Cancer Ther.*, 2020, **19**, 1385–1394.
64 N. D. Bodyak, R. Mosher, A. V. Yurkovetskiy, M. Yin, C. Bu, P. R. Conlon, D. R. Demady, M. J. DeVit, D. R. Gumerov, V. R. Gurijala, W. Lee, D. McGillicuddy, P. U. Park, L. L. Poling, M. Protopova, L. Qin, C. A. Stevenson, E. Ter-Ovanesyan, A. Uttard, D. Xiao, J. Xu, L. Xu,

D. A. Bergstrom and T. B. Lowinger, *Mol. Cancer Ther.*, 2021, **20**, 896–905.
65 A. V. Yurkovetskiy, N. D. Bodyak, M. Yin, J. D. Thomas, S. M. Clardy, P. R. Conlon, C. A. Stevenson, A. Uttard, L. Qin, D. R. Gumerov, E. Ter-Ovanesyan, C. Bu, A. J. Johnson, V. R. Gurijala, D. McGillicuddy, M. J. DeVit, L. L. Poling, M. Protopopova, L. Xu, Q. Zhang, P. U. Park, D. A. Bergstrom and T. B. Lowinger, *Mol. Cancer Ther.*, 2021, **20**, 885–895.
66 L. Li, A. Hau, W. Tong, M. Lau, T. Zhu, K. Fells, A. Wei, X. Li, D. Deng, Y. Sun, E. Kovacs, A. Khasanov, Z. Yan, P. Zhu, H. Zhou, H. Ji, H. Li and H. Zhang, *Cancer Res.*, 2020, **80**, LB–227.
67 Q. Li, L. Wang, J. Zhang, G. Zhao, Z. Liu, X. Ma and J. Jiang, *Clin. Transl. Sci.*, 2023, **16**, 1232–1242.
68 J. Zhang, R. Liu, S. Gao, W. Li, Y. Chen, Y. Meng, C. Liu, W. Jin, J. Wu, Y. Wang, Y. Hao, S. Yi, Y. Qing, J. Ge and X. Hu, *npj Breast Cancer*, 2023, **9**, 28.
69 F. Han, F. Wang, Y.-R. Shi, Y. Guo, X.-L. Shu, S. Pan, S.-H. Qu, P. Zhang, Y. Jiang, M.-J. Xu, K. Lei, S. Qu, F. Lei, X. Lv, Y.-Q. Xiang and R.-H. Xu, *Ann. Oncol.*, 2023, **34**, S559.
70 B. Akla, M. Broussas, N. Loukili, A. Robert, C. Beau-Larvor, M. Malissard, N. Boute, T. Champion, J.-F. Haeuw, A. Beck, M. Perez, C. Dreyfus, M. Pavlyuk, E. Chetaille and N. Corvaia, *Mol. Cancer Ther.*, 2020, **19**, 168–177.
71 C. Kollmannsberger, T. K. Choueiri, D. Y. C. Heng, S. George, F. Jie, R. Croitoru, S. Poondru and J. A. Thompson, *Oncologist*, 2021, **26**, 182–e361.
72 A. L. Ho, D. Adkins, J. H. Lorch, J. S. Thomas and J. S. Grewal, *J. Clin. Oncol.*, 2023, **41**, TPS6107.
73 L. Kujtan and J. Subramanian, *Transl. Lung Cancer Res.*, 2023, **12**, 1826–1829.
74 A. Rizzo, A. Cusmai, S. Acquafredda, L. Rinaldi and G. Palmiotti, *Expert Opin. Invest. Drugs*, 2022, **31**, 495–498.
75 CAB Portfolio – BioAtla, **https://www.bioatla.com/cabportfolio/**, accessed March 13, 2024.
76 J. Shen, R. Pachynski, L. Nordquist, N. Adra, M. Bilen, R. Aggarwal, Z. Reichert, M. Schweizer, D. Xu, M. Patel, J. Zhang, W. Shi, D. Z. L'Heureux and S. Tagawa, *Cancer Res.*, 2023, **83**, CT121.
77 M. L. Maitland, J. C. Sachdev, M. R. Sharma, V. Moreno, V. Boni, S. Kummar, E. Stringer-Reasor, N. Lakhani, A. R. Moreau, D. Xuan, R. Li, E. L. Powell, A. Jackson-Fisher, M. Bowers, S. Alekar, X. Xin, A. W. Tolcher and E. Calvo, *Clin. Cancer Res.*, 2021, **27**, 4511–4520.
78 R. P. Lyon, M. W. Schmitt, M. Jonas, C. E. Franz, E. S. Trueblood, R. Yumul, L. Westendorf and M. C. Ryan, *Cancer Res.*, 2020, **80**, 2906.
79 K. Jhaveri, H. Han, E. Dotan, D.-Y. Oh, C. Ferrario, A. Tolcher, K.-W. Lee, C.-Y. Liao, Y.-K. Kang, Y. H. Kim, E. Hamilton, A. Spira, N. Patel, C. Karapetis, S. Y. Rha, L. Boyken, J. Woolery and P. Bedard, *Ann. Oncol.*, 2022, **33**, S749–S750.
80 Y. H. Park, H. K. Ahn, J.-Y. Kim, J. S. Ahn, Y.-H. Im, S.-H. Kim, S. Lee, H.-S. CHUNG and S. J. Park, *J. Clin. Oncol.*, 2020, **38**, 3551.
81 G. R. Pettit, S. B. Singh, F. Hogan, P. Lloyd-Williams, D. L. Herald, D. D. Burkett and P. J. Clewlow, *J. Am. Chem. Soc.*, 1989, **111**, 5463–5465.
82 F. Roux, I. Maugras, J. Poncet, G. Niel and P. Jouin, *Tetrahedron*, 1994, **50**, 5345–5360.
83 T. Shioiri and Y. Hamada, *Synlett*, 2001, **2001**, 184–201.
84 C. Mordant, S. Reymond, H. Tone, D. Lavergne, R. Touati, B. Ben Hassine, V. Ratovelomanana-Vidal and J.-P. Genet, *Tetrahedron*, 2007, **63**, 6115–6123.
85 W. Zhou, X.-D. Nie, Y. Zhang, C.-M. Si, Z. Zhou, X. Sun and B.-G. Wei, *Org. Biomol. Chem.*, 2017, **15**, 6119–6131.
86 World Intellectual Property Organization, WO02088172A2, 2002.
87 K. M. Bajjuri, Y. Liu, C. Liu and S. C. Sinha, *ChemMedChem*, 2011, **6**, 54–59.
88 G. R. Pettit , J. Barkoczy, *US Pat.*, US5635483A, 1997.
89 S. Yokosaka, A. Izawa, C. Sakai, E. Sakurada, Y. Morita and Y. Nishio, *Bioorg. Med. Chem.*, 2018, **26**, 1643–1652.
90 M. Akaiwa, T. Martin and B. A. Mendelsohn, *ACS Omega*, 2018, **3**, 5212–5221.
91 R. Ratnayake, S. P. Gunasekera, J. J. Ma, L. H. Dang, T. J. Carney, V. J. Paul and H. Luesch, *Eur. J. Biol. Chem. Res.*, 2020, **21**, 2356–2366.
92 G. M. Cragg, D. G. I. Kingston and D. J. Newman, *Anticancer Agents from Natural Products*, CRC Press, Boca Raton, 1st edn, 2005.
93 M. Lopus, *Mol. Cell. Biochem.*, 2013, **382**, 93–102.
94 A. Ray, T. Okouneva, T. Manna, H. P. Miller, S. Schmid, L. Arthaud, R. Luduena, M. A. Jordan and L. Wilson, *Cancer Res.*, 2007, **67**, 3767–3776.
95 M. K. Hu and W. S. Huang, *J. Pept. Res.*, 1999, **54**, 460–467.
96 R. S. Marks, D. L. Graham, J. A. Sloan, S. Hillman, S. Fishkoff, J. E. Krook, S. H. Okuno, J. A. Mailliard, T. R. Fitch and F. Addo, *Am. J. Clin. Oncol.*, 2003, **26**(4), 336–337.
97 P. Kerbrat, V. Dieras, N. Pavlidis, A. Ravaud, J. Wanders and P. Fumoleau, *Eur. J. Cancer*, 2003, **39**, 317–320.
98 J. Smyth, M. Boneterre, J. Schellens, H. Calvert, G. Greim, J. Wanders and A. Hanauske, *Ann. Oncol.*, 2001, **12**(4), 509–511.
99 D. A. Gianolio, C. Rouleau, W. E. Bauta, D. Lovett, W. R. Cantrell Jr, A. Recio 3rd, P. Wolstenholme-Hogg, M. Busch, P. Pan, J. E. Stefano, H. M. Kramer, J. Goebel, R. D. Krumbholz, S. Roth, S. M. Schmid and B. A. Teicher, *Cancer Chemother. Pharmacol.*, 2012, **70**, 439–449.
100 D. J. Newman and G. M. Cragg, *Mar. Drugs*, 2017, **15**, 99.
101 G. Casi, N. Huguenin-Dezot, K. Zuberbühler, J. Scheuermann and D. Neri, *J. Am. Chem. Soc.*, 2012, **134**, 5887–5892.
102 G. R. Pettit, D. L. Herald, S. B. Singh, T. J. Thornton and J. T. Mullaney, *J. Am. Chem. Soc.*, 1991, **113**, 6692–6693.
103 G. R. Pettit, T. J. Thornton, J. T. Mullaney, M. R. Boyd, D. L. Herald, S.-B. Singh and E. J. Flahive, *Tetrahedron*, 1994, **50**, 12097–12108.
104 K. Akaji, Y. Hayashi, Y. Kiso and N. Kuriyama, *J. Org. Chem.*, 1999, **64**, 405–411.

105 N. Patino, E. Frérot, N. Galeotti, J. Poncet, J. Coste, M.-N. Dufour and P. Jouin, *Tetrahedron*, 1992, **48**, 4115–4122.
106 R. Bai, M. C. Edler, P. L. Bonate, T. D. Copeland, G. R. Pettit, R. F. Ludueña and E. Hamel, *Mol. Pharmacol.*, 2009, **75**, 218–226.
107 R. E. Schwartz, C. F. Hirsch, D. F. Sesin, J. E. Flor, M. Chartrain, R. E. Fromtling, G. H. Harris, M. J. Salvatore, J. M. Liesch and K. Yudin, *J. Ind. Microbiol.*, 1990, **5**, 113–123.
108 C. Weiss, E. Figueras, A. N. Borbely and N. Sewald, *J. Pept. Sci.*, 2017, **23**, 514–531.
109 G. Trimurtulu, I. Ohtani, G. M. L. Patterson, R. E. Moore, T. H. Corbett, F. A. Valeriote and L. Demchik, *J. Am. Chem. Soc.*, 1994, **116**, 4729–4737.
110 V. A. Verma, T. H. Pillow, L. DePalatis, G. Li, G. L. Phillips, A. G. Polson, H. E. Raab, S. Spencer and B. Zheng, *Bioorg. Med. Chem. Lett.*, 2015, **25**, 864–868.
111 M. Kobayashi, S. Aoki, N. Ohyabu, M. Kurosu, W. Wang and I. Kitagawa, *Tetrahedron Lett.*, 1994, **35**, 7969–7972.
112 T. Leao, G. Castelão, A. Korobeynikov, E. A. Monroe, S. Podell, E. Glukhov, E. E. Allen, W. H. Gerwick and L. Gerwick, *Proc. Natl. Acad. Sci. U. S. A.*, 2017, **114**, 3198–3203.
113 M. Eggen, C. J. Mossman, S. B. Buck, S. K. Nair, L. Bhat, S. M. Ali, E. A. Reiff, T. C. Boge and G. I. Georg, *J. Org. Chem.*, 2000, **65**, 7792–7799.
114 R. M. Iacobazzi, C. Annese, A. Azzariti, L. D'Accolti, M. Franco, C. Fusco, G. La Piana, V. Laquintana and N. Denora, *ACS Med. Chem. Lett.*, 2013, **4**, 1189–1192.
115 J. Kitagaki, G. Shi, S. Miyauchi, S. Murakami and Y. Yang, *Anticancer Drugs*, 2015, **26**, 259–271.
116 D. Panda, K. DeLuca, D. Williams, M. A. Jordan and L. Wilson, *Proc. Natl. Acad. Sci. U. S. A.*, 1998, **95**, 9313–9318.
117 M. J. Edelman, D. R. Gandara, P. Hausner, V. Israel, D. Thornton, J. DeSanto and L. A. Doyle, *Lung Cancer*, 2003, **39**, 197–199.
118 M. Eggen and G. I. Georg, *Med. Res. Rev.*, 2002, **22**, 85–101.
119 Q. Lai, M. Wu, R. Wang, W. Lai, Y. Tao, Y. Lu, Y. Wang, L. Yu, R. Zhang, Y. Peng, X. Jiang, Y. Fu, X. Wang, Z. Zhang, C. Guo, W. Liao, Y. Zhang, T. Kang, H. Chen, Y. Yao, L. Gou and J. Yang, *Eur. J. Med. Chem.*, 2020, **199**, 112364.
120 D. Su, K. R. Kozak, J. Sadowsky, S.-F. Yu, A. Fourie-O'Donohue, C. Nelson, R. Vandlen, R. Ohri, L. Liu, C. Ng, J. He, H. Davis, J. Lau, G. Del Rosario, E. Cosino, J. dela Cruz-Chuh, Y. Ma, D. Zhang, M. Darwish, W. Cai, C. Chen, H. Zhou, J. Lu, Y. Liu, S. Kaur, K. Xu and T. H. Pillow, *Bioconjugate Chem.*, 2018, **29**, 1155–1167.
121 C. Weiss, B. Sammet and N. Sewald, *Nat. Prod. Rep.*, 2013, **30**, 924–940.
122 J. J. Schmidt, Y. Khatri, S. I. Brody, C. Zhu, H. Pietraszkiewicz, F. A. Valeriote and D. H. Sherman, *ACS Chem. Biol.*, 2020, **15**, 524–532.
123 Z. Q. Beck, C. C. Aldrich, N. A. Magarvey, G. I. Georg and D. H. Sherman, *Biochemistry*, 2005, **44**, 13457–13466.
124 S. Eißler, A. Stoncius, M. Nahrwold and N. Sewald, *Synthesis*, 2006, **22**, 3747–3789.
125 K. L. Bolduc, S. D. Larsen and D. H. Sherman, *Chem. Commun.*, 2012, **48**, 6414–6416.
126 S. Eissler, M. Nahrwold, B. Neumann, H.-G. Stammler and N. Sewald, *Org. Lett.*, 2007, **9**, 817–819.
127 C. A. Mast, S. Eißler, A. Stončius, H.-G. Stammler, B. Neumann and N. Sewald, *Chem.–Eur. J.*, 2005, **11**, 4667–4677.
128 Y. Ding, C. M. Rath, K. L. Bolduc, K. Håkansson and D. H. Sherman, *J. Am. Chem. Soc.*, 2011, **133**, 14492–14495.
129 E. Figueras, A. Borbély, M. Ismail, M. Frese and N. Sewald, *Beilstein J. Org. Chem.*, 2018, **14**, 1281–1286.
130 P. Bai, W. Yan and J. Yang, *Cytoskeleton*, 2024, **81**(6–7), 255–263.
131 M. S. Bousquet, J. J. Ma, R. Ratnayake, P. A. Havre, J. Yao, N. H. Dang, V. J. Paul, T. J. Carney, L. H. Dang and H. Luesch, *ACS Chem. Biol.*, 2016, **11**, 1322–1331.
132 N. J. Mabjeesh, D. Escuin, T. M. LaVallee, V. S. Pribluda, G. M. Swartz, M. S. Johnson, M. T. Willard, H. Zhong, J. W. Simons and P. Giannakakou, *Cancer Cell*, 2003, **3**, 363–375.
133 M. Carbonaro, D. Escuin, A. O'Brate, M. Thadani-Mulero and P. Giannakakou, *J. Biol. Chem.*, 2012, **287**, 11859–11869.
134 A. Gangjee, R. K. Pavana, M. A. Ihnat, J. E. Thorpe, B. C. Disch, A. Bastian, L. C. Bailey-Downs, E. Hamel and R. Bai, *ACS Med. Chem. Lett.*, 2014, **5**, 480–484.
135 Y. Lu, J. Chen, M. Xiao, W. Li and D. D. Miller, *Pharm. Res.*, 2012, **29**, 2943–2971.
136 L. Davis, M. Recktenwald, E. Hutt, S. Fuller, M. Briggs, A. Goel and N. Daringer, *Cancers*, 2022, **14**, 1259.
137 X. Yuan, W. Ruan, B. Bobrow, P. Carmeliet and H. K. Eltzschig, *Nat. Rev. Drug Discovery*, 2024, **23**, 175–200.
138 J. Fares, M. Y. Fares, H. H. Khachfe, H. A. Salhab and Y. Fares, *Signal Transduction Targeted Ther.*, 2020, **5**, 1–17.
139 H. Y. K. Yip and A. Papa, *Cells*, 2021, **10**, 659.
140 Z. Du and C. M. Lovly, *Mol. Cancer*, 2018, **17**, 58.
141 E. Witsch, M. Sela and Y. Yarden, *Physiology*, 2010, **25**, 85–101.
142 C. K. Barlowe and E. A. Miller, *Genetics*, 2013, **193**, 383–410.
143 Y. Nyathi, B. M. Wilkinson and M. R. Pool, *Biochim. Biophys. Acta, Mol. Cell Res.*, 2013, **1833**, 2392–2402.
144 S. Itskanov and E. Park, *Cold Spring Harbor Perspect. Biol.*, 2023, **15**(1), a041250.
145 S. Itskanov, L. Wang, T. Junne, R. Sherriff, L. Xiao, N. Blanchard, W. Q. Shi, C. Forsyth, D. Hoepfner, M. Spiess and E. Park, *Nat. Chem. Biol.*, 2023, **19**, 1063–1071.
146 H. Luesch, W. Y. Yoshida, R. E. Moore, V. J. Paul and T. H. Corbett, *J. Am. Chem. Soc.*, 2001, **123**, 5418–5423.
147 K.-C. Huang, Z. Chen, Y. Jiang, S. Akare, D. Kolber-Simonds, K. Condon, S. Agoulnik, K. Tendyke, Y. Shen, K.-M. Wu, S. Mathieu, H. Choi, X. Zhu, H. Shimizu, Y. Kotake, W. H. Gerwick, T. Uenaka, M. Woodall-Jappe and K. Nomoto, *Mol. Cancer Ther.*, 2016, **15**, 1208–1216.

148 R. A. Medina, D. E. Goeger, P. Hills, S. L. Mooberry, N. Huang, L. I. Romero, E. Ortega-Barría, W. H. Gerwick and K. L. McPhail, *J. Am. Chem. Soc.*, 2008, **130**, 6324–6325.
149 D. Tranter, A. O. Paatero, S. Kawaguchi, S. Kazemi, J. D. Serrill, J. Kellosalo, W. K. Vogel, U. Richter, D. R. Mattos, X. Wan, C. C. Thornburg, S. Oishi, K. L. McPhail, J. E. Ishmael and V. O. Paavilainen, *ACS Chem. Biol.*, 2020, **15**, 2125–2136.
150 H. Luesch, W. Y. Yoshida, R. E. Moore and V. J. Paul, *Bioorg. Med. Chem.*, 2002, **10**, 1973–1978.
151 K. Tidgewell, N. Engene, T. Byrum, J. Media, T. Doi, F. A. Valeriote and W. H. Gerwick, *Chembiochem*, 2010, **11**, 1458–1466.
152 S. Matthew, P. J. Schupp and H. Luesch, *J. Nat. Prod.*, 2008, **71**, 1113–1116.
153 M. Gutiérrez, T. L. Suyama, N. Engene, J. S. Wingerd, T. Matainaho and W. H. Gerwick, *J. Nat. Prod.*, 2008, **71**, 1099–1103.
154 C. C. Thornburg, E. S. Cowley, J. Sikorska, L. A. Shaala, J. E. Ishmael, D. T. A. Youssef and K. L. McPhail, *J. Nat. Prod.*, 2013, **76**, 1781–1788.
155 H. Luesch, S. K. Chanda, R. M. Raya, P. D. DeJesus, A. P. Orth, J. R. Walker, J. C. Izpisúa Belmonte and P. G. Schultz, *Nat. Chem. Biol.*, 2006, **2**, 158–167.
156 Y. Liu, B. K. Law and H. Luesch, *Mol. Pharmacol.*, 2009, **76**, 91–104.
157 A. O. Paatero, J. Kellosalo, B. M. Dunyak, J. Almaliti, J. E. Gestwicki, W. H. Gerwick, J. Taunton and V. O. Paavilainen, *Cell Chem. Biol.*, 2016, **23**, 561–566.
158 W. Shi, D. Lu, C. Wu, M. Li, Z. Ding, Y. Li, B. Chen, X. Lin, W. Su, X. Shao, Z. Xia, L. Fang, K. Liu and H. Li, *Biochem. Biophys. Res. Commun.*, 2021, **547**, 52–58.
159 Q.-Y. Chen, Y. Liu and H. Luesch, *ACS Med. Chem. Lett.*, 2011, **2**, 861–865.
160 Q.-Y. Chen, Y. Liu, W. Cai and H. Luesch, *J. Med. Chem.*, 2014, **57**, 3011–3029.
161 G. Yao, W. Wang, L. Ao, Z. Cheng, C. Wu, Z. Pan, K. Liu, H. Li, W. Su and L. Fang, *J. Med. Chem.*, 2018, **61**, 8908–8916.
162 H. Luesch and V. O. Paavilainen, *Nat. Prod. Rep.*, 2020, **37**, 717–736.
163 W. Cai, R. Ratnayake, M. Wang, Q.-Y. Chen, K. P. Raisch, L. H. Dang, B. K. Law and H. Luesch, *Curr. Res. Pharmacol. Drug Discov.*, 2021, **2**, 100053.
164 J. Chen and C. J. Forsyth, *J. Am. Chem. Soc.*, 2003, **125**, 8734–8735.
165 D. Ma, B. Zou, G. Cai, X. Hu and J. O. Liu, *Chem.–Eur. J.*, 2006, **12**, 7615–7626.
166 Z.-Y. Mao, C.-M. Si, Y.-W. Liu, H.-Q. Dong, B.-G. Wei and G.-Q. Lin, *J. Org. Chem.*, 2017, **82**, 10830–10845.
167 E. M. Tarsis, E. J. Rastelli, S. E. Wengryniuk and D. M. Coltart, *Tetrahedron*, 2015, **71**, 5029–5044.
168 W. Cai, R. Ratnayake, M. H. Gerber, Q.-Y. Chen, Y. Yu, H. Derendorf, J. G. Trevino and H. Luesch, *Invest. New Drugs*, 2019, **37**, 364–374.
169 W. Cai, Q.-Y. Chen, L. H. Dang and H. Luesch, *ACS Med. Chem. Lett.*, 2017, **8**, 1007–1012.
170 V. Kunz, K. S. Bommert, J. Kruk, D. Schwinning, M. Chatterjee, T. Stühmer, R. Bargou and K. Bommert, *Sci. Rep.*, 2020, **10**, 18419.
171 Z. Zhao, D. A. Pissarnitski, X. Huang, A. Palani, Z. Zhu, W. J. Greenlee, L. A. Hyde, L. Song, G. Terracina, L. Zhang and E. M. Parker, *ACS Med. Chem. Lett.*, 2017, **8**, 1002–1006.
172 J. W. A. Kinnaird, P. Y. Ng, K. Kubota, X. Wang and J. L. Leighton, *J. Am. Chem. Soc.*, 2002, **124**, 7920–7921.
173 S. Kiyooka, Y. Kaneko, M. Komura, H. Matsuo and M. Nakano, *J. Org. Chem.*, 1991, **56**, 2276–2278.
174 Y. Onda, Y. Masuda, M. Yoshida and T. Doi, *J. Med. Chem.*, 2017, **60**, 6751–6765.
175 D. Dhakal, D. Kallifidas, M. Chen, S. Kokkaliari, Q.-Y. Chen, V. J. Paul, Y. Ding and H. Luesch, *Org. Lett.*, 2023, **25**, 2238–2242.
176 A. M. Hau, J. A. Greenwood, C. V. Löhr, J. D. Serrill, P. J. Proteau, I. G. Ganley, K. L. McPhail and J. E. Ishmael, *PLoS One*, 2013, **8**, e65250.
177 J. D. Serrill, X. Wan, A. M. Hau, H. S. Jang, D. J. Coleman, A. K. Indra, A. W. G. Alani, K. L. McPhail and J. E. Ishmael, *Invest. New Drugs*, 2016, **34**, 24–40.
178 S. Kazemi, S. Kawaguchi, C. E. Badr, D. R. Mattos, A. Ruiz-Saenz, J. D. Serrill, M. M. Moasser, B. P. Dolan, V. O. Paavilainen, S. Oishi, K. L. McPhail and J. E. Ishmael, *Biochem. Pharmacol.*, 2021, **183**, 114317.
179 W. He, H.-B. Qiu, Y.-J. Chen, J. Xi and Z.-J. Yao, *Tetrahedron Lett.*, 2014, **55**, 6109–6112.
180 G. Yao, Z. Pan, C. Wu, W. Wang, L. Fang and W. Su, *J. Am. Chem. Soc.*, 2015, **137**, 13488–13491.
181 C. Wu, Z. Cheng, D. Lu, K. Liu, Y. Cheng, P. Wang, Y. Zhou, M. Li, X. Shao, H. Li, W. Su and L. Fang, *J. Med. Chem.*, 2021, **64**, 991–1000.
182 T. Kitamura, R. Suzuki, S. Inuki, H. Ohno, K. L. McPhail and S. Oishi, *ACS Med. Chem. Lett.*, 2022, **13**, 105–110.
183 A. H. L. Bong and G. R. Monteith, *Biochim. Biophys. Acta, Mol. Cell Res.*, 2018, **1865**, 1786–1794.
184 A. Arbabian, J.-P. Brouland, P. Gélébart, T. Kovàcs, R. Bobe, J. Enouf and B. Papp, *BioFactors*, 2011, **37**, 139–149.
185 M. Periasamy and A. Kalyanasundaram, *Muscle Nerve*, 2007, **35**, 430–442.
186 X. Zhai, A. M. Sterea and Y. El Hiani, *Cells*, 2020, **9**, 1536.
187 L. Peterková, E. Kmoníčková, T. Ruml and S. Rimpelová, *J. Med. Chem.*, 2020, **63**, 1937–1963.
188 N. Kurisawa, A. Iwasaki, K. Teranuma, S. Dan, C. Toyoshima, M. Hashimoto and K. Suenaga, *J. Am. Chem. Soc.*, 2022, **144**, 11019–11032.
189 M. Morita, H. Ogawa, O. Ohno, T. Yamori, K. Suenaga and C. Toyoshima, *FEBS Lett.*, 2015, **589**, 1406–1411.
190 T. Teruya, H. Sasaki, K. Kitamura, T. Nakayama and K. Suenaga, *Org. Lett.*, 2009, **11**, 2421–2424.
191 Y. Sagara and G. Inesi, *J. Biol. Chem.*, 1991, **266**, 13503–13506.
192 B. J. Abbott, D. S. Fukuda, D. E. Dorman, J. L. Occolowitz, M. Debono and L. Farhner, *Antimicrob. Agents Chemother.*, 1979, **16**, 808–812.
193 D. C. McMullen, W. S. Kean, A. Verma, J. T. Cole and W. D. Watson, *Biol. Proced. Online*, 2012, **14**, 4.

194 S. Kokkaliari, D. Luo, V. J. Paul and H. Luesch, *Mar. Drugs*, 2023, **21**, 378.
195 M. Morita, O. Ohno, T. Teruya, T. Yamori, T. Inuzuka and K. Suenaga, *Tetrahedron*, 2012, **68**, 5984–5990.
196 A. Watanabe, O. Ohno, M. Morita, T. Inuzuka and K. Suenaga, *Bull. Chem. Soc. Jpn.*, 2015, **88**, 1256–1264.
197 E. Sato, M. Sato, Y. Tanabe, N. Nakajima, A. Ohkubo and K. Suenaga, *J. Org. Chem.*, 2017, **82**, 6770–6777.
198 E. Sato, Y. Tanabe, N. Nakajima, A. Ohkubo and K. Suenaga, *Org. Lett.*, 2016, **18**, 2047–2049.
199 Y. Liu, Y. Sun, Y. Guo, X. Shi, X. Chen, W. Feng, L.-L. Wu, J. Zhang, S. Yu, Y. Wang and Y. Shi, *Int. J. Biol. Sci.*, 2023, **19**, 897–915.
200 C. Wang and R. J. Youle, *Annu. Rev. Genet.*, 2009, **43**, 95–118.
201 C. M. Pfeffer and A. T. K. Singh, *Int. J. Mol. Sci.*, 2018, **19**, 448.
202 C. Du, M. Fang, Y. Li, L. Li and X. Wang, *Cell*, 2000, **102**, 33–42.
203 A. M. Chinnaiyan, *Neoplasia*, 1999, **1**, 5–15.
204 D. Luo, R. Ratnayake, K. R. Atanasova, V. J. Paul and H. Luesch, *Biochem. Pharmacol.*, 2023, **213**, 115608.
205 B. A. Carneiro and W. S. El-Deiry, *Nat. Rev. Clin. Oncol.*, 2020, **17**, 395–417.
206 W. Wrasidlo, A. Mielgo, V. A. Torres, S. Barbero, K. Stoletov, T. L. Suyama, R. L. Klemke, W. H. Gerwick, D. A. Carson and D. G. Stupack, *Proc. Natl. Acad. Sci. U. S. A.*, 2008, **105**, 2313–2318.
207 P. Orning and E. Lien, *J. Leukocyte Biol.*, 2021, **109**, 121–141.
208 X. Huang, W. Huang, L. Li, X. Sun, S. Song, Q. Xu, L. Zhang, B.-G. Wei and X. Deng, *Mol. Pharm.*, 2016, **13**, 3756–3763.
209 W. A. Abdel-Naime, A. Kimishima, A. Setiawan, J. R. Fahim, M. A. Fouad, M. S. Kamel and M. Arai, *Mar. Drugs*, 2020, **18**, 555.
210 N. Rohwer and T. Cramer, *Drug Resistance Updates*, 2011, **14**, 191–201.
211 Y. Miyamoto, A. Iwasaki, H. Fujimura, C. Kudo, N. Kurisawa, O. Ohno and K. Suenaga, *J. Org. Chem.*, 2023, **88**, 3208–3216.
212 A. Tripathi, J. Puddick, M. R. Prinsep, M. Rottmann and L. T. Tan, *J. Nat. Prod.*, 2010, **73**, 1810–1814.
213 D. Luo, M. Y. Putra, T. Ye, V. J. Paul and H. Luesch, *Mar. Drugs*, 2019, **17**, 83.
214 A. Tripathi, J. Puddick, M. R. Prinsep, M. Rottmann, K. P. Chan, D. Y.-K. Chen and L. T. Tan, *Phytochemistry*, 2011, **72**, 2369–2375.
215 K. Suenaga, T. Mutou, T. Shibata, T. Itoh, T. Fujita, N. Takada, K. Hayamizu, M. Takagi, T. Irifune, H. Kigoshi and K. Yamada, *Tetrahedron*, 2004, **60**, 8509–8527.
216 B. Han, H. Gross, D. E. Goeger, S. L. Mooberry and W. H. Gerwick, *J. Nat. Prod.*, 2006, **69**, 572–575.
217 Y. Nakao, W. Y. Yoshida, Y. Takada, J. Kimura, L. Yang, S. L. Mooberry and P. J. Scheuer, *J. Nat. Prod.*, 2004, **67**, 1332–1340.
218 K. Hagimoto, S. Tojo, T. Teruya, M. Yoshida and H. Kigoshi, *Tetrahedron*, 2024, **154**, 133871.
219 K. Sueyoshi, M. Kaneda, S. Sumimoto, S. Oishi, N. Fujii, K. Suenaga and T. Teruya, *Tetrahedron*, 2016, **72**, 5472–5478.
220 A. Tripathi, W. Fang, D. T. Leong and L. T. Tan, *Mar. Drugs*, 2012, **10**, 1126–1137.
221 S. Sato, A. Murata, T. Orihara, T. Shirakawa, K. Suenaga, H. Kigoshi and M. Uesugi, *Chem. Biol.*, 2011, **18**, 131–139.
222 A. Signorile, G. Sgaramella, F. Bellomo and D. De Rasmo, *Cells*, 2019, **8**, 71.
223 M. Kaneda, K. Sueyoshi, T. Teruya, H. Ohno, N. Fujii and S. Oishi, *Org. Biomol. Chem.*, 2016, **14**, 9093–9104.
224 M. Kaneda, S. Kawaguchi, N. Fujii, H. Ohno and S. Oishi, *ACS Med. Chem. Lett.*, 2018, **9**, 365–369.
225 L. Dai, B. Chen, H. Lei, Z. Wang, Y. Liu, Z. Xu and T. Ye, *Chem. Commun.*, 2012, **48**, 8697–8699.
226 W. Huang, R.-G. Ren, H.-Q. Dong, B.-G. Wei and G.-Q. Lin, *J. Org. Chem.*, 2013, **78**, 10747–10762.
227 J. Gorges and U. Kazmaier, *Org. Lett.*, 2018, **20**, 2033–2036.
228 O. Ohno, A. Iwasaki, K. Same, C. Kudo, E. Aida, K. Sugiura, S. Sumimoto, T. Teruya, E. Tashiro, S. Simizu, K. Matsuno, M. Imoto and K. Suenaga, *Org. Lett.*, 2022, **24**, 4547–4551.
229 N. Kotoku, R. Ishida, H. Matsumoto, M. Arai, K. Toda, A. Setiawan, O. Muraoka and M. Kobayashi, *J. Org. Chem.*, 2017, **82**, 1705–1718.
230 R. Ishida, H. Matsumoto, S. Ichii, M. Kobayashi, M. Arai and N. Kotoku, *Chem. Pharm. Bull.*, 2019, **67**, 210–223.
231 L. M. Nogle and W. H. Gerwick, *Org. Lett.*, 2002, **4**, 1095–1098.
232 C. Zhang, C. B. Naman, N. Engene and W. H. Gerwick, *Mar. Drugs*, 2017, **15**, 121.
233 K. S. Taylor, C. Zhang, E. Glukhov, W. H. Gerwick and T. L. Suyama, *J. Nat. Prod.*, 2021, **84**, 865–870.
234 T. L. Suyama and W. H. Gerwick, *Org. Lett.*, 2008, **10**, 4449–4452.
235 Q. Zhang, S. Wang, J. Chen and Z. Yu, *Int. J. Med. Sci.*, 2019, **16**, 424–442.
236 I.-C. Chen, B. Sethy and J.-P. Liou, *Front. Cell Dev. Biol.*, 2020, **8**, 576391.
237 X. Qiu, L. Zhu, H. Wang, Y. Tan, Z. Yang, L. Yang and L. Wan, *Bioorg. Med. Chem.*, 2021, **52**, 116510.
238 X. Peng, Z. Sun, P. Kuang and J. Chen, *Eur. J. Med. Chem.*, 2020, **208**, 112831.
239 A. Bowers, N. West, J. Taunton, S. L. Schreiber, J. E. Bradner and R. M. Williams, *J. Am. Chem. Soc.*, 2008, **130**, 11219–11222.
240 Y. Ying, K. Taori, H. Kim, J. Hong and H. Luesch, *J. Am. Chem. Soc.*, 2008, **130**, 8455–8459.
241 K. Taori, V. J. Paul and H. Luesch, *J. Am. Chem. Soc.*, 2008, **130**, 1806–1807.
242 C. M. Pavlik, C. Y. B. Wong, S. Ononye, D. D. Lopez, N. Engene, K. L. McPhail, W. H. Gerwick and M. J. Balunas, *J. Nat. Prod.*, 2013, **76**, 2026–2033.
243 J. Hong and H. Luesch, *Nat. Prod. Rep.*, 2012, **29**, 449–456.
244 Y. Liu, L. A. Salvador, S. Byeon, Y. Ying, J. C. Kwan, B. K. Law, J. Hong and H. Luesch, *J. Pharmacol. Exp. Ther.*, 2010, **335**, 351–361.

245 A. Yurek-George, A. R. L. Cecil, A. H. K. Mo, S. Wen, H. Rogers, F. Habens, S. Maeda, M. Yoshida, G. Packham and A. Ganesan, *J. Med. Chem.*, 2007, **50**, 5720–5726.
246 M. Law, P. Corsino, S. Jahn, B. Davis, S. Chen, B. Patel, K. Pham, J. Lu, B. Sheppard, P. Nørgaard, J. Hong, P. Higgins, J.-S. Kim, H. Luesch and B. Law, *Oncogene*, 2013, **32**, 1316–1329.
247 L. A. Salvador, H. Park, F. H. Al-Awadhi, Y. Liu, B. Kim, S. L. Zeller, Q.-Y. Chen, J. Hong and H. Luesch, *ACS Med. Chem. Lett.*, 2014, **5**, 905–910.
248 S. Kashiwagi, M. Yashiro, T. Takashima, S. Nomura, S. Noda, H. Kawajiri, T. Ishikawa, K. Wakasa and K. Hirakawa, *Br. J. Cancer*, 2010, **103**, 249–255.
249 L.-C. Wu, Z.-S. Wen, Y.-T. Qiu, X.-Q. Chen, H.-B. Chen, M.-M. Wei, Z. Liu, S. Jiang and G.-B. Zhou, *ACS Med. Chem. Lett.*, 2013, **4**, 921–926.
250 F. H. Al-Awadhi, L. A. Salvador-Reyes, L. A. Elsadek, R. Ratnayake, Q.-Y. Chen and H. Luesch, *ACS Chem. Neurosci.*, 2020, **11**, 1937–1943.
251 Y.-H. Zhou, X. Wu, F. Tan, Y.-X. Shi, T. Glass, T. J. Liu, K. Wathen, K. R. Hess, J. Gumin, F. Lang and W. K. A. Yung, *J. Neurooncol.*, 2005, **71**, 223–229.
252 C. Xu, G. Liu, H. Ji, W. Chen, D. Dai, Z. Chen, D. Zhou, L. Xu, H. Hu, W. Cui, L. Chang, Q. Zha, L. Li, S. Duan and Q. Wang, *Mol. Med. Rep.*, 2018, **18**, 4297–4302.
253 A. A. Bowers, T. J. Greshock, N. West, G. Estiu, S. L. Schreiber, O. Wiest, R. M. Williams and J. E. Bradner, *J. Am. Chem. Soc.*, 2009, **131**, 2900–2905.
254 D. J. Clausen, W. B. Smith, B. E. Haines, O. Wiest, J. E. Bradner and R. M. Williams, *Bioorg. Med. Chem.*, 2015, **23**, 5061–5074.
255 J. M. Guerra-Bubb, A. A. Bowers, W. B. Smith, R. Paranal, G. Estiu, O. Wiest, J. E. Bradner and R. M. Williams, *Bioorg. Med. Chem. Lett.*, 2013, **23**, 6025–6028.
256 X. Li, Z. Tu, H. Li, C. Liu, Z. Li, Q. Sun, Y. Yao, J. Liu and S. Jiang, *ACS Med. Chem. Lett.*, 2013, **4**, 132–136.
257 B. Kim, H. Park, L. A. Salvador, P. E. Serrano, J. C. Kwan, S. L. Zeller, Q.-Y. Chen, S. Ryu, Y. Liu, S. Byeon, H. Luesch and J. Hong, *Bioorg. Med. Chem. Lett.*, 2014, **24**, 3728–3731.
258 P. Bhansali, C. L. Hanigan, L. Perera, R. A. Casero and L. M. V. Tillekeratne, *Eur. J. Med. Chem.*, 2014, **86**, 528–541.
259 J. Almaliti, A. A. Al-Hamashi, A. T. Negmeldin, C. L. Hanigan, L. Perera, M. K. H. Pflum, R. A. Jr. Casero and L. M. V. Tillekeratne, *J. Med. Chem.*, 2016, **59**, 10642–10660.
260 B. Kim, R. Ratnayake, H. Lee, G. Shi, S. L. Zeller, C. Li, H. Luesch and J. Hong, *Bioorg. Med. Chem.*, 2017, **25**, 3077–3086.
261 G. Poli, R. Di Fabio, L. Ferrante, V. Summa and M. Botta, *ChemMedChem*, 2017, **12**, 1917–1926.
262 P. Bhansali, C. L. Hanigan, R. A. Jr. Casero and L. M. V. Tillekeratne, *J. Med. Chem.*, 2011, **54**, 7453–7463.
263 J. Su, Y. Qiu, K. Ma, Y. Yao, Z. Wang, X. Li, D. Zhang, Z. Tu and S. Jiang, *Tetrahedron*, 2014, **70**, 7763–7769.
264 D. J. Clausen, W. B. Smith, B. E. Haines, O. Wiest, J. E. Bradner and R. M. Williams, *Bioorg. Med. Chem.*, 2015, **23**, 5061–5074.
265 J. A. Souto, E. Vaz, I. Lepore, A.-C. Pöppler, G. Franci, R. Álvarez, L. Altucci and Á. R. de Lera, *J. Med. Chem.*, 2010, **53**, 4654–4667.
266 B. Zhang, G. Shan, Y. Zheng, X. Yu, Z.-W. Ruan, Y. Li and X. Lei, *Mar. Drugs*, 2019, **17**, 333.
267 M. Yu, L. A. Salvador, S. K. B. Sy, Y. Tang, R. S. P. Singh, Q.-Y. Chen, Y. Liu, J. Hong, H. Derendorf and H. Luesch, *Mar. Drugs*, 2014, **12**, 1623–1640.
268 X. Wang, B. C. Waschke, R. A. Woolaver, Z. Chen, G. Zhang, A. D. Piscopio, X. Liu and J. H. Wang, *Cancer Immunol. Res.*, 2019, **7**, 1318–1331.
269 X. Liu, J. Phillips, D. Ungermannove, C. G. Nasveschuk and G. Zhang, *US Pat.*, 20130203681A1, 2014.
270 A. R. Schreiber, J. A. Kagihara, B. R. Corr, S. L. Davis, C. Lieu, S. S. Kim, A. Jimeno, D. R. Camidge, J. Williams, A. M. Heim, A. Martin, J. A. DeMattei, N. Holay, T. A. Triplett, S. G. Eckhardt, K. Litwiler, J. Winkler, A. D. Piscopio and J. R. Diamond, *Cancers*, 2023, **16**, 91.
271 OnKure Therapeutics – Scientific Publications, **https://onkuretherapeutics.com/pipeline/publications/**, accessed October 26, 2024.
272 T. Seiser, F. Kamena and N. Cramer, *Angew. Chem., Int. Ed.*, 2008, **47**, 6483–6485.
273 C. G. Nasveschuk, D. Ungermannova, X. Liu and A. J. Phillips, *Org. Lett.*, 2008, **10**, 3595–3598.
274 Y. Ying, K. Taori, H. Kim, J. Hong and H. Luesch, *J. Am. Chem. Soc.*, 2008, **130**, 8455–8459.
275 A. K. Ghosh and S. Kulkarni, *Org. Lett.*, 2008, **10**, 3907–3909.
276 Q. Xiao, L.-P. Wang, X.-Z. Jiao, X.-Y. Liu, Q. Wu and P. Xie, *J. Asian Nat. Prod. Res.*, 2010, **12**, 940–949.
277 Q.-Y. Chen, P. R. Chaturvedi and H. Luesch, *Org. Process Res. Dev.*, 2018, **22**, 190–199.
278 Y. Gao, N. T. Nihira, X. Bu, C. Chu, J. Zhang, A. Kolodziejczyk, Y. Fan, N. T. Chan, L. Ma, J. Liu, D. Wang, X. Dai, H. Liu, M. Ono, A. Nakanishi, H. Inuzuka, B. J. North, Y.-H. Huang, S. Sharma, Y. Geng, W. Xu, X. S. Liu, L. Li, Y. Miki, P. Sicinski, G. J. Freeman and W. Wei, *Nat. Cell Biol.*, 2020, **22**, 1064–1075.
279 S. M. Gromek, J. A. deMayo, A. T. Maxwell, A. M. West, C. M. Pavlik, Z. Zhao, J. Li, A. J. Wiemer, A. Zweifach and M. J. Balunas, *Bioorg. Med. Chem.*, 2016, **24**, 5183–5196.
280 Q. Liu, W. Lu, M. Ma, J. Liao, A. Ganesan, Y. Hu, S. Wen and P. Huang, *RSC Adv.*, 2014, **5**, 1109–1112.
281 R. Randino, P. Gazzerro, R. Mazitschek and M. Rodriquez, *Bioorg. Med. Chem.*, 2017, **25**, 6486–6491.
282 G. D. Roodman, *Leukemia*, 2009, **23**, 435–441.
283 A. T. Nunes and C. M. Annunziata, *Semin. Oncol.*, 2017, **44**, 377–380.
284 T. A. M. Gulder and B. S. Moore, *Angew Chem. Int. Ed. Engl.*, 2010, **49**, 9346–9367.
285 A. G. Solimando, E. Malerba, P. Leone, M. Prete, C. Terragna, M. Cavo and V. Racanelli, *Front. Oncol.*, 2022, **12**, 1–17.
286 A. Markham, *Drugs*, 2020, **80**, 1607–1613.

287 A. R. Pereira, A. J. Kale, A. T. Fenley, T. Byrum, H. M. Debonsi, M. K. Gilson, F. A. Valeriote, B. S. Moore and W. H. Gerwick, *ChemBioChem*, 2012, **13**, 810–817.
288 J. Almaliti, B. Miller, H. Pietraszkiewicz, E. Glukhov, C. B. Naman, T. Kline, J. Hanson, X. Li, S. Zhou, F. A. Valeriote and W. H. Gerwick, *Eur. J. Med. Chem.*, 2019, **161**, 416–432.
289 J. Almaliti, P. Fajtová, J. Calla, G. M. LaMonte, M. Feng, F. Rocamora, S. Ottilie, E. Glukhov, E. Boura, R. T. Suhandynata, J. D. Momper, M. K. Gilson, E. A. Winzeler, W. H. Gerwick and A. J. O'Donoghue, *Chem.–Eur. J.*, 2023, **29**, e202203958.
290 N. Sin, K. B. Kim, M. Elofsson, L. Meng, H. Auth, B. H. B. Kwok and C. M. Crews, *Bioorg. Med. Chem. Lett.*, 1999, **9**, 2283–2288.
291 H.-J. Zhou, M. A. Aujay, M. K. Bennett, M. Dajee, S. D. Demo, Y. Fang, M. N. Ho, J. Jiang, C. J. Kirk, G. J. Laidig, E. R. Lewis, Y. Lu, T. Muchamuel, F. Parlati, E. Ring, K. D. Shenk, J. Shields, P. J. Shwonek, T. Stanton, C. M. Sun, C. Sylvain, T. M. Woo and J. Yang, *J. Med. Chem.*, 2009, **52**, 3028–3038.
292 D. B. B. Trivella, A. R. Pereira, M. L. Stein, Y. Kasai, T. Byrum, F. A. Valeriote, D. J. Tantillo, M. Groll, W. H. Gerwick and B. S. Moore, *Chem. Biol.*, 2014, **21**, 782–791.
293 G. M. LaMonte, J. Almaliti, B. Bibo-Verdugo, L. Keller, B. Y. Zou, J. Yang, Y. Antonova-Koch, P. Orjuela-Sanchez, C. A. Boyle, E. Vigil, L. Wang, G. M. Goldgof, L. Gerwick, A. J. O'Donoghue, E. A. Winzeler, W. H. Gerwick and S. Ottilie, *J. Med. Chem.*, 2017, **60**, 6721–6732.
294 H. Yin and A. D. Flynn, *Annu. Rev. Biomed. Eng.*, 2016, **18**, 51–76.
295 R. M. Epand, C. Walker, R. F. Epand and N. A. Magarvey, *Biochim. Biophys. Acta, Biomembr.*, 2016, **1858**, 980–987.
296 S. Nishimura and N. Matsumori, *Nat. Prod. Rep.*, 2020, **37**, 677–702.
297 M. A. Ghannoum and L. B. Rice, *Clin. Microbiol. Rev.*, 1999, **12**, 501–517.
298 L. A. Salvador-Reyes, J. Sneed, V. J. Paul and H. Luesch, *J. Nat. Prod.*, 2015, **78**, 1957–1962.
299 L. A. Elsadek, J. H. Matthews, S. Nishimura, T. Nakatani, A. Ito, T. Gu, D. Luo, L. A. Salvador-Reyes, V. J. Paul, H. Kakeya and H. Luesch, *Chembiochem*, 2021, **22**, 1790–1799.
300 S. K. Patra, *Biochim. Biophys. Acta, Rev. Cancer*, 2008, **1785**, 182–206.
301 G. Preta, *Front. Cell Dev. Biol.*, 2020, **8**, 1–10.
302 C.-L. Shao, R. G. Linington, M. J. Balunas, A. Centeno, P. Boudreau, C. Zhang, N. Engene, C. Spadafora, T. S. Mutka, D. E. Kyle, L. Gerwick, C.-Y. Wang and W. H. Gerwick, *J. Org. Chem.*, 2015, **80**, 7849–7855.
303 C.-L. Shao, X.-F. Mou, F. Cao, C. Spadafora, E. Glukhov, L. Gerwick, C.-Y. Wang and W. H. Gerwick, *J. Nat. Prod.*, 2018, **81**, 211–215.
304 L. Keller, J. L. Siqueira-Neto, J. M. Souza, K. Eribez, G. M. LaMonte, J. E. Smith and W. H. Gerwick, *Molecules*, 2020, **25**, 1604.
305 S. Nishimura, *J. Antibiot.*, 2021, **74**, 769–785.
306 J. B. MacMillan and T. F. Molinski, *Org. Lett.*, 2002, **4**, 1535–1538.
307 L. A. Salvador, V. J. Paul and H. Luesch, *J. Nat. Prod.*, 2010, **73**, 1606–1609.
308 A. Quintard, C. Sperandio and J. Rodriguez, *Org. Lett.*, 2018, **20**, 5274–5277.
309 D. Fiorito, S. Keskin, J. M. Bateman, M. George, A. Noble and V. K. Aggarwal, *J. Am. Chem. Soc.*, 2022, **144**, 7995–8001.
310 A. Ramos, S. Sadeghi and H. Tabatabaeian, *Int. J. Mol. Sci.*, 2021, **22**, 9451.
311 H. Luesch, W. Y. Yoshida, R. E. Moore, V. J. Paul and S. L. Mooberry, *J. Nat. Prod.*, 2000, **63**, 611–615.
312 K. E. Milligan, B. L. Marquez, R. T. Williamson and W. H. Gerwick, *J. Nat. Prod.*, 2000, **63**, 1440–1443.
313 G. G. Harrigan, W. Y. Yoshida, R. E. Moore, D. G. Nagle, P. U. Park, J. Biggs, V. J. Paul, S. L. Mooberry, T. H. Corbett and F. A. Valeriote, *J. Nat. Prod.*, 1998, **61**, 1221–1225.
314 J. C. Kwan, R. Ratnayake, K. A. Abboud, V. J. Paul and H. Luesch, *J. Org. Chem.*, 2010, **75**, 8012–8023.
315 X. Liang, S. Matthew, Q.-Y. Chen, J. C. Kwan, V. J. Paul and H. Luesch, *Org. Lett.*, 2019, **21**, 7274–7278.
316 B. Han, K. L. McPhail, H. Gross, D. E. Goeger, S. L. Mooberry and W. H. Gerwick, *Tetrahedron*, 2005, **61**, 11723–11729.
317 B. L. Marquez, K. S. Watts, A. Yokochi, M. A. Roberts, P. Verdier-Pinard, J. I. Jimenez, E. Hamel, P. J. Scheuer and W. H. Gerwick, *J. Nat. Prod.*, 2002, **65**, 866–871.
318 D. D. Zhang and E. Chapman, *Nat. Prod. Rep.*, 2020, **37**, 797–826.
319 A. L. Herbert, M. Fu, C. M. Drerup, R. S. Gray, B. L. Harty, S. D. Ackerman, T. O'Reilly-Pol, S. L. Johnson, A. V. Nechiporuk, B. A. Barres and K. R. Monk, *Proc. Natl. Acad. Sci. U. S. A.*, 2017, **114**, E9153–E9162.
320 J. H. Matthews, X. Liang, V. J. Paul and H. Luesch, *ACS Chem. Biol.*, 2018, **13**, 1189–1199.
321 S. Wu, H. Lu and Y. Bai, *Cancer Med.*, 2019, **8**, 2252–2267.
322 H. Liu, Y. Liu, Z. Wang, X. Xing, A. R. Maguire, H. Luesch, H. Zhang, Z. Xu and T. Ye, *Chem.–Eur. J.*, 2013, **19**, 6774–6784.
323 H. Liu, Y. Liu, X. Xing, Z. Xu and T. Ye, *Chem. Commun.*, 2010, **46**, 7486–7488.
324 A. Thorburn, *J. Thorac. Oncol.*, 2007, **2**, 461–465.
325 R. Trivedi and D. P. Mishra, *Front. Oncol.*, 2015, **5**, 69.
326 K. Papenfort and B. L. Bassler, *Nat. Rev. Microbiol.*, 2016, **14**, 576–588.
327 X. Liang, Q.-Y. Chen, G. M. Seabra, S. Matthew, J. C. Kwan, C. Li, V. J. Paul and H. Luesch, *J. Nat. Prod.*, 2021, **84**, 779–789.
328 M. Hosseini, H. Kringelum, A. Murray and J. E. Tønder, *Org. Lett.*, 2006, **8**, 2103–2106.
329 V. Ruiz-Torres, J. A. Encinar, M. Herranz-López, A. Pérez-Sánchez, V. Galiano, E. Barrajón-Catalán and V. Micol, *Molecules*, 2017, **22**, 1037.
330 E. Muratspahić, M. Freissmuth and C. W. Gruber, *Trends Pharmacol. Sci.*, 2019, **40**, 309–326.

331 H. Qamar, K. Hussain, A. Soni, A. Khan, T. Hussain and B. Chénais, *Molecules*, 2021, **26**, 247.
332 F. H. Al-Awadhi and H. Luesch, *Nat. Prod. Rep.*, 2020, **37**, 827–860.
333 I. Lerman and S. R. Hammes, *Steroids*, 2018, **133**, 96–101.
334 S. Srinivasan, T. Kryza, J. Batra and J. Clements, *Nat. Rev. Cancer*, 2022, **22**, 223–238.
335 Q.-Y. Chen, D. Luo, G. M. Seabra and H. Luesch, *Bioorg. Med. Chem.*, 2020, **28**, 115756.
336 L. Hedstrom, *Chem. Rev.*, 2002, **102**, 4501–4524.
337 S. U. Seo, S. M. Woo, S.-S. Im, Y. Jang, E. Han, S. H. Kim, H. Lee, H.-S. Lee, J.-O. Nam, E. Gabrielson, K. Min and T. K. Kwon, *Cell Death Dis.*, 2022, **13**, 1–13.
338 T. Yadati, T. Houben, A. Bitorina and R. Shiri-Sverdlov, *Cells*, 2020, **9**, 1679.
339 F. Farris, V. Matafora and A. Bachi, *J. Exp. Clin. Cancer Res.*, 2021, **40**, 147.
340 C.-W. Chou, Y.-K. Huang, T.-T. Kuo, J.-P. Liu and Y.-P. Sher, *Int. J. Mol. Sci.*, 2020, **21**, 7790.
341 S. Köcher, J. Rey, J. Bongard, A. N. Tiaden, M. Meltzer, P. J. Richards, M. Ehrmann and M. Kaiser, *Angew. Chem., Int. Ed.*, 2017, **56**, 8555–8558.
342 M. Nishio, Y. Umezawa, M. Hirota and Y. Takeuchi, *Tetrahedron*, 1995, **51**, 8665–8701.
343 I. Nakanishi, T. Kinoshita, A. Sato and T. Tada, *Biopolymers*, 2000, **53**, 434–445.
344 S. P. Gunasekera, M. W. Miller, J. C. Kwan, H. Luesch and V. J. Paul, *J. Nat. Prod.*, 2010, **73**, 459–462.
345 W. Wang, S. A. Nag and R. Zhang, *Curr. Med. Chem.*, 2015, **22**, 264–289.
346 F. H. Al-Awadhi, V. J. Paul and H. Luesch, *Chembiochem*, 2018, **19**, 815–825.
347 F. Yokokawa and T. Shioiri, *Tetrahedron Lett.*, 2002, **43**, 8673–8677.
348 D. Luo, Q.-Y. Chen and H. Luesch, *J. Org. Chem.*, 2016, **81**, 532–544.
349 D. Luo and H. Luesch, *ACS Med. Chem. Lett.*, 2020, **11**, 419–425.
350 K. Taori, V. J. Paul and H. Luesch, *J. Nat. Prod.*, 2008, **71**, 1625–1629.
351 F. H. Al-Awadhi, L. A. Salvador, B. K. Law, V. J. Paul and H. Luesch, *Mar. Drugs*, 2017, **15**, 290.
352 E. Zafrir-Ilan and S. Carmeli, *Tetrahedron*, 2010, **66**, 9194–9202.
353 N. H. Thuan, T. T. An, A. Shrestha, N. X. Canh, J. K. Sohng and D. Dhakal, *Front. Chem.*, 2019, **7**, 2296–2646.
354 A. Rauf, A. A. Khalil, A. Olatunde, M. Khan, S. Anwar, A. Alafnan and K. R. Rengasamy, *Pharmacol. Res.*, 2021, **166**, 105521.
355 B. Breznik, A. Mitrović, T. T. Lah and J. Kos, *Biochimie*, 2019, **166**, 233–250.
356 J. C. Kwan, E. A. Eksioglu, C. Liu, V. J. Paul and H. Luesch, *J. Med. Chem.*, 2009, **52**, 5732–5747.
357 F. H. Al-Awadhi, B. K. Law, V. J. Paul and H. Luesch, *J. Nat. Prod.*, 2017, **80**, 2969–2986.
358 F. H. Al-Awadhi, R. Ratnayake, V. J. Paul and H. Luesch, *Bioorg. Med. Chem.*, 2016, **24**, 3276–3282.
359 Z. Li, H. Li, F. Jiang, Z. Wang and W. Zhang, *Bioorg. Med. Chem.*, 2022, **57**, 116646.
360 S. Yang, W. Zhang, N. Ding, J. Lo, Y. Liu, M. J. Clare-Salzler, H. Luesch and Y. Li, *Bioorg. Med. Chem.*, 2012, **20**, 4774–4780.
361 A. Lawer, J. Nesvaderani, G. M. Marcolin and L. Hunter, *Tetrahedron*, 2018, **74**, 1278–1287.
362 B. Zhang, S. Li and W. Shui, *Front. Chem.*, 2022, **10**, 843502.
363 P. K. Chaudhary and S. Kim, *Cells*, 2021, **10**, 3288.
364 L. A. Salvador-Reyes, N. Engene, V. J. Paul and H. Luesch, *J. Nat. Prod.*, 2015, **78**, 486–492.
365 F. H. Al-Awadhi, B. Gao, M. A. Rezaei, J. C. Kwan, C. Li, T. Ye, V. J. Paul and H. Luesch, *J. Med. Chem.*, 2018, **61**, 6364–6378.
366 H. Lin, S. Sun, X. Lu, P. Chen, C. Chen, W. Liang and C. Peng, *Int. Immunopharmacol.*, 2017, **51**, 124–130.
367 M. Bekiari, in *Blue Planet Law: The Ecology of our Economic and Technological World*, ed. M. da G. Garcia and A. Cortês, Springer International Publishing, Cham, 2023, pp. 237–252.
368 I. E. Cock and M. J. Cheesman, *Molecules*, 2023, **28**, 7127.
369 Q. Zhou, K. Hotta, Y. Deng, R. Yuan, S. Quan and X. Chen, *Microorganisms*, 2021, **9**, 2551.
370 M. Baunach, A. Guljamow, M. Miguel-Gordo and E. Dittmann, *Nat. Prod. Rep.*, 2024, **41**, 347–369.
371 K. Scherlach and C. Hertweck, *Nat. Commun.*, 2021, **12**, 3864.
372 S. Ponziani, G. Di Vittorio, G. Pitari, A. M. Cimini, M. Ardini, R. Gentile, S. Iacobelli, G. Sala, E. Capone, D. J. Flavell, R. Ippoliti and F. Giansanti, *Int. J. Mol. Sci.*, 2020, **21**, 5510.
373 M. Liu, A. P. Martyn and R. J. Quinn, *Nat. Prod. Rep.*, 2022, **39**, 2292–2307.
374 J. Manochkumar, A. K. Cherukuri, R. S. Kumar, A. I. Almansour, S. Ramamoorthy and T. Efferth, *Comput. Biol. Med.*, 2023, **165**, 107425.

